

Dose-effect autonomic responses to ocular surface stimulation

by

Emmanuel Alabi

A thesis

presented to the University of Waterloo

in fulfillment of the

thesis requirement for the degree of

Doctor of Philosophy

in

Vision Science

Waterloo, Ontario, Canada, 2018

©Emmanuel Alabi 2018

## **Examining Committee Membership**

The following served on the Examining Committee for this thesis. The decision of the Examining Committee is by majority vote.

External Examiner	MARIA CARMEN ACOSTA Associate Professor
-------------------	--

Supervisor	TREFFORD SIMPSON Professor
------------	-------------------------------

Internal Member	NATALIE HUTCHINGS Associate Professor
-----------------	--

Internal Member	VIVIAN CHOH Associate Professor
-----------------	------------------------------------

Internal-external Member	PAUL STOLEE Professor
--------------------------	--------------------------

## **AUTHOR'S DECLARATION**

I hereby declare that I am the sole author of this thesis. This is a true copy of the thesis, including any required final revisions, as accepted by my examiners.

I understand that my thesis may be made electronically available to the public.

## Abstract

### Introduction:

The ocular surface is one of the most densely innervated superficial tissues of the human body supplied extensively by autonomic and sensory nerve fibres. Studies have shown that ocular surface sensory neurons respond to thermal, chemical and mechanical stimuli, but investigation into the functional response of the autonomic nervous system (ANS) to ocular surface stimulation is lacking. The ANS is cardinal to human functioning as it acts below the level of consciousness to regulate the internal organs of the body thus controlling secretory cells, smooth muscle and cardiac muscle. Within the eye the ANS is responsible for the control of pupillary reflexes, accommodation and regulation of blood flow, thus monitoring these mechanisms can provide information about ANS functionality. **The primary objective** of this research was to determine the response of the ANS to ocular surface stimuli by measuring pupil size, conjunctival blood flow and accommodation changes after the delivery of noxious and innocuous corneal stimuli.

### Methods:

A computerised Belmonte pneumatic esthesiometer was used to determine detection thresholds (using ascending method of limits), and to randomly deliver mechanical and chemical stimuli from levels of detection threshold (100% threshold) to twice the threshold (200% threshold) in 50% steps, to the central cornea of 43 healthy subjects, aged 19 - 35 years. Statistical analyses were performed using SPSS (Chicago, SPSS Inc.) and  $p \leq 0.05$  was considered statistically significant.

**Chapter 3:** 15 participants enrolled in this study. For each suprathreshold stimulus a spectrophotometer (Spectrascan650; Photoresearch Inc, Chatsworth, VA) was used to measure ipsi- and contralateral redness before and after delivery of the corneal stimulus, the change in redness represented the ocular vascular response to noxious stimuli.

Conjunctival redness between the stimulated and unstimulated eye was analyzed using dependent t-tests. The effects of stimulus intensity and modality on conjunctival redness were analyzed using repeated measures ANOVA. Tukey HSD tests were used for all post hoc analysis.

**Chapter 4:** 15 participants were enrolled in this study. For each suprathreshold stimulus, imaging of the stimulated and unstimulated eye was performed using two

modified and calibrated Logitech c920 digital cameras (Logitech c920; Logitech International S.A., Newark, CA), for 4 seconds before (pre-stimulus capture) and 4 seconds after the delivery of the stimulus (post-stimulus capture). The data were processed with a custom segmentation algorithm to help identify the pupils and pupil diameter (average of horizontal and vertical measures) was measured using ImageJ software (NIH, Bethesda, MD). Pupil dilation response differences between the ipsi- and contralateral eye was analyzed using dependent t-tests. The effect of stimulus intensity, modality and sex of subjects were analyzed using repeated measures

### **Chapter 5**

13 participants were enrolled in Part A. For each suprathreshold stimulus the accommodative response at a sampling rate of 25Hz, over a 5 second period (while the subjects fixated on a high contrast (85%) color cartoon frame at 66cm) prior to (baseline) and after stimulus delivery was acquired with an eccentric infra-red (IR) photorefractor (Power Refractor, Multi-channel Systems, Reutlingen, Germany). The accommodative response for the left and right eye were averaged. Quantitative differences in accommodative response, stimulus intensity and modality were analyzed using repeated measures ANOVA.

The data used in Part B were acquired from the same subjects in Part A. The pupil response (while the eyes were accommodating to a 66cm target) to ocular surface stimulation was acquired using the same device and methods as in Part A. Quantitative differences in pupil response, stimulus intensity and modality were analyzed using repeated measures ANOVA.

### **Results:**

### **Chapter 3**

In mechanical and chemical stimulation experiments, the stimulated eye became redder than the unstimulated eye (all dependent t-test  $p > 0.05$ ). On average, redness increased from baseline as the corneal stimulus intensity increased. This happened regardless of whether mechanical or chemical stimulation occurred (ANOVA  $p < 0.05$ ). At 200% threshold, conjunctival redness was greater than all stimulus intensities (Tukey HSD, all  $p < 0.05$ ). There was a difference between chemical and mechanical stimulation based on stimulus intensity (ANOVA  $p < 0.05$ ), chemical stimulation produced greater conjunctival redness than mechanical stimulation at all stimulation levels (all Tukey HSD  $p < 0.05$ ).

**Chapter 4:** In mechanical and chemical stimulation experiments, there was no difference in pupil responses between the stimulated eye and the unstimulated eye, (all dependent T-test  $p > 0.05$ ). On average, pupil diameter increased from baseline as the corneal stimulus intensity increased. This happened regardless of whether mechanical or chemical stimulation occurred (ANOVA  $p < 0.05$ ). At 200% threshold, pupil diameter was greater than at all stimulus intensities (Tukey HSD, all  $p < 0.05$ ). There was a difference in pupil diameter between male and female subjects based on stimulus intensity (ANOVA  $p < 0.05$ ); females had greater pupil diameters than males at levels of 150% threshold and 200% threshold (all Tukey HSD  $p < 0.05$ ).

### **Chapter 5**

Part A: On average, accommodation increased from baseline as the corneal stimulus intensity increased. This happened regardless of whether mechanical or chemical stimulation occurred (ANOVA  $p < 0.05$ ). At 200% threshold, accommodation was greater than all stimulus intensities (Tukey HSD, all  $p < 0.05$ ). There was no difference in accommodation between chemical and mechanical stimulation based on stimulus intensity.

Part B: On average, pupil constriction response (during accommodation) was different between baseline and 200% threshold but there was no dose dependent pupil response to ocular surface stimulation. This happened regardless of whether mechanical or chemical stimulation occurred (ANOVA  $p < 0.05$ ). There was no difference in pupil response between chemical and mechanical stimulation based on stimulus intensity (ANOVA  $p > 0.05$ ).

### **Conclusion:**

Suprathreshold stimulation of the cornea appears to evoke dose dependent autonomic responses in the pupils, conjunctival vasculature and the accommodative mechanism. These autonomic measures are accessible, relative easy and cost effective to acquire. The components that respond to noxious corneal stimulation are linked in a homeostatic loop of complex sympathetic, parasympathetic and sensory neural control and therefore, understanding the characteristics of the local stimulus-response neural circuitry relating nociceptive stimuli to autonomic nervous functionality is important. It also promises the development of clinical procedures and instruments to better understand how these neural responses are impacted by pain.

## **Acknowledgements**

I would like to extend my greatest gratitude to my supervisor Dr Trefford Simpson for his guidance and patience throughout my study. It is a privilege to work an individual who possesses a continuum of scientific knowledge and ideas. Thank you for giving me the independence to carry out this research. Above all thank you for supporting me through out my masters and PhD.

I would like to thank my committee members Dr Vivian Choh and Dr Natalie Hutchings for their helpful comments and suggestions. I am grateful to my internal/external examiner Dr Paul Stolee and my external examiner Dr Maria Carmen Acosta for reviewing my thesis.

.

My sincere acknowledgements to Varadhu and Dr Yunwei Feng for their assistance in the lab. Many thanks to the Graduate officers (Dr Daphne McCulloch and Dr Ben Thompson) and graduate coordinator - Stephanie Forsyth for all their assistance and keeping me on track. I would like to thank Dr Hovis for giving me many laughs during his course that I TA'd for 6 years.

I thank all GIVS members, staff and faculty of the school of Optometry for providing a pleasant work environment.

## **Dedication**

To my mother – Thank you!

## Table of Contents

Examining Committee Membership.....	ii
AUTHOR'S DECLARATION .....	iii
Abstract .....	iv
Acknowledgements .....	vii
Dedication .....	viii
Table of Contents .....	ix
List of Figures .....	xiii
List of Tables.....	xvi
List of Abbreviations.....	xvii
Chapter 1 Literature Review .....	1
1.1 Introduction .....	1
1.2 The Cornea .....	1
1.2.1 Corneal Epithelium.....	1
1.2.2 Bowman's Layer .....	2
1.2.3 Corneal Stroma.....	2
1.2.4 Descemet's Membrane .....	3
1.2.5 Corneal Endothelium.....	3
1.3 The Conjunctiva .....	3
1.3.1 Bulbar Conjunctiva.....	4
1.3.2 Palpebral Conjunctiva .....	5
1.4 Tears .....	5
1.4.1 Tear Production .....	6
1.4.2 Lacrimal Glands .....	6
1.4.3 Accessory Lacrimal Glands.....	6
1.4.4 Meibomian Glands .....	7
1.5 Ocular Surface Innervation.....	7
1.5.1 Conjunctival Innervation .....	9
1.6 Functions of Ocular Surface Neurons .....	10
1.6.1 Mechano-sensory, Polymodal and Cold Sensitive Neurons.....	11
1.6.2 Sensations arising from the ocular surface.....	14

1.7 The Autonomic Nervous System .....	14
1.7.1 The Pupils .....	15
1.7.2 Pupillary light reflex .....	16
1.8 Accommodation .....	18
1.9 Innervation of the Conjunctiva .....	19
1.10 Pain .....	20
1.10.1 History of Pain .....	20
1.10.2 Transmission of Pain.....	22
1.10.3 Trigeminal Pathway .....	24
1.11 Psychophysical Techniques .....	24
1.12 Classical methods of psychophysical measurement .....	26
1.12.1 Method of Adjustments.....	26
1.12.2 Method of Limits .....	26
1.12.3 Method of constant stimuli .....	28
1.13 Devices for the measurement of ocular surface .....	29
1.13.1 The Cochet-Bonnet esthesiometer .....	29
1.13.2 Pneumatic esthesiometers .....	29
1.13.3 Comparison of Cochet-Bonnet and pneumatic esthesiometers.....	31
1.14 Psychophysical scaling .....	31
1.14.1 Stevens Power Law.....	32
1.15 Suprathreshold scaling on the ocular surface.....	33
1.16 Colour Science .....	34
Chapter 2 Rationale.....	35
2.1 Introduction.....	35
2.2 Experiments on the conjunctival blood flow response .....	35
2.3 Experiments on the pupillary response .....	36
2.4 Experiments on the Accommodative Reflex .....	37
2.5 Summary .....	38
Chapter 3.....	39
Conjunctival redness response to corneal mechanical and chemical stimulation.....	39
3.1 Introduction.....	39

3.2 Materials and Methods .....	41
3.2.1 Sample .....	41
3.2.2 Computer-controlled Belmonte Esthesiometer .....	41
3.2.3 Nociceptive Stimuli .....	43
3.2.4 Stimulus Delivery .....	44
3.2.5 Redness Measurements .....	45
3.2.6 Analyses .....	47
3.3 Results .....	47
3.3.1 Effects of Stimulus Intensity on Conjunctival Redness .....	47
3.3.2 Effects of Stimulus Modality and Stimulus Intensity on Conjunctival Redness .....	48
3.3.3 Relationship Between Stimulated and Unstimulated Eye .....	50
3.3.4 Relationship Between Conjunctival Redness and Stimulus Intensity .....	51
3.4 Discussion .....	55
3.5 Conclusion.....	59
Chapter 4 Pupil Response to Noxious Ocular Surface Stimulation .....	60
4.1 Introduction .....	60
4.2 Methods .....	62
4.2.1 Subjects .....	62
4.2.2 Computer-controlled Belmonte Esthesiometer .....	63
4.2.3 Nociceptive Stimuli .....	63
4.2.4 Stimulus Delivery .....	64
4.2.5 Data Processing and Pupil Size Measurements .....	64
4.2.6 Analyses .....	65
4.3 Results .....	66
4.3.1 Effects of Stimulus Intensity on Pupil Diameter .....	66
4.3.2 Effects of Stimulus Modality and Stimulus Intensity on Pupil Diameter .....	66
4.3.3 Relationship Between Ipsi- and Contralateral Eye .....	66
4.3.4 Effects of Sex and Stimulus Intensity on Pupil Diameter .....	77
4.4 Discussion .....	78
4.5 Conclusion.....	82
Chapter 5 Part A - Accommodative Response to Ocular Surface Stimulation .....	83

5.1 Introduction.....	83
5.2 Methods.....	85
5.2.1 Subjects .....	85
5.2.2 Power Refractor .....	85
5.2.3 Computer-controlled Belmonte Esthesiometer .....	86
5.2.4 Nociceptive Stimuli.....	87
5.2.5 Stimulus Delivery .....	87
5.2.6 Analyses.....	89
5.3 Results.....	90
5.4 Discussion.....	100
5.4.1 Part A - Accommodative Response to Ocular Surface Stimulation.....	100
Part B – Pupil Response to Ocular Surface Stimulation in the Accommodating Eye .....	104
5.4.2 Subjects .....	105
5.4.3 Power Refractor .....	105
5.4.4 Computer-controlled Belmonte Esthesiometer .....	106
5.4.5 Nociceptive Stimuli.....	106
5.4.6 Stimulus Delivery .....	107
5.5 Analyses.....	108
5.6 Results.....	109
5.7 Discussion.....	114
5.8 Conclusion .....	117
Chapter 6.....	118
General Discussion .....	118
Chapter 7 Future Work .....	126
Letter of Copyright Permission.....	128
Bibliography .....	129

## List of Figures

Figure A: The path travelled by nerves in the cornea (above). Impulse activity of functional types of neurons that can be found in the cornea.....	13
Figure 1: Enface image of the computerized Belmonte esthesiometer and calibrated video display (A). Image displaying the nozzle of the computerized Belmonte esthesiometer used in stimulus delivery to the ocular surface (B).....	43
Figure 2: Stimulus and ROI locations for the left eye. X represents the stimulus location, N represents the ROI for the nasal conjunctiva, and T represents the ROI for the temporal conjunctiva.....	46
Figure 3: Mean conjunctival redness across the different stimulus intensities for chemical (red) and mechanical (blue) corneal stimulation experiments (error bars denote 95% confidence interval). .....	49
Figure 4: Box-plot of the conjunctival redness between the stimulated and the unstimulated eye after 200% threshold corneal mechanical stimulation. ....	50
Figure 5: Box-plot of the conjunctival redness between the stimulated and the unstimulated eye after 200% threshold corneal mechanical stimulation. ....	51
Figure 6: The relationship between conjunctival redness and stimulus intensity during mechanical stimulation of the cornea. An average redness increase of 0.018 (CIEu') is expected from baseline to 200% threshold. ....	53
Figure 7: The relationship between conjunctival redness and stimulus intensity during chemical stimulation of the cornea. An average redness increase of 0.043 (CIEu') is expected from baseline to 200% threshold. ....	54
Figure 8: Box-plot of pupil response between the ipsilateral (stimulated) and the contralateral (unstimulated) eye after corneal mechanical stimulation (error bars denote 95% confidence interval).....	67

Figure 9: Box-plot of pupil response between the ipsilateral (stimulated) and the contralateral (unstimulated) eye after corneal chemical stimulation (error bars denote 95% confidence interval).....	68
Figure 10: Pre- and post-stimulus pupil diameter for mechanical corneal stimulation for male and female subjects. ....	71
Figure 11: Pre- and post-stimulus pupil diameter for chemical corneal stimulation for male and female subjects. ....	73
Figure 12: Mean pupil diameter across different stimulus intensities for mechanical (blue) and chemical (red) corneal stimulation experiments (error bars denote 95% confidence interval). ....	76
Figure 13: Mean pupil diameter across different chemical stimulus intensities for male (blue) and female (red) subjects (error bars denote 95% confidence interval). ....	77
Figure 14: Image of the Power Refractor (Multi-channel Co, Reutlingen, Germany). ....	86
Figure 15:Pre-stimulus accommodative response for all subjects in the mechanical (left) and chemical (right) corneal stimulation experime .....	91
Figure 16:Post-stimulus accommodative response for all subjects in the mechanical (left) and chemical (right) corneal stimulation experiments.....	92
Figure 17: Accommodative response across different stimulus intensities for mechanical (blue) and chemical (red) corneal stimulation experiments (error bars denote 95% confidence interval). ....	95
Figure 18: Box-plot of accommodative response between baseline and 0% stimulus intensities for the mechanical corneal stimulation experiment (error bars denote 95% confidence interval). ....	96
Figure 19: Box-plot of accommodative response between baseline and 0% stimulus intensities for the chemical corneal stimulation experiment (error bars denote 95% confidence interval). ....	97
Figure 20: The relationship between accommodation and stimulus intensity per subject during mechanical stimulation of the cornea. ....	98

Figure 21: The relationship between accommodation and stimulus intensity per subject during chemical stimulation of the cornea. ....	99
Figure 22: Pupil response (in the accommodating eye) across different stimulus intensities for mechanical (blue) and chemical (red) corneal stimulation experiments (error bars denote 95% confidence interval). ....	111
Figure 23: The relationship between pupil response and stimulus intensity per subject during mechanical stimulation of the cornea. ....	112
Figure 24: The relationship between pupil response and stimulus intensity per subject during chemical stimulation of the cornea. ....	113

## List of Tables

Table 1: Results from a mixed model analysis displaying the relationship between conjunctival redness and stimulus intensity in mechanical corneal stimulation experiments (the slope estimates are referenced to the highest stimulus level). .....	52
Table 2: Results from a mixed model analysis displaying the relationship between conjunctival redness and stimulus intensity in chemical corneal stimulation experiments (the slope estimates are referenced to the highest stimulus level). .....	52
Table 3: The values for the non-linear regression model for pupil response used mechanical and chemical corneal stimulation experiments. ....	69
Table 4: Pupil sizes at the different time points as determined by the non-linear model $y=C+(B*((A*time)/(EXP(A*time))))$ for male and female subjects. ....	74
Table 5: Mean $\pm$ (SD) pupil size between males and females for mechanical and chemical corneal stimulation experiments. ....	75
Table 6: Mean ( $\pm$ SD) accommodative response across the different stimulus intensities in mechanical and chemical corneal stimulation experiments. ....	93
Table 7: Mean ( $\pm$ SD) pupil response across the different stimulus intensities in mechanical and chemical corneal stimulation experiments. ....	109

## List of Abbreviations

ANOVA	Analysis of variance
ANS	Autonomic nervous system
ASIC	Acid-sensitive ion channel
CGRP	Calcitonin gene related peptides
CNS	Central nervous system
CO <sub>2</sub>	Carbon Dioxide
DL	Difference threshold
EW	Edinger-Westphal
ENAC	Epithelium sodium channels
LC	Locus coeruleus
LGB	Lateral geniculate body
NDHN	Nociceptive dorsal horn neurons
PNS	Peripheral nervous system
VAS	Visual analogue scale
V1	Primary visual cortex
VR1	Vanilloid receptor -1

# **Chapter 1**

## **Literature Review**

### **1.1 Introduction**

The ocular surface comprises the cornea and its key support tissue, the conjunctiva. In a wider anatomical and physiological sense, the tear film, Meibomian glands and the ocular mucosal adnexa (i.e., the lacrimal gland and the lacrimal drainage system) also contribute to the ocular surface[1].

### **1.2 The Cornea**

The cornea is the transparent avascular part of the eye that plays a cardinal role in ocular refraction and acts as a protective mechanism. Anteriorly to posteriorly, the cornea is made up of five major layers: epithelium, Bowman's layer, stroma, Descemet's Layer and the endothelial layer[2].

#### **1.2.1 Corneal Epithelium**

The outermost layer of the cornea is known as the epithelium. It borders the Bowman's layer and the tear film. The epithelial part of the cornea is approximately 55  $\mu\text{m}$  thick[3]. It is thicker inferiorly, thinner superiorly and thicker nasally than temporally[4]. It is made up of a basal cell layer and about four to five layers of non-keratinized, tiled squamous cells which are bound together by occluding junctions. These tight junctions form an efficient barrier against disease-causing microorganisms and the loss of fluid.

Superficially, the corneal epithelium has two to three layers of flattened squamous cells, and a few layers of wing cells bordered by a layer of columnar basal cells[5].

### **1.2.2 Bowman's Layer**

The Bowman's layer is a thin layer separating the corneal epithelium from the stroma. The central Bowman's layer thickness is approximately 17 $\mu$ m, and it remains constant from the center to the mid-periphery. The thicknesses at the nasal and temporal periphery is 20  $\mu$ m and 19  $\mu$ m respectively, and comprises collagen fibrils found in random distribution[6]. Damage to the Bowman's layer can lead to adherence of the corneal epithelium to the stroma which results in the disruption of the structural integrity of the ocular surface. It is thus evident that this membrane is important in the support and maintenance of corneal structure[7].

### **1.2.3 Corneal Stroma**

The stroma is predominantly composed of collagen, glycoprotein and water. The stroma takes up about 90% of the total volume of the cornea[8]. It has the tendency to take in fluid and keeps the cornea transparent at all times through the process of controlled dehydration. However, there are times where the cornea can lose transparency. This occurs when there is disruption of the cellular limiting layers which in turn leads to the inflow of fluids that affects the orderly arrangement of stromal lamellae and causes an increase in the scattering of light. Intrusion of the stromal lamellae by immune cells such as macrophages tends to reduce the transparency of the cornea as well.[9].

#### **1.2.4 Descemet's Membrane**

The Descemet's membrane is a thick basement membrane measuring about 5–10  $\mu\text{m}$  in thickness. It is a bi-layered membrane with the anterior layer made up of a mixture of proteoglycans and collagen lamellae. The posterior layer is glassy in appearance and is produced by the endothelium cells below it[10].

#### **1.2.5 Corneal Endothelium**

The corneal endothelium is a single layer consisting of hexagonal cells that do not have the ability to regenerate. The normal density of corneal endothelial cells in adults is approximately 2500 cells/ $\text{mm}^2$  and it is reduced by about 0.6% yearly[11]. The endothelium performs an essential function of maintaining the hydration of the cornea by imbibing water and other substances[12]. When the endothelial cells' density is reduced to approximately 800 cells/ $\text{mm}^2$ , it may lead to corneal decompensation, causing corneal edema and loss of corneal transparency, which disrupts vision. Similarly, the reduced numbers of endothelial cells leads to increased size to compensate for the lost cells[13]. Through the use of an active adenosine triphosphate (ATP) and bicarbonate-dependent pump, the endothelium regulates the cornea's state of hydration thus helping to keep the cornea clear at all times[14]. For nourishment, nutrients pass through the endothelium via simple and facilitated diffusion[12].

### **1.3 The Conjunctiva**

The conjunctiva forms a border to the margin of the cornea and eyelids and lines the eyeball at the sclera. It overlays the sclera up to the 1.5 mm transition zone between the cornea and

the conjunctiva known as the limbus[15]. Six or more layers of non-keratinized columnar and cuboidal cells can be found in the conjunctiva and towards the fornix there can be up to 12 cell layers. There are mucus apocrine gland cells known as goblet cells found among the epithelial cells of the conjunctiva[16]. Feng and Simpson[3] showed the human conjunctival epithelial thickness to be around  $44.9 \pm 3.4 \mu\text{m}$  (mean  $\pm$  SD) and other research suggests the conjunctiva stromal thickness measurements are around  $197 \mu\text{m}$ [17]. The conjunctiva is divided into 3 parts: bulbar conjunctiva, palpebral conjunctiva and forniceal conjunctiva.

### **1.3.1 Bulbar Conjunctiva**

The bulbar conjunctiva consists of a layered secretory epithelium interfaced with a basement membrane overlaying the substantia propria which is a vascularized connective tissue substrate. The substantia propria is a highly vascularized, loose connective tissue[18].

Cuboidal epithelial cells, Langerhans cells, goblet cells, lymphocytes and melanocytes, are some the cell types found in the bulbar conjunctiva which is about six layers in thickness[19]. Apical cell junctions, desmosomes and gap junctions control what permeates the conjunctiva[17, 20].

Parasympathetic activation causes the release of granules from mucous-secreting goblet cells that constitute about 5–15% of the conjunctival epithelial basal cells[20]. The highest density of goblet cells occurs in the inferior nasal bulbar conjunctiva and tarsal conjunctiva.

The bulbar conjunctiva is inferiorly bordered by and loosely attached to Tenon's capsule. There is a more rigid attachment of the conjunctiva to Tenon's fascia as we approach the limbus. In this region, the epithelium gradually changes to flatter and less cuboidal epithelial cell morphology. Once the bulbar conjunctiva transitions into the limbus, radiating folds known as the palisades of Vogt can be observed, the stem cells of the cornea can be found in this location[21, 22].

### **1.3.2 Palpebral Conjunctiva**

The lining of the posterior surface of the eyelids is known as the palpebral conjunctiva. It consists of three major parts: 1) the marginal conjunctiva - this stretches from eyelid margin to the tarsus, 2) the sub-tarsal conjunctiva that covers the tarsal plate and 3) the orbital conjunctiva that stretches from the tarsus to the fornix[5].

### **1.4 Tears**

The precorneal tear film consists of three major layers that collectively work to help maintain the optical quality of the eye, it also coats the ocular surface providing a protective function[23]. The three layers are the aqueous, lipid and mucous layers. The aqueous layer is the middle component of this tri-layer complex, it is produced by the lacrimal gland and forms a protective barrier against microorganisms and regulates the osmotic pressure of the tears. The lipid layer is produced by the Meibomian glands and overlays the aqueous layer, proving a hydrophobic barrier for the tears[24]. The mucous layer is closest to the corneal epithelium, it is supplied by the goblet cells of the conjunctiva and is responsible for the hydrophilic components of the tear film[25].

### **1.4.1 Tear Production**

There are several factors that can influence the production of tears. The production of tears can be grouped into psycho-emotional, basal and reflex tearing. Psycho-emotional tears are the tears one experiences in emotional states such as sadness, anger or happiness. Basal tears are in constant production and are responsible for keeping the eyes lubricated and nourished always. Reflex tearing is the tear production associated with irritation of the ocular surface[26].

### **1.4.2 Lacrimal Glands**

The lacrimal gland is divided into two lobes (the orbital and palpebral lobes) by the lateral horn of the levator aponeurosis[27].

The lacrimal gland develops from the outgrowth of the pouch conjunctiva, while the adnexal accessory glands develop after the main lacrimal glands form[28]. The lacrimal gland produces water, electrolytes and proteins for the tear film. While the protein component is synthesized by the lacrimal gland itself, the water and electrolyte components originate from the blood supply and travel across the apical membrane into the duct system of the lacrimal gland[29].

### **1.4.3 Accessory Lacrimal Glands**

The glands of Wolfring and Krause are accessory glands found towards the superior fornix of the conjunctiva. They are smaller than the lacrimal gland but also produce water, electrolytes and proteins that are secreted as part of the tears. These glands form part of the lacrimal system. [27].

#### **1.4.4 Meibomian Glands**

The Meibomian or tarsal glands are large, secretory structures found within the tarsal plate of the eyelids. On average, there are about 32 glands in the superior eyelid while about 25 can be found in the inferior eyelid[2]. The secretion produced by the tarsal glands are oily due to a high lipid content. A few substances that make up this oily secretion includes, but is not limited to sterols, waxy esters, fatty acids and cholesterol[30]. The secretions from the Meibomian gland forms the lipid layer of the tear film and is responsible for the prevention of evaporation of water from the tear film[30].

#### **1.5 Ocular Surface Innervation**

The cornea is one of the most densely innervated structures in the human body and the nerve branches supplying the cornea are derived from the cranial nerve (V) also known as the trigeminal nerve[31]. The cell bodies of the neurons of the trigeminal nerve aggregate to form the gasserian or semilunar ganglion which is located just adjacent to the brainstem. The semilunar ganglion has two major roots, the motor and sensory roots and these bundles of nerve fiber connect the ganglion directly to the brainstem. The trigeminal nerve, as its name “tri” indicates, has three major branches; the ophthalmic (V1), maxillary (V2) and mandibular (V3) branches. With the exception of the optic nerve all sensory neurons of the eye are linked with the ophthalmic branch of the trigeminal nerve. The ophthalmic division splits into three branches, namely the frontal, lacrimal and nasociliary nerves. The nasociliary nerve is responsible for the transmission of all the somatosensory information that leaves the eye[13]. The nasociliary nerve is divided into the long and short ciliary nerves and collectively these nerves contain sympathetic, parasympathetic and sensory

fibers. All these fibers leave the eye through the sclera in close approximation to the optic nerve and aggregate at the ciliary ganglion which is about 10mm behind the eye. Sensory receptors on the cornea, conjunctiva and parts of the sclera all converge to form the long ciliary nerve[32].

Impulses from the trigeminal ganglion cells are transmitted by the ophthalmic division of the trigeminal nerve[2]. After exiting the trigeminal ganglion cells, nerve fibers travel suprachoroidally and branch to form nerve bundles that come to rest uniformly around the corneoscleral limbus to form the limbal plexus[32].

The nerve fibers in the transition zone from conjunctiva to cornea then lose their myelin sheath as they enter the cornea, traveling parallel to the ocular surface. At this point, these nerve fibers make a degree turn and the majority of the fibers proceed towards the outermost layer of the cornea, the epithelium. However, there are some nerve fibers that end up in the stroma of the cornea[13].

The lacrimal gland is innervated by autonomic and sensory bundles[33]. There is an unequal autonomic innervation to the lacrimal gland because there is a greater parasympathetic supply in comparison to sympathetic input.

The sympathetic pathway to the lacrimal gland can be traced from the preganglionic neurons in the ciliospinal center of Budge (segments C8 to T2 of the spinal cord). The nerve fibers from this region project to the superior cervical ganglion via the sympathetic trunk. At this point the sympathetic fibers join parasympathetic nerves and travel through the pterygopalatine ganglion. They finally terminal in the lacrimal gland via the zygomatic

division of the second branch of the trigeminal nerve (V2)[2]. The sympathetic pathway in the lacrimal gland innervates smooth muscle and small blood vessels within the gland[5]. The preganglionic parasympathetic supply to the lacrimal gland begins at the level of the pons where the lacrimal nucleus is located. The nerve fibers then project towards the sphenopalatine ganglion (or pterygopalatine ganglion) via branches of the facial nerve known as the superficial and deep petrosal nerves. Upon reaching the pterygopalatine ganglion the nerves synapse and postganglionic fibers then head to the lacrimal gland by passing through the maxillary branch of the trigeminal nerve[33]. The axons continue their journey from the maxillary nerve through the zygomatico-temporal nerve where communicating branches carry the axons to join the lacrimal nerve. The axons finally terminate in secretory cells of the lacrimal gland and also on blood vessels within this area[34]. Acetylcholine and vasoactive intestinal peptide (VIP) are the main neurotransmitters for the parasympathetic lacrimal gland activity. While acetylcholine binds to M3 muscarinic receptors, VIP binds to VIP receptors, all located in the cellular membranes of the glandular acinar cells[34].

Sensory fibers innervate the lacrimal gland via the lacrimal branch of the ophthalmic division of the trigeminal nerve. Substance P and calcitonin gene-related peptide are released from the sensory receptors found on the lacrimal nerve causing lacrimation[35].

### **1.5.1 Conjunctival Innervation**

As mentioned above the conjunctiva is extensively supplied by the ophthalmic division of the fifth cranial nerve. Sensory neurons from the conjunctiva are the terminals of branches

of the lacrimal nerve, the frontal nerve (supratrochlear and infraorbital divisions), and the nasociliary nerve (infratrochlear division). These nerves also constitute a majority of the innervation of the eyelid[36]. There is evidence some of the neurons in the conjunctiva can also be traced to nerves that branch off the second division of the trigeminal nerve, specifically the infraorbital nerve but this is only on studies done in monkeys[37]. Finally, the rest of the neurons in the conjunctiva, especially towards the limbus, are innervated by autonomic and sensory bundles from the ciliary nerve. Most of these bundles end up as free unmyelinated nerve endings in the conjunctiva and together they form the sub-epithelial plexus which can be found more anteriorly in the substantia propria of the conjunctiva[36].

### **1.6 Functions of Ocular Surface Neurons**

The cornea is one of the most densely innervated superficial tissues of the human body supplied extensively by sensory and autonomic nerve fibers. There is a greater supply of parasympathetic fibers in the cornea in comparison to sympathetic fibers. The nerve supply of the cornea and conjunctiva consists of a small number of primary sensory neurons located in the ciliary ganglion and their population is approximately 1.5% of the total number of neurons of the ganglion. As mentioned earlier, the axons reach the cornea via the long and short ciliary nerves[32, 38-40].

Depending on the existence and thickness of myelin sheath, corneal neurons can be grouped into myelinated A-delta type neurons and unmyelinated C-type corneal neurons[41]. The size of the myelin sheath influences the conduction velocity of nerve

impulses from the cornea to the central nervous system (CNS). The conduction velocity is higher in the axons of neurons of A-delta type fibers[42-44].

### **1.6.1 Mechano-sensory, Polymodal and Cold Sensitive Neurons**

The three functional types of neurons that can be found within the cornea are mechano-sensory (mechanonociceptors), polymodal and cold sensitive neurons (Figure A). Mechanonociceptors, which make up about 20% of the corneal neurons, respond to mechanical forces sufficient to damage corneal epithelial cells[45]. Corneal mechanonociceptors are most likely responsible for the sharp painful feeling produced by any mechanical contact with the surface of the cornea similar to that experienced in the skin[46] and tooth pulp[47].

Polymodal nociceptors are the main source of nerve impulse activity that is caused by mechanical and chemical irritation, heat and damaging cold[39, 43-45, 48, 49]. Approximately 70% of corneal sensory receptors are polymodal nociceptors [39, 42, 45]. Polymodal nociceptors are activated when exposed to temperatures above 39°C[45, 48, 50]. Polymodal nociceptors respond to many endogenous chemicals released by inflammatory cells on the ocular surface such as protons, potassium ions, prostaglandins and arachidonic acid metabolites, amines, cytokines, and kinins[51]. During the stages of inflammation, locally released mediators stimulate the polymodal nociceptors, leading to an incessant firing which produces feelings of pain[32, 42]. Polymodal nociceptors respond to their activating stimuli with a continuous but irregular discharge of impulses that

continue if the stimulus is sustained. The impulse discharge of polymodal nociceptors signals the presence of a noxious stimulus and encodes its intensity and duration.

Cold-sensitive receptors represent about 10–15% of the total population of corneal nociceptors[52, 53]. They discharge spontaneously at rest and increase their firing rate when the temperature of the corneal surface decreases (below 33.8C) and they appear to be momentarily silent upon warming[54-56]. It has been suggested that the increase in firing rate when the temperature of the cornea drops is due to evaporation at the corneal surface, the application of cold solutions or the blowing of cold air on the cornea[54-56]. Cold receptors can detect and process a change in minute temperature variations of 0.18C or less, thus allowing the perception of corneal temperature reductions of that magnitude as a conscious sensation of cooling[49, 55-58].

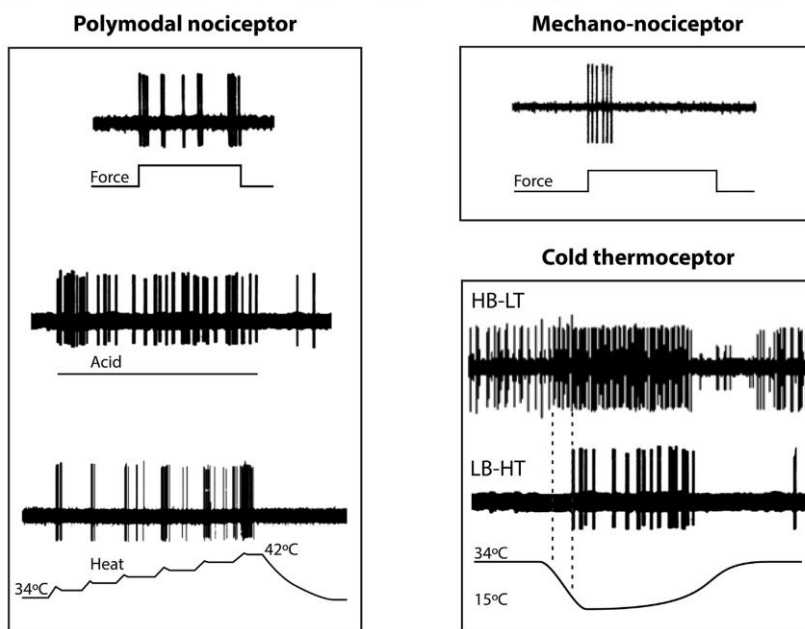
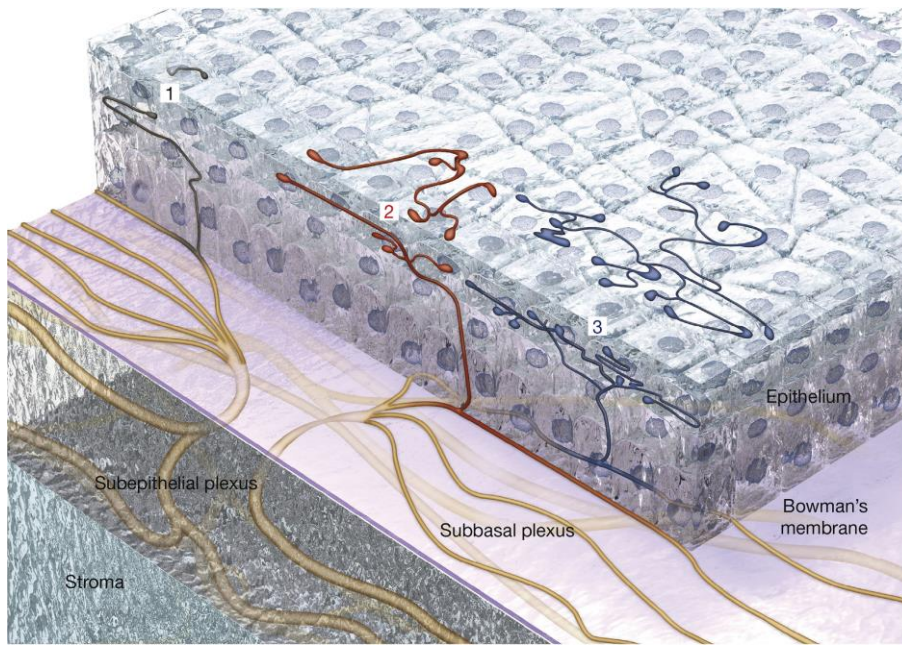


**Figure A: The path travelled by nerves in the cornea (above). Impulse activity of functional types of neurons that can be found in the cornea (below).**

(Reproduced with permission from - Belmonte, Carlos, et al. "TFOS DEWS II pain and sensation report." *The Ocular Surface* 15.3 (2017): 407.)

Receptive fields are areas of ocular surface tissue that are innervated by sensory fibers arriving from the ophthalmic division of the trigeminal nerve[42]. When a receptive field is activated, there is firing of nerve impulses due to depolarization of the nerve terminals. Mechanonociceptors and polymodal nociceptors have large receptive fields within the cornea and, to some extent, the episclera[51, 59]. Cold receptors on the other hand have fewer receptive fields in the cornea though even smaller cold sensing receptor fields can be found in the region of the limbus[56, 60].

### **1.6.2 Sensations arising from the ocular surface**

When delivering mechanical, chemical or thermal stimulation to the ocular surface, irritation and cold are the major sensations experienced[61-63]. The possible activation of A $\delta$  mechanosensory and polymodal nociceptors results in a scratchy and irritating acute sensation while the application of chemical stimuli decreases corneal pH and results in an unpleasant burning and stinging pain that lasts longer even after removal of the stimulus. The sensations involving thermal stimulation have been described with words such as irritating, warmth and cooling[42, 44, 48, 62, 64].

### **1.7 The Autonomic Nervous System**

The human nervous system is made up of the CNS and the peripheral nervous system (PNS). Together, the brain and the spinal cord form the CNS which in turn controls the whole body through the peripheral somatic and autonomic nervous system[65]. The nervous system interacts with the body and surrounding environments to bring about adaptive behavior[66].

The autonomic nervous system (ANS) consists of a group of nerves and nerve cells that control various processes in the body[67]. The ANS is divided into three major parts: the sympathetic nervous system, parasympathetic nervous system and enteric nervous system[68]. The enteric nervous system contains the only group of neurons outside the CNS which forms circuits that are able to bring about autonomic reflex activity[69]. Some of the body functions controlled by the ANS include breathing, blood pressure, urination, defecation, sexual response, digestion, body temperature, production of body fluids, balance of water and electrolytes and metabolism[70].

The ANS is controlled by a part of the brain called the hypothalamus[68]. The ANS regulates various ocular functions like pupil dilatation, pupillary constriction and accommodation. These functions are performed by the eye's intrinsic muscles found in the ciliary body and the iris, and the nerve supply to these structures is by post ganglionic fibers of the superior cervical ganglion[71]. The ANS also influences ocular blood flow, which is controlled through innervation of the optic nerve vasculature, retina, choroid, ciliary body and the iris[72].

### **1.7.1 The Pupils**

While the primary function of the pupillary reflex is to regulate the amount of light entering the eye, there are various cognitive processes which result in dilation of the pupil including: habituation, sexual and political preference, fatigue, and level of mental effort[73]. A study conducted by Steinhauer et al.[74], revealed that there is a significant effect of sustained tasks on pupil diameter. This study, conducted on human subjects, revealed that sustained

difficult tasks cause an inhibition on the parasympathetic pathway, resulting in pupillary dilation. Other experiments have suggested that the pupil diameter tends to enlarge with increasing task demand and pain[73, 75-77].

Children with autism have been found to have restricted pupillary constriction, suggesting that there is lower parasympathetic modulation[78]. Individuals who experience migraines have been found to have altered pupillary responses; subtle sympathetic and parasympathetic abnormalities in the pupil during the migraine have been shown to exist[79]. Amblyopic patients have also been shown to have delayed pupillary responses[80].

### **1.7.2 Pupillary light reflex**

The integrity of the visual system can be assessed often by the pupillary light reflex[81]. Photostimulation of rods and cones in the outer retina initiates the pupillary light reflex[82]. The balance between the sympathetic and the parasympathetic system input will determine the pupillary response. For example, an increased parasympathetic innervation will cause a resultant pupillary constriction while a decreased innervation will result in pupillary dilatation[83].

Pupillary constriction is achieved through parasympathetic connection via the sphincter muscles while pupillary dilatation is achieved through a sympathetic pathway to dilator muscles[84]. Photosensitive cells containing melanopsin have been found under retinal ganglion cells. According to Do and Yau (2010), “these intrinsically photosensitive retinal ganglion cells (ipRGC’s) comprise approximately 2 percent of overall RGC population and

project to areas of the brain that regulate non imaging forming functions to light”[82]. These functions include pupillary light reflex and circadian related actions such as modulation of sleep-wake states, sudden suppression of melatonin and photo entrainment[82].

The retinal ganglion cells (RGC) have been thought to mediate the afferent branch of the pupillary light reflex where melanopsin is the photosensitive pigment[85]. The activation of RGCs that contain melanopsin is not only intrinsic but also extrinsic, through the activation of rods and cones in the outer retina[86].

The input to intrinsically photosensitive retinal ganglion cells in normal retina is predominantly from rod and cone photoreceptors. By themselves, ipRGCs have been shown to modulate sustained pupillary size in response to different light levels[82]. Genetic removal of ipRGCs in mice eliminates the pupillary response to light, which indicates that the melanopsin ipRGCs serve as a required channel for transmission of impulses to reach the olivary pretectal nucleus[85].

The afferent nerve fibers extend from the retina to the midbrain at the pretectal nucleus. These nerve fibers move along the optic nerve via the optic chiasma where nerve fibers coming from nasal retina decussate and thus move along the opposite optic tract to terminate at the contralateral pretectal nucleus[5].

The nerve fibers coming from the temporal retina terminate at the ipsilateral pretectal nucleus. These nerve fibers remain uncrossed thus travelling at the same side of the optic

tract and each pretectal nucleus is connected with Edinger-Westphal nucleus of both sides. The basis of consensual light reflex lies in this connection[87].

Preganglionic fibers in the ventrosegmental and anterio-medial nucleus make up the efferent pathway of the pupillary light response[82]. These fibers arise from the midbrain area and travel along the oculomotor nerve[5]. The preganglionic nerve fibers leave the mesencephalon traveling via the inferior division of the ocular oculomotor nerve (III cranial nerve) to the ciliary ganglion. The oculomotor nerve also contains motor fibers that innervate skeletal muscles which control eyelids and eye movement[82]. At the level of the ciliary ganglion, motor fibers separate. The sphincter papillae is innervated by post ganglionic nerve fibers that travel along the short ciliary nerves[5].

Smooth muscles of the mammalian iris are normally under autonomic control with the iris sphincter muscles being modulated by the neurotransmitter acetylcholine and the iris dilator muscles being modulated by the neurotransmitter norepinephrine[5].

## **1.8 Accommodation**

Accommodation is the eye's ability to alter its refractive power to bring closer items into focus on the retina. As primates age, the eyes ability to carry out this task reduces[88] and one experiences the complete loss of accommodation by the age of 55[89].

In the accommodative state, the ciliary muscle contracts causing the suspensory zonules of Zinn to relax, which in turn causes the crystalline lens to take a more convex shape, the dioptric power of the eye. In disaccommodation the opposite occurs and the lens assumes a flatter shape[90].

As is typical, the accommodative mechanism contains an afferent and efferent pathway. Accommodation is a reflex that is visually guided and so, requires a visual stimulus for it to normally occur. The optic nerve constitutes the afferent pathway of the accommodative mechanism. The preganglionic neurons of the Edinger-Westphal nucleus sends impulses to the ciliary ganglion and from the ciliary ganglion, the impulses travel towards the ciliary muscle forming the efferent pathway[91]. Accommodative control in humans is primarily driven by the oculomotor nerve's parasympathetic innervation of the ciliary muscle. Positive accommodation of up to 20 diopters is modulated by the action of the neurotransmitter acetylcholine on post-synaptic muscarinic (M3) receptors on ciliary smooth muscle and tends to occur in 1 second or less[92]. Contrary to previous ideas that the sympathetic arm of the ANS had no role in accommodation, research indicates that sympathetic innervation causes an inhibitory effect on the parasympathetic activity and influences accommodation at far by up to 1.5 diopters[93]. This action is primarily modulated by neurotransmitter noradrenaline on b2 receptors in ciliary smooth muscle and tends to occur much more slowly (10 – 40 seconds)[91, 94].

### **1.9 Innervation of the Conjunctiva**

As mentioned above, the conjunctiva is supplied by the ophthalmic division of the fifth cranial nerve. Sensory neurons from the conjunctiva are the terminals of branches of the lacrimal nerve, the frontal nerve (supratrochlear and infraorbital divisions) and the nasociliary nerve (infratrochlear division). These nerves also constitute a majority of the innervation of the eyelid[36]. Some of the neurons in the conjunctiva can also be traced to

nerves that branch off the second division of the trigeminal nerve, specifically the infraorbital nerve[2]. Finally, the rest of the neurons in the conjunctiva, especially towards the limbus, are by autonomic and sensory bundles from the ciliary nerve. Most of these bundles end up as free unmyelinated nerve endings in the conjunctiva and together they form the sub-epithelial plexus which can be found more anteriorly in the substantia propria of the conjunctiva. The nerves from the sub-epithelial plexus eventually terminate on the blood vessels in the conjunctiva, on epithelial cells or end up as sensory receptors[36].

## **1.10 Pain**

The International Association for the Study of Pain has defined pain as, “an unpleasant sensory and emotional experience associated with actual or potential tissue damage, or described in terms of such damage”[95]. The word “pain” has also been used to describe the experiences associated with discomfort and other unpleasant feelings. Williams and Craig[96] have recently worked on an updated definition of pain to be, “a distressing experience associated with actual or potential tissue damage with sensory, emotional, cognitive, and social components.” Whichever definition one may be inclined to use, it is clear that pain is subjective and has an affective dimension as well as elements of bodily sensation[96].

### **1.10.1 History of Pain**

Ideas about pain have been in existence for centuries. However, towards the end of the nineteenth century there were three dominant, yet opposing, views of pain. One of the views, which had its origins from ancient philosophy, implied that pain was an emotion[97].

Avicenna (AD 980 – 1037) proposed that pain was a specific sensation which has its own sensory processing organs[98]. The third view about pain within that era was proposed by Erb (1874). He believed that pain was as a result of intense activation of afferent systems that serve other sensations. Psychologists and some physicians followed this theory[99]. In the 1900s, Sherrington suggested the existence of the nociceptor, free nerve endings of nerve fibers, activated by stimuli, capable of causing damage to the tissues[100]. Other suggestions about pain were discussed by Hardy, Wolff and Goodell[101], who proposed that pain consists of sensory components related to the stimulation of sensory nerve terminals and processing components embodying distress and emotional reactions. Beecher (1957), proposed a similar concept but used the terms “primary” and “secondary” pain components for the sensory and emotional representation of pain respectively. Tursky[102] introduced sensory (qualitative), intensity (quantitative), and reactive (agony, distress) components of pain. Melzack and Casey[103] suggested an interactive model and further described pain in terms of three hierarchical levels: a sensory-discriminative component (e.g., quality, intensity, location), a cognitive-evaluative component (e.g., thoughts due to the cause and significance of the pain), and a motivational–affective component (e.g., depression, anxiety)[103]. In summary, from the numerous ideas about pain, it is evident that pain consists of sensory, emotional, and cognitive dimensions that contribute to the transmission and modulation of painful stimuli.

Pain plays an important physiological role as it provides the body with a warning of potential or actual damage[104]. Pain can be divided into four major groups: nociceptive,

psychogenic, neuropathic, and idiopathic[105]. Nociceptive pain is usually as a consequence of injury and results from the activation of pain-sensing afferents of the sensory system by harmful stimuli. We are able to measure nociceptive pain through methods applied in sensory physiology[104, 105]. Psychogenic pain, also termed psychalgia, occurs when pain is mainly sustained by psychological influence which may include mental, behavioral or emotional factors[106]. Examples of psychogenic pain include some headache and back pain. Neuropathic pain occurs due to direct injury or disease of the CNS or the peripheral nerves[107]. The pain can sometimes be disproportionate to the degree of tissue damage. On occasion, neuropathic pain serves no protective function as it can occur without nociception[107]. Finally, idiopathic pain exists when there is no evidence as to the etiology of pain or lack of reasonable inferences about the supporting pathophysiology of pain[108]. It is not uncommon to have a mixture of nociceptive and neuropathic pain, a phenomenon which has been described as mixed pain[109].

### **1.10.2 Transmission of Pain**

Nociceptors are sensory receptors that are involved in the detection of noxious (harmful) stimuli. They transform the unpleasant stimuli into electrical signals, which are then conducted to the CNS. Nociceptors are the free nerve endings of primary afferent A-delta and C fibers. They are distributed throughout the body (skin, viscera, muscles joints, meninges) and can be stimulated by mechanical, thermal or chemical stimuli. An example of mechanical stimulation is pressure and an example of thermal stimulation is extreme

heat. Chemical stimuli, which may include inflammatory mediators such as bradykinin, serotonin, prostaglandins, cytokines, and H<sup>+</sup>, are released from damaged tissue and can stimulate nociceptors directly. They can also act to reduce the activation threshold of nociceptors so that the stimulation required to cause activation is less. This process is called primary sensitization[110].

There are four major processes involved in nociception: transduction, transmission, perception and modulation. Transduction begins when nociceptors of A-delta and C fibers of primary afferent neurons respond to noxious stimuli such as mechanical, chemical or thermal stimulation[111]. The noxious stimulation causes a release of chemical mediators from the affected cells. These mediators include, but are not limited to, prostaglandin, bradykinin, substance P, serotonin, histamine and potassium. The release of these mediators leads to the exchange of sodium and potassium ions (de-polarization and re-polarization) at the cellular membrane level and this results in an action potential and generation of a pain impulse[112]. Transduction can also occur directly through transducer channels. For example, heat acts directly on capsaicin channels to alter potassium ions and cyclic GMP. Other transducer channels that can cause an action potential that leads to a pain impulse include acid-sensing ion channels (contributes to chemical sensitivity) and the mechanically sensitive ion channel, Piezo2.

The general transmission of a pain impulse can be divided in three major stages, which begins with the transduction of pain impulses from the nociceptors to electrical signals and conduction of the electrical information along the A-delta and C nociceptor nerve fibers to

dorsal horn of the spinal cord. The nociceptor fibers terminate at the dorsal horn of the spinal cord where a synaptic cleft can be found between the fibers and the nociceptive dorsal horn neurons (NDHN)[111]. Excitatory neurotransmitters such as ATP, glutamate, bradykinin, nitric oxide, substance P and calcitonin gene related peptides (CGRP), are released to cause the transmission of the pain impulse across the synaptic cleft. The second stage involves the transmission of the pain impulse from the NDHN to the brain stem via two major ascending pathways, the spinothalamic pathway and the spinoparabrachial pathway. The final stage of pain transmission involves the impulse moving through the cortex, thalamus and higher levels of the brain[113].

### **1.10.3 Trigeminal Pathway**

The trigeminal pathway involves the transmission of noxious stimuli from the region of the face via the nerve fibers originating from the nerve cells in the maxillary and ophthalmic regions of the trigeminal ganglion, and cranial nuclei VII, IX, and X[104]. The nerve fibers enter the brainstem and travel towards the medulla, where they innervate a subdivision of the trigeminal nuclear complex. From the trigeminal nuclear complex, the nerve fibers ascend and enter the thalamus on the contra lateral side. From the thalamus, the trigeminal information is sent to the primary sensory cortex[104].

### **1.11 Psychophysical Techniques**

In 1860, Fechner[114] came up with the term “psychophysics” that describes the relationship between ‘stimulus’ in the physical dimension and ‘sensation’ in the psychological dimension. The development of psychophysics paved the way for the

identification of the relationship between the internal sensory events and perceptual responses to the external stimuli[115].

One of the basic functions of a sensory system is to identify and distinguish between energy changes within the environment. Thresholds are boundary values in the stimulus continuum that indicate the existence of a stimulus or a difference in the stimulus response [115]. Thresholds can be divided into: 1) Absolute (or detection) threshold (RL) which indicates the presence of the stimulus and 2) Difference thresholds (DL) which refer to the change in the stimulus. Sensory threshold measurements play a crucial role in the valuation of any sensory system.

Absolute threshold is defined as the smallest amount of stimulus intensity needed to produce a sensation or the stimulus intensity required to detect that stimulus 50% of the time[116]. When a sensory threshold is reached, the stimulus needs to be increased or decreased by a certain amount to sense a change in the sensation produced by the stimulus. The amount of change in a stimulus ( $\Delta\phi$ ) required to produce a just noticeable (sensory) difference (JND) is called the difference threshold[116]. A larger change ( $\Delta\phi$ ) is needed to identify changes in greater intensity stimuli than that of lower stimuli intensities. According to Weber's law[116], "the increase or decrease in the intensity of the stimuli that is just noticeably different ( $\Delta\phi$ ) is always a constant fraction ( $c$ ) of the starting intensity of the stimulus ( $\phi$ )". Weber's law holds for a range of the intensities. However, Weber's fraction tends to be high at lower stimulus intensities, possibly because of the noise in the sensory system or the stimulus.

Thresholds vary with time due to external and internal sources[117]. Hence, several measurements of the threshold value are typically averaged to estimate the sensory threshold. External sources of variation can be due to the random fluctuations in the stimulus itself or the environment/experimental settings in which the test is conducted. Internally, noise in the neurological system can be one of the contributors to the variations, along with other factors like psychological biases and attention[116].

## **1.12 Classical methods of psychophysical measurement**

### **1.12.1 Method of Adjustments**

The method of adjustments is a simple and fast way to identify absolute and difference thresholds. In this procedure the participant alters the stimulus intensity until it is just perceived or until it becomes just imperceptible (ascending and descending absolute thresholds, respectively) or appears to be just noticeably different from some other standard stimulus (when performing difference threshold measurements)[117]. The intensity of the stimulus at this point is the subject's threshold. Ideally, the two kinds of measurement, that is, the trials in which the stimulus intensity is decreased (descending trials) and the trials of increasing stimulus intensity (ascending trials), are swapped several times and the results are averaged to attain the threshold estimate[118].

### **1.12.2 Method of Limits**

In comparison to some of the classical methods of psychophysical measurements, the method of limits is less time consuming[119]. When performing the method of limits, stimuli well above or below the threshold are presented and their intensities are

successively changed in small, equal amounts until the boundary of sensation is obtained. [119]. The stimuli are typically presented numerous times in a descending or ascending manner. The initial stimulus intensity is well above threshold when using the descending series trial, the intensity is then decreased in equal interval steps until it can no longer be perceived. For an ascending series trial, the initial stimulus intensity is below threshold and the intensity is increased until the presence of the sensation is communicated by the observer. The series comes to an end when the transition point in sensation is obtained. Ascending and descending series most likely yield slight but systematic variances in thresholds[119], thus the two types of series are often applied in alternation and the results are averaged to attain the threshold estimate.

When it comes to determining the difference threshold using the method of limits, a standard and comparison stimulus is presented concurrently or sequentially. While the intensity of the standard stimulus is kept the same, the intensity of the comparison stimulus is altered in small steps. The comparison stimulus is either initially less (ascending series) or initially greater (descending series) in magnitude than the standard. A series ends when the subject's response switches from "lesser" to "greater" or vice versa. The difference threshold is then the intensity difference between the stimuli of the first trial on which the response differs from the previous one[119].

Two types of errors that can be encountered when using the method of limit are error of expectation and error of habituation[119]. The error of expectation happens when the observer anticipates the arrival of the stimulus and reports the change in sensation before

it occurs. When the error of expectation occurs in ascending trials, the thresholds are falsely low, and vice versa in descending trials. The error of habituation happens when the observer develops an inclination to repeat the same response even after the threshold point has been reached. In ascending trials, the error of habituation falsely increases the thresholds and vice versa in descending trials.

### **1.12.3 Method of constant stimuli**

The method of constant stimuli is a procedure whereby the experimenter selects about four to nine stimulus values which, on the basis of an earlier exploration (perhaps by using the method of limits or adjustment), are expected to contain the threshold value. This fixed set of stimuli is delivered multiple times in a random order that guarantees each stimulus will occur as many times as the other stimuli in the set[119]. Once the stimulus has been delivered, the subject then replies as to whether the stimulus was perceived (in the case of the absolute threshold) or whether the intensity was higher or lower than that of a standard (in the case of the difference threshold). Once each stimulus intensity has been presented several times (about 20 times), the proportion of “detected” and “not detected” responses is calculated for each stimulus level. The data are then plotted with stimulus intensity along the x-axis and proportion of perceived stimuli along the y-axis. The result is a graph that is referred to as a psychometric function. A chief shortcoming is that it is quite time-consuming because many trials are required[116].

### **1.13 Devices for the measurement of ocular surface**

In 1894 Von Frey carried out some of the earliest experiments on corneal sensitivity using varying lengths of horse hair waxed to a glass rod[120]. Boberg Ans[121] and Cochet-Bonnet[122] updated Von Frey's device by using nylon monofilament to replace the horse hair for corneal sensitivity measurements.

#### **1.13.1 The Cochet-Bonnet esthesiometer**

The Cochet-Bonnet esthesiometer is made up of a nylon thread attached to a probe that is either handheld or mounted on an apparatus[122]. During the test procedure, the nylon thread is touched to the cornea, perpendicularly. The subject then reports he/she felt the thread. The corneal threshold is defined by the amount of mechanical force caused by the thread against the cornea, which is inferred from the bending of the thread.

A few studies[63, 123-126]have identified disadvantages associated with using the Cochet-Bonnet esthesiometer. The Cochet-Bonnet esthesiometer has a truncated stimulus intensity range[126], and most of the stimuli are suprathreshold. Corneal sensitivity measurements can be influenced by environmental conditions, such as humidity, and age of the thread[127, 128]. Finally, patient apprehension causes a false increase of sensitivity[63, 128].

#### **1.13.2 Pneumatic esthesiometers**

Pneumatic esthesiometers[48, 63, 129, 130] were developed after the Cochet-Bonnet type providing a greater range of stimulus intensities. The Belmonte esthesiometer and the modified Waterloo Belmonte esthesiometer are described below.

The Belmonte esthesiometer[48] has two medical grade gas cylinders, one containing compressed air and the other containing 98.5% CO<sub>2</sub>. The cylinders are connected through regulators to a directional control valve that electronically controls the flow of air and CO<sub>2</sub> separately. This allows for the accurate control of the CO<sub>2</sub> proportion of the output gas mixture and air. The resultant flow of air is measured by a flowmeter and transferred to a probe mounted on a modified slit lamp. The probe contains a temperature-controlling apparatus that warms or cools the gas as well as a solenoid valve that directs the output of gas.

During stimulation, a pulse generator directs the gas mixture to the tip of the probe by changing the direction of flow from the electronic valve towards the ocular surface. This produces a short pulse of gas with defined temperature, CO<sub>2</sub> concentration, and flow rate for a period of 1-10 seconds. In the absence of stimulation, the gas flowing through the valve is diverted back to the probe and enters a CO<sub>2</sub> meter that monitors the concentration of the gas mixture.

The Waterloo Belmonte esthesiometer[130] is a Belmonte esthesiometer modified at the University of Waterloo that utilizes computer-controlled combinations of air, CO<sub>2</sub> flow and temperature. In addition, there is custom software used to define & control the psychophysical method and stimulus attributes. A button box, used in recording subject responses, is attached to the esthesiometer. The distance between the probe and ocular surface, and its orthogonal alignment are constantly monitored using a calibrated video

camera. In addition to this, there are two cameras attached to the esthesiometer that are used to record the pupils during some of the experiments.

### **1.13.3 Comparison of Cochet-Bonnet and pneumatic esthesiometers**

Corneal sensitivity measurements using the Cochet-Bonnet esthesiometer most likely activates the  $A\delta$  mechanosensory nociceptors because the device's nylon thread provides mechanical force on the cornea[43]. Pneumatic esthesiometers on the other hand have the ability to activate mechanosensory, polymodal and cold receptors because of their ability to deliver mechanical, chemical and thermal stimulation[43]. The probe does not come into contact with the surface of the eye so patient apprehension and damage to the corneal epithelium can potentially be avoided. Also, pneumatic esthesiometers provide greater repeatability of measurements, and more control of stimulus characteristics than the Cochet-Bonnet esthesiometers[123, 129, 131]. With the Cochet-Bonnet esthesiometer, corneal threshold is measured in terms of pressure (millibars) while for the pneumatic esthesiometer the threshold is measured in terms of flow rate (ml/min)[123, 126].

### **1.14 Psychophysical scaling**

Psychophysical scaling is the process of quantifying mental events, especially sensation and perception, and determining the relationship between quantitative measures of mental events and quantitative measures of physical stimuli[132]. Both absolute and differential thresholds are concerned with the physical dimension of a stimulus as such, possess no information about the resulting sensation evoked by the stimulus. Psychophysical scaling is important because it provides a relationship between the input and output of a sensory

system in a quantitative way[133]. The intensity of a stimulus and its resulting sensation do not always stand in a one-to-one relationship and, as such, the changes in stimulus intensity and the corresponding changes in sensation must be empirically studied.

Plotting the magnitudes of a sensory attribute against the corresponding physical values of the stimulus results in a psychophysical relationship called the psychophysical magnitude function. A psychophysical magnitude function is unique to each sensory modality and stimulus condition, and can help understand the operation of the sensory system.

There are three major types of psychophysical scaling techniques: bisection scaling, discrimination, and magnitude estimation techniques[132]. In bisection scaling (also known as equisection scaling) subjects adjust stimuli to partition a sensory continuum into equal intervals. In discrimination scaling, subjects make ordinal discrimination judgments of stimuli. When using the magnitude estimation technique, subjects make direct numerical estimations of the sensation magnitudes produced by different stimuli and adjust stimuli to match numbers presented by the experimenter.

#### **1.14.1 Stevens Power Law**

In 1957, Stevens[134] proposed that the relationship between sensation magnitude and stimulus intensity was a power function, which became known as the Power law that is stated as:

$$\Psi = k (\Phi)^b$$

$\Psi$  is the sensation magnitude,  $\Phi$  is the stimulus intensity,  $k$  is an arbitrary constant determining the scale unit and  $b$  is the power exponent that depends on the stimulus

conditions and sensory modality. The value of the exponent partly determines the shape of the function where  $\Psi$  is plotted against  $\Phi$ . The relationship is negatively accelerated when less than 1.00 and positively accelerated when the exponent is greater than 1.00.

### **1.15 Suprathreshold scaling on the ocular surface**

The Cochet-Bonnet esthesiometer was the initial device used for psychophysical scaling of ocular surface thresholds. The method of magnitude estimation with a free modulus was used to determine corneal thresholds. A power function with an exponent of 1.01 was postulated to represent the relationship between the apparent magnitude of corneal threshold and the pressure applied on the cornea[135]. The researchers further predicted the exponents to represent a lower bound because of the tendency for magnitude estimation to underestimate the value of the exponent[136].

A few years later, the introduction of non-contact pneumatic esthesiometers paved the way for less harmful approach to psychophysical scaling of the ocular surface[48, 91, 137, 138]. Carlos Belmonte et al,[48] showed the exponential intensity-response curves for mechanical and chemical stimuli to be 0.58 and 0.63, respectively. Feng and Simpson[137] reported the corneal transducer function for mechanical stimuli to be 0.82 and that of chemical stimuli to 1.08. Chen et al[62] found the relationship between the magnitude of pain and CO<sub>2</sub> concentration to be a power function with an adjusted exponent of 1.12. Situ and Simpson[138] carried out sensory transduction experiments in the central and peripheral corneal locations and reported exponents of 1.38 and 1.19, respectively for mechanical stimuli, and 0.97 and 0.96, respectively for chemical stimuli.

## 1.16 Colour Science

Colour can be described by its 3 main properties: hue, saturation and luminance[139, 140]. Hue is what we refer to as the colour itself. Examples of hues are red, yellow, and blue. Saturation is the quantity of white in a colour[139]. When there is a large amount of white present in a colour, the colour tends to be pastel-like and less saturated. When there is zero white in a colour it is said to be saturated. To explain saturation, take the colour periwinkle, which is a mixture of blue and white. Thus, periwinkle and blue have the same hue, but different levels of saturation. The third component is luminance, which is the measure of intensity of a colour[140].

There are different colour systems and many of them have been utilized to measure the hue, saturation and luminance of colour[139, 141]. The CIE system (The Commission Internationale de L'Éclairage)[141] is for colour specification that was developed so that the visible spectrum could be expressed in a quantitative way[141]. The CIE system may be represented by a chromaticity diagram and is based on the spectral power distribution parameters (SPD)[139-141]. SPD refer to the classification of the power of light at specific wavelengths as viewed by the eye[140].

Spectroradiometers are used to measure the SPD of any colour and information about the saturation and luminance of that specific colour can be acquired[140]. For some experiments in my research, the CIE L' u' v' colour space diagram was the colour system of choice and the variable u' was used to denote and quantify ocular redness in a similar way in which it was utilized in previous experiments[142-146].

## **Chapter 2**

### **Rationale**

#### **2.1 Introduction**

The literature review in the previous chapter identifies the ocular surface as one of the most densely innervated superficial tissues of the human body, supplied extensively by parasympathetic, sympathetic and sensory nerve fibres. Sensory neurons and their response to thermal, chemical and mechanical stimuli were also discussed; however, I was unable to discuss research into the functional response of the autonomic nervous system (ANS) to ocular surface stimulation because research into this has not been performed.

The ANS is cardinal to human functioning as it acts below the level of consciousness to regulate the organs of the body thus controlling secretory cells, smooth muscle and cardiac muscle [1]. With respect to the eye, the ANS is responsible for the control of pupillary reflexes, accommodation and regulation of blood flow[2-4]. Monitoring the impact of sensory stimulation of the ocular surface on these mechanisms provides novel information about ANS functionality in healthy individuals and, as such, the primary objective of this research was to determine the response of the ANS to ocular surface stimulation by measuring pupil size, ocular vascular variations and changes in the accommodative state of the eye after the delivery of noxious and innocuous stimuli.

#### **2.2 Experiments on the conjunctival blood flow response**

The conjunctiva is an integral component of the ocular surface and has an extensive blood supply[5]. The blood vessels in the bulbar conjunctiva are a terminal vascular bed of the human internal carotid artery, which in turn is the main blood supply of the cerebral

cortex[6]. Information derived from the response of conjunctival blood vessels to local painful stimulation may be applicable to other parts of the body[7, 8]; however, there is no previous research on the response of conjunctival vasculature to ocular surface stimulation. In my first set of experiments (Chapter 3) I sought to evaluate the conjunctival redness response to noxious ocular surface stimulation. Under controlled settings, I delivered mechanical and chemical suprathreshold stimuli to the cornea. For each suprathreshold stimulus delivered, a spectrophotometer (Spectrascan650; Photoresearch Inc, Chatsworth, VA) was used to measure the ipsilateral and contralateral conjunctival chromaticity, an estimate of conjunctival redness, before and after delivery of the ocular surface stimulus. The change in redness represented the conjunctival vascular response to noxious stimuli.

### **2.3 Experiments on the pupillary response**

The size of our pupils can provide information regarding psychological states such as attention[9] and can also provide information regarding emotional changes[10]. Theoretically, pain or feelings of discomfort (such as those that are evoked by suprathreshold stimulation of the cornea) have an effect on the ANS due to the connection between sensory and autonomic neurons found in the neural circuitry of the ocular surface[11, 12], but this theoretical observation has never been examined empirically in humans.

In the second set of experiments (Chapter 4) I sought to evaluate the pupillary response to noxious ocular surface stimulation. Under controlled settings, I delivered mechanical and chemical suprathreshold stimuli to the cornea. For each suprathreshold stimulus, ipsilateral

and contralateral pupil sizes were each captured by two modified digital cameras (Logitech c920; Logitech International S.A., Newark, CA). The changes in pupil diameter from before to after stimulus delivery represented the pupillary response to ocular surface discomfort.

## **2.4 Experiments on the Accommodative Reflex**

Accommodation, the eye's ability to focus and maintain clear vision at near, is an important reflex mechanism driven by complex autonomic neuro-circuitry[13]. The previous chapter discussed the interconnectivity between the neural pathways that are responsible for both accommodation and ocular surface nociception yet, there are no studies examining how the accommodative system responds to ocular surface noxious stimuli.

In my final set of experiments (Chapters 5), I evaluated the accommodative response to noxious ocular surface stimulation and the relationship between pupil size and accommodative response to corneal stimulation. I delivered mechanical and chemical suprathreshold stimuli to the cornea, under controlled room temperature, illumination and humidity. For each suprathreshold stimulus delivered, a photorefractor (Power Refractor, Multichannel Co, Reutlingen, Germany) was used to measure the accommodative response in the left and right eyes before and after delivery of the ocular surface stimulus. The change in accommodation represented the accommodative response to noxious ocular surface stimulation.

## **2.5 Summary**

Collectively, the set of experiments enable us, for the first time, to begin to characterise the local stimulus-response neural circuitry by characterising the dose-effect relationships between ocular surface stimulation and autonomic responses. This in and of itself is important, and sets the foundation for the development of clinical methods and laboratory tools to better understand how these mechanisms are disrupted in neurodegenerative conditions, such as Parkinson Disease. Finally, this understanding provides a framework to enable us to develop novel objective metrics of ocular surface pain, something very important in non-communicative patients and in infants.

## Chapter 3

### **Conjunctival redness response to corneal mechanical and chemical stimulation.**

#### **3.1 Introduction**

The mucous membrane that covers the inner surface of the eyelids and the outer surface of the ocular globe is known as the palpebral and bulbar conjunctiva, respectively. The bulbar conjunctiva represents some parts of systemic circulation as it is a terminal vascular bed of the human internal carotid artery, which in turn is the main blood supply of the cerebral cortex[1]. The conjunctiva is transparent, and because of this, blood flow can be studied in vivo and non-invasively as there is uncomplicated optical resolution, in comparison to, say, retinal vasculature[2]. Another factor that aids the use of the conjunctiva as a model to study microcirculation is the high contrast between the reddish blood vessels and the whitish sclera[3]. Our ability to view the blood vessels in the conjunctiva comes with some advantages.

The physiological attributes of bulbar conjunctival blood vessels are similar to that of blood vessels found within the tissue of other parts of the body, previous research indicates that there is no difference between the composition of the blood within the bulbar and that of capillaries in other parts of the body[4, 5]. It is thus possible to assume that information derived from the influence of ocular surface stimulation on conjunctival blood vessel dynamics may be applicable to the rest of the body[6, 7].

The bulbar conjunctiva has an extensive supply of blood vessels that give off a reddish hue due to the blood flowing in them. The amount of redness observed within the conjunctiva

is termed conjunctival redness[8]. A greater conjunctival redness value indicates an increase in the in the cross-sectional diameter of the blood vessels on the anterior portion of the eye which leads to an increase in the volume of blood in the bulbar conjunctival, anterior scleral and limbal vessels, otherwise known as conjunctival hyperemia[9]. Anatomically, conjunctival hyperemia can be classified into limbal, palpebral and bulbar. Initiators of conjunctival hyperemia include, but are not limited to, diurnal variations, chemicals, contact lens wear, fatigue, the presence of foreign bodies, hormonal levels, an unstable tear film, ocular discomfort/corneal pain and dry eye disease[10].

The conjunctival vasculature is innervated by both sympathetic and parasympathetic arms of the autonomic nervous system (ANS)[11]. Parasympathetic and sympathetic nerve fibres from the facial nerve have been shown to have nerve terminal endings in the conjunctival blood vessel walls[12]. The ANS is responsible for the regulation of blood flow (homeostasis) on the surface of the eye. This is important as the transportation of a variety of molecules including oxygen and white blood cells serve nutritional and immunologic functions respectively for the anterior eye[13] and, as such, major changes in ocular surface blood flow could have effects on these nutritional and immunologic functions.

Cells on the ocular surface, like other cells in the human body, generate by-products that they cannot retain due to inadequate storage and/or toxicity and blood flow is responsible for the disposal of these by-products. It is thus expected that an increase or decrease in conjunctival blood flow will influence these metabolic factors which will in turn impact the integrity and normal functioning of ocular surface components.

Stimulation of the human cornea by chemical, mechanical and thermal applications elicit sensations of irritation, pain and discomfort[14-16]. These sensations have been mentioned to cause changes in conjunctival blood flow[10]; however, their effect on the anterior eye's microcirculation has not been evaluated in a quantitative way. The purpose of this study was to characterize the ocular redness levels in healthy participants by investigating redness changes that occur with the application of suprathreshold corneal mechanical and chemical stimulation.

## **3.2 Materials and Methods**

### **3.2.1 Sample**

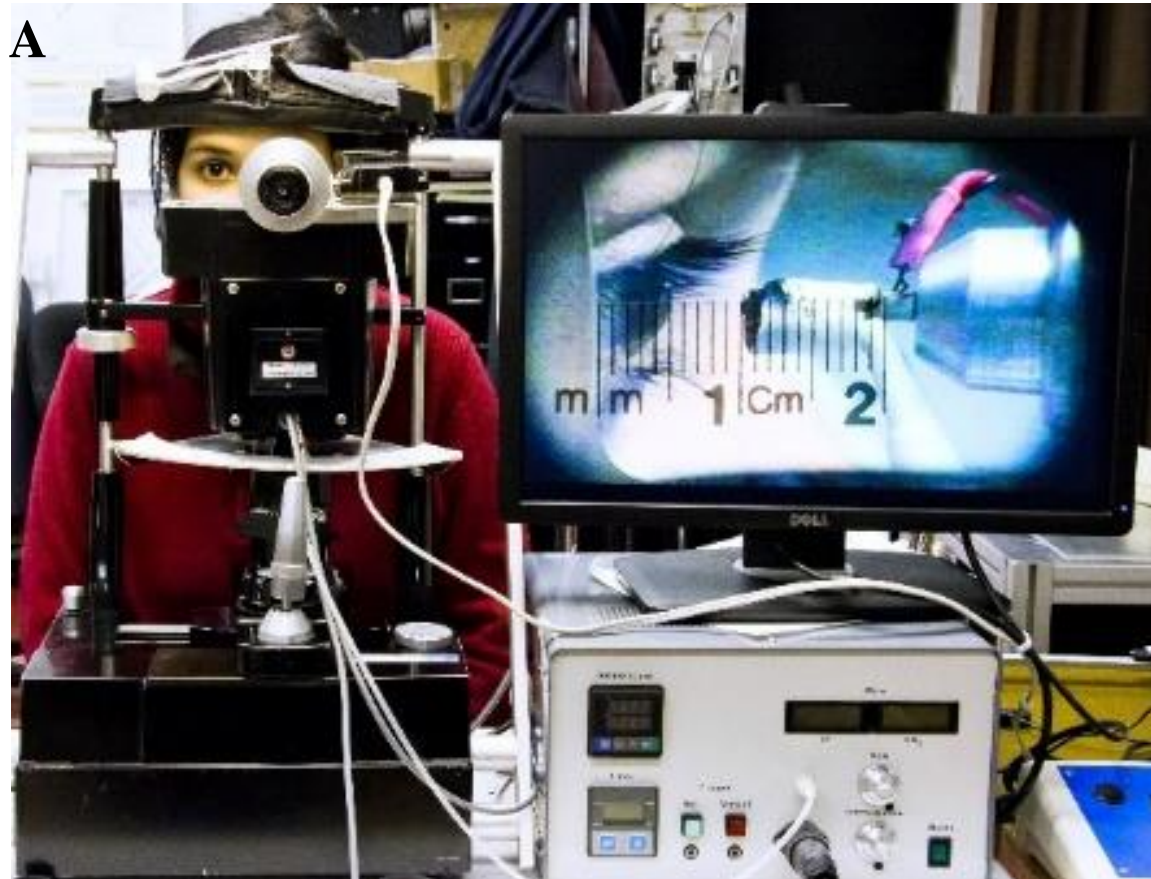
Ethics clearance was obtained from the Office of Research Ethics at the University of Waterloo before commencement of the study. Eligible subjects (healthy adults below the age of 36 with no ocular surface disorders) signed an informed consent document before enrolment in the study.

The eligibility of participants was determined at a screening appointment. The sample consisted of 15 healthy participants (7 males and 8 females) with an average age of 32.5 years (range 20-35 years). Subjects with any self-reported vascular disorders were excluded from the study.

### **3.2.2 Computer-controlled Belmonte Esthesiometer**

The device used for the delivery of mechanical and chemical stimuli to the ocular surface consists of a control box that electronically regulates the mixture of air and carbon dioxide (CO<sub>2</sub>). The flow rates of air and concentration of CO<sub>2</sub> are separately controlled by two

digital flow controllers. Within the nozzle assembly is a thermostat to control temperature. A calibrated video camera was used to ensure that the stimulus was orthogonal to, and the nozzle tip was 5mm from the ocular surface.



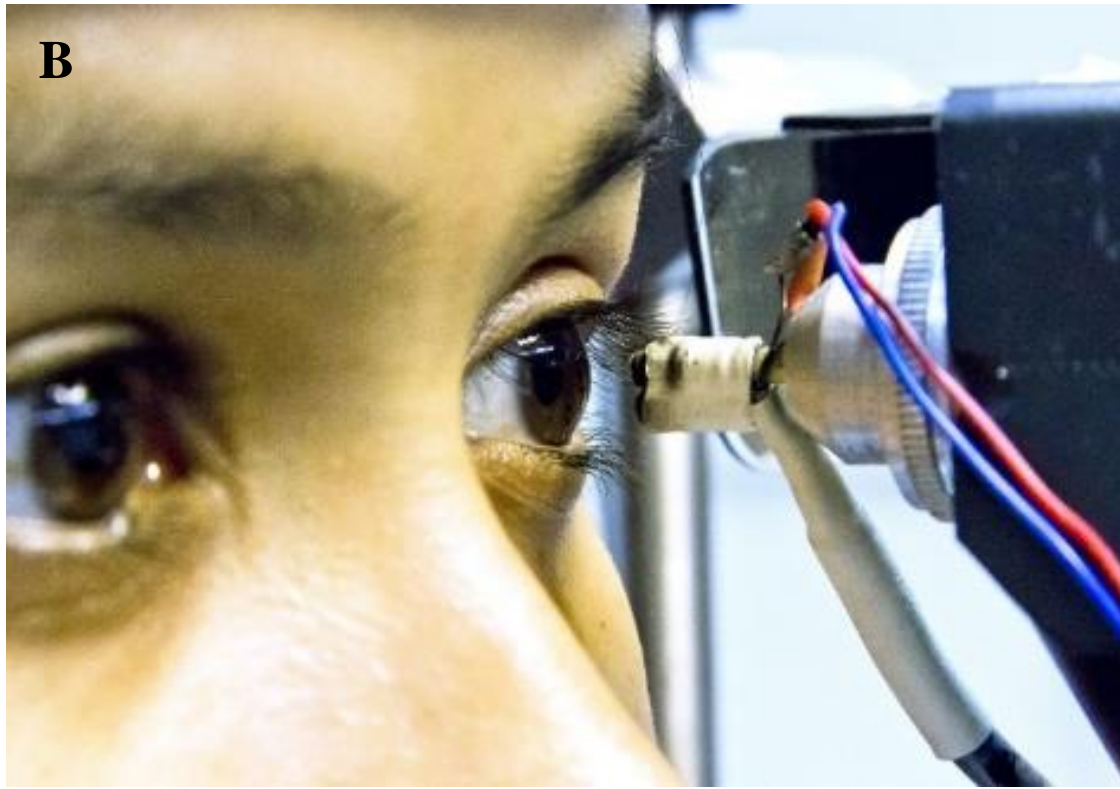


**Figure 1: Enface image of the computerized Belmonte esthesiometer and calibrated video display (A). Image displaying the nozzle of the computerized Belmonte esthesiometer used in stimulus delivery to the ocular surface (B).**

### **3.2.3 Nociceptive Stimuli**

Mechanical stimuli consisted of a series of air pulses with varying flow rates from 0 to 200 ml/min and chemical stimulation was delivered by increasing the concentration of CO<sub>2</sub> in the air. An ascending methods of limits[17] was used to determine mechanical and chemical detection thresholds of the cornea. Attributes of psychophysical methods were based on previous methods in the lab [14].

The mechanical threshold, which is the lowest air flow rate (with CO<sub>2</sub> set at 0%) that the subject could detect, was first determined. The flow-rate steps were set at 10 mL/min, and the mechanical threshold was the average of three readings when the subject first reported the stimulus. For determining the chemical threshold, the flow rate of air was set at half the initially determined mechanical threshold, and CO<sub>2</sub> was added to the air in increments of 5% CO<sub>2</sub>. The chemical threshold was the average of three first reports of stimulus detection.

### **3.2.4 Stimulus Delivery**

The stimulus was presented at the corneal apex of the left eye while subjects viewed a fixation target that was 3 meters away. With the help of the two Logitech cameras situated on each side of the esthesiometer, the experimenter positioned the tip of the esthesiometer so that it was approximately perpendicular to the corneal surface during stimulus delivery. The temperature of the air was set to 50°C, this decreased to 33.4°C at the ocular surface at room temperature of 23°C. This was calibrated using a custom electronic thermometer positioned 5 mm from the probe tip (which corresponds to the position of the ocular surface in the experiments). The duration of the stimulus was 3 seconds and it was delivered to the ocular surface immediately after a blink. The subject blinked freely between trials. The next stimulus was triggered after the sensation caused by the last stimulus had disappeared completely.

Once the mechanical and chemical thresholds were determined, a sham (0% threshold – no stimulus was delivered, the esthesiometer intensity setting was zero) and three stimuli were

then delivered to the subject in random order, in both the mechanical and chemical stimulation experiments – stimulus at 0% threshold (sham), stimulus at 100% threshold, stimulus at 150% threshold, and stimulus at 200% threshold. The conjunctival redness levels prior to stimulus delivery (baseline) and after stimulus delivery were compared.

### **3.2.5 Redness Measurements**

For the measurements of conjunctival redness, chromaticity ( $u'$ ) values were taken using the SpectraScan PR650 Spectrophotometer (Photoresearch Inc, Chatsworth, VA) immediately after stimulus delivery for three seconds. The PR650 measures luminance and chromaticity and calculates the equivalent CIE value. The photometer was mounted on a modified slit-lamp that also had an external illumination source, fixation targets, and a measuring tape attached to it. The measuring tape was used to monitor and ensure that a fixed distance was maintained between the photometer and the participant's eye during conjunctival redness measurements.

The nasal and temporal conjunctiva of the participants' right and left eyes were viewed with the slit lamp and a region of interest (ROI) was selected and used for all subsequent measurements. For the nasal conjunctiva of the right and left eye, the ROI was a  $5\text{mm}^2$  spot (corresponding to the area of the photometer's black circular target) that was horizontally displaced about 3mm away from the limbus, towards the direction of the nose. The ROI of the temporal conjunctiva was the same in size as that of the nasal conjunctiva; however, the location was 3mm away from the limbus, towards the outer canthus. An illustration of the ROI for the left eye can be seen in Figure 2.

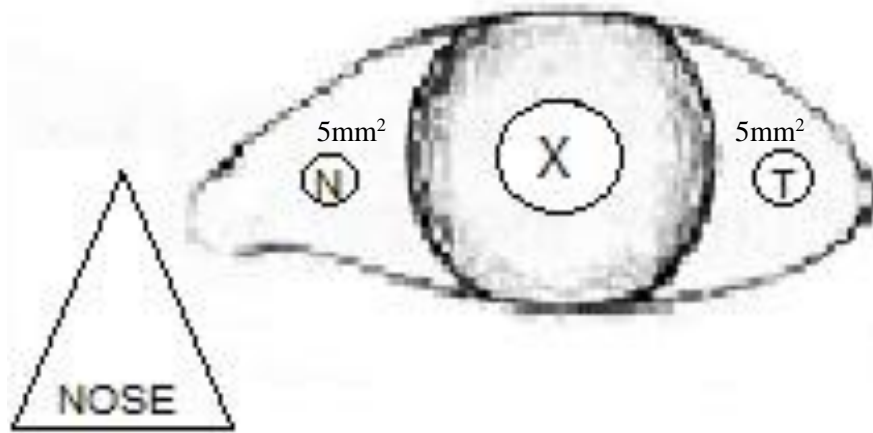


**Figure 2: Stimulus and ROI locations for the left eye. X represents the stimulus location, N represents the ROI for the nasal conjunctiva, and T represents the ROI for the temporal conjunctiva.**

The ROI measurements were taken in a random order under controlled illumination. The participant sat at the instrument and looked at a fixation target to their left or right (depending on the ROI being measured). Looking at the left target was for the temporal measurements of the right eye and the nasal measurements of the left eye, and vice versa. The chromaticity (CIEu') of a ROI was measured with the photometer. The examiner looked through the eye piece and positioned a black measuring spot (approximately 5 mm diameter) on the temporal/nasal bulbar conjunctiva on top of the ROI. Three measurements of redness were taken on both eyes and averaged. To ensure consistent results, no adjustments were made to the eye piece or the lateral position of the photometer.

### **3.2.6 Analyses**

Conjunctival redness differences between the stimulated and unstimulated eye was analyzed using dependent T-tests. Linear mixed effects analyses were used to investigate the relationship between conjunctival redness, and stimulus intensity. Quantitative differences in conjunctival redness, stimulus modality, and stimulus intensity were analyzed using repeated measures (RM) ANOVA. Tukey HSD tests were used for all post hoc analysis. SPSS for Windows, Version 16.0 (Chicago, SPSS Inc.) was used for data analysis procedures. A probability value of 0.05 or less was assumed to be significant.

### **3.3 Results**

Measurements of conjunctival redness at baseline (before each measurement session), 0% threshold (the catch trials when the esthesiometer intensity setting was zero) and with mechanical and chemical stimulation of differing intensities stratified by modality are shown in Figure 3.

#### **3.3.1 Effects of Stimulus Intensity on Conjunctival Redness**

On average, redness increased from baseline as the corneal apical stimulus intensity increased. This happened regardless of whether mechanical or chemical stimulation occurred (ANOVA  $F(4,476) = 194.7, p < 0.05$ ). At 200% threshold, conjunctival redness was greater than all stimulus intensities (Tukey HSD, all  $p < 0.05$ ).

Baseline conjunctival redness values for the chemical and mechanical stimulation experiments were not different (ANOVA  $F(118) = 0.8, p > 0.05$ ) and at 0% threshold there was no difference in redness for the chemical and mechanical stimulation experiments (ANOVA  $F(118) = 0.8, p > 0.05$ )

### **3.3.2 Effects of Stimulus Modality and Stimulus Intensity on Conjunctival Redness**

There was a difference between chemical and mechanical stimulation based on stimulus intensity (ANOVA  $F(4,472) = 61.1, p < 0.05$ ). Chemical stimulation produced greater conjunctival redness than mechanical stimulation at 100% threshold, 150% threshold, and 200% threshold (all Tukey HSD  $p < 0.05$ ).

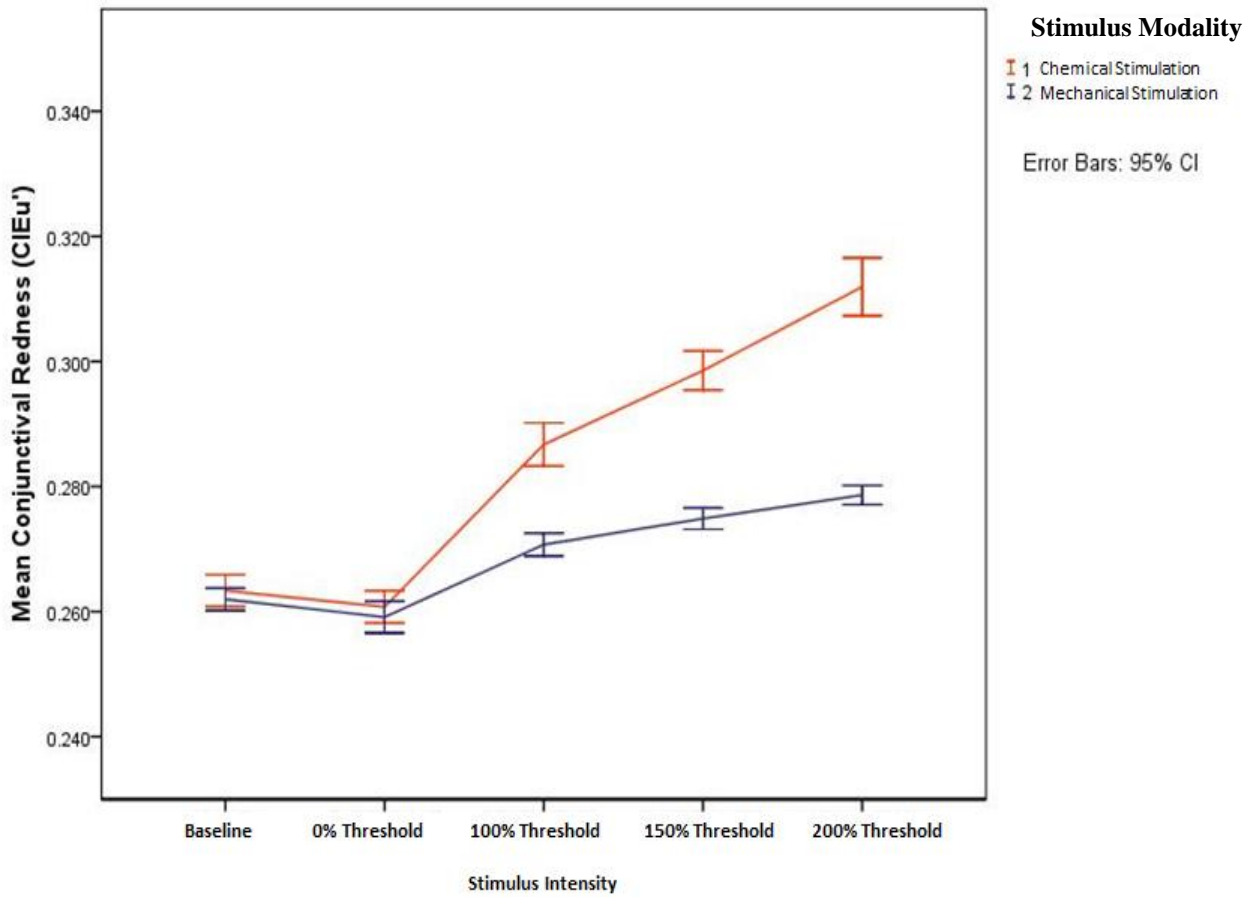


**Figure 3: Mean conjunctival redness across the different stimulus intensities for chemical (red) and mechanical (blue) corneal stimulation experiments (error bars denote 95% confidence interval).**

### 3.3.3 Relationship Between Stimulated and Unstimulated Eye

With mechanical stimulation of the cornea, the ipsilateral eye (stimulated eye [left eye]) became redder than the contralateral (unstimulated) eye (dependent t-test  $t(29) = 34.7$   $p < 0.05$ ). A similar result occurred with chemical stimulation of the dependent t-test  $t(29) = 14.3$   $p < 0.05$ ).

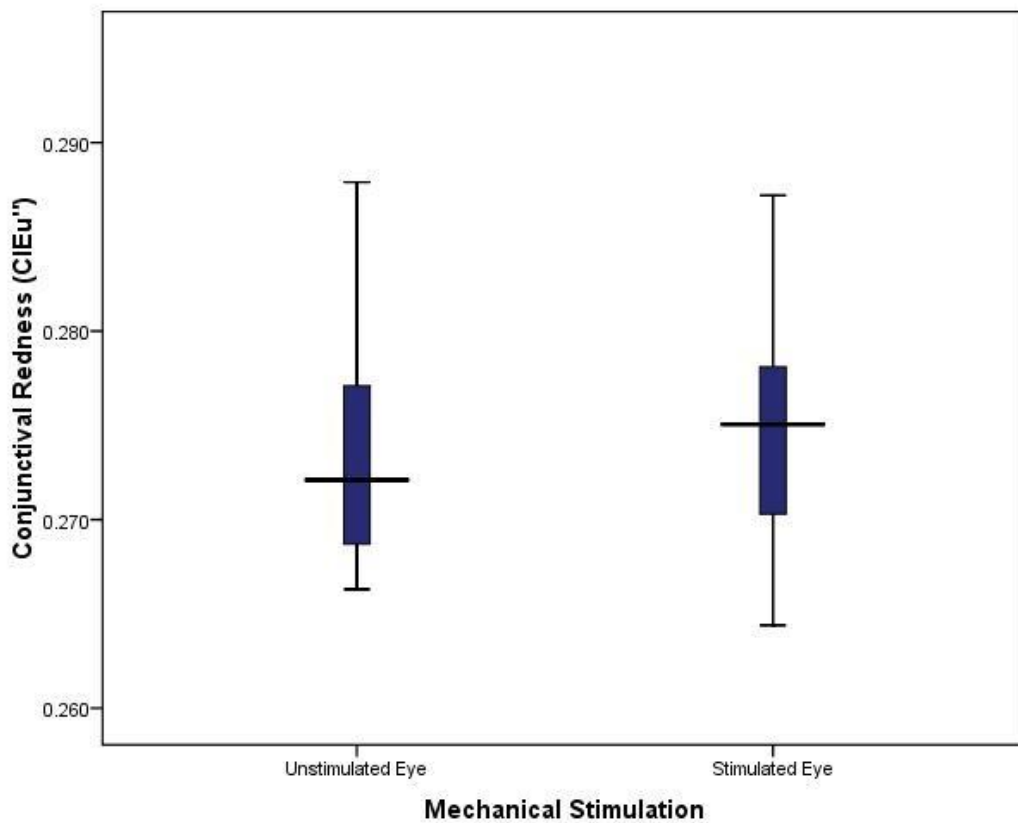


**Figure 4: Box-plot of the conjunctival redness between the stimulated and the unstimulated eye after 200% threshold corneal mechanical stimulation.**

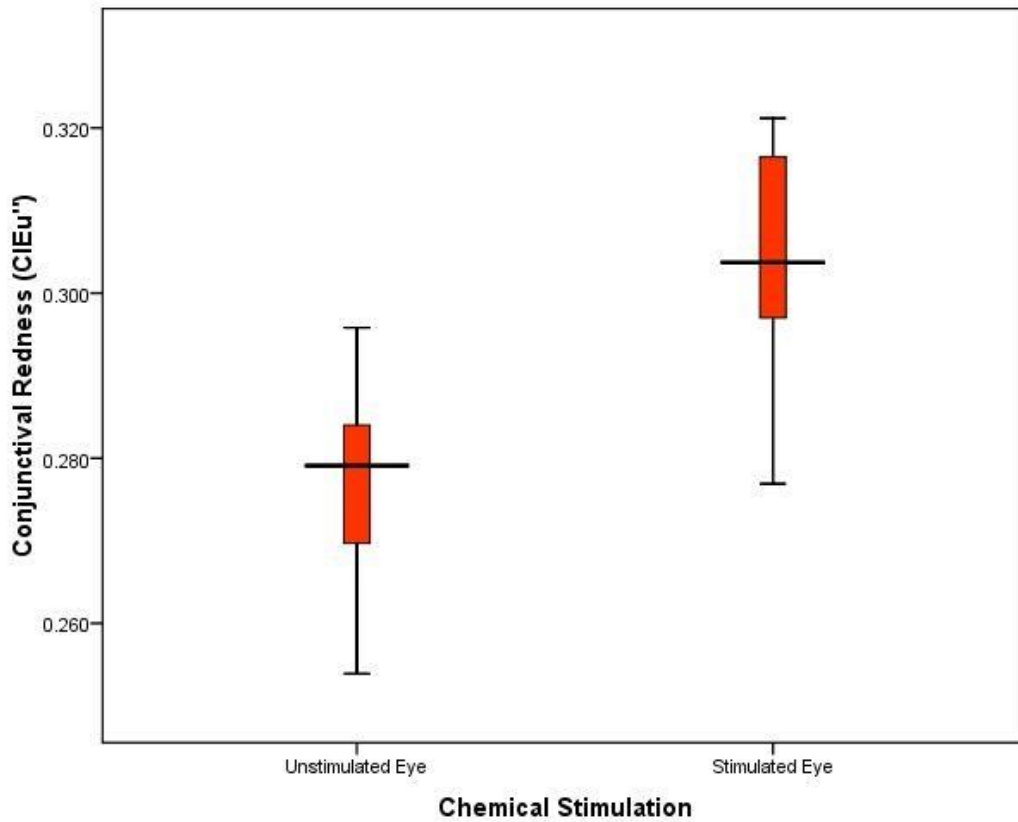


**Figure 5: Box-plot of the conjunctival redness between the stimulated and the unstimulated eye after 200% threshold corneal mechanical stimulation.**

### **3.3.4 Relationship Between Conjunctival Redness and Stimulus Intensity**

A linear mixed effects analysis was used to find the relationship between conjunctival redness and stimulus intensity. Stimulus intensity was entered as fixed effects in the model. As random effects, intercepts for participants as well as by-participant random slopes for the effect of stimulus intensity was entered. Below is a table summarizing the results of the model. The best model for both mechanical and chemical stimulation was one that incorporated random effects of the intercept and slope.

**Table 1: Results from a mixed model analysis displaying the relationship between conjunctival redness and stimulus intensity in mechanical corneal stimulation experiments (the slope estimates are referenced to the highest stimulus level).**

Parameter	Estimate for Mechanical	Significance
Intercept	0.279	0.001
Baseline	-0.018	0.001
Threshold	-0.008	0.001
150% Threshold	-0.004	0.046

**Table 2: Results from a mixed model analysis displaying the relationship between conjunctival redness and stimulus intensity in chemical corneal stimulation experiments (the slope estimates are referenced to the highest stimulus level).**

Parameter	Estimate for Chemical	Significance
Intercept	0.311	0.001
Baseline	-0.043	0.001
Threshold	-0.025	0.001
150 Threshold	-0.013	0.001

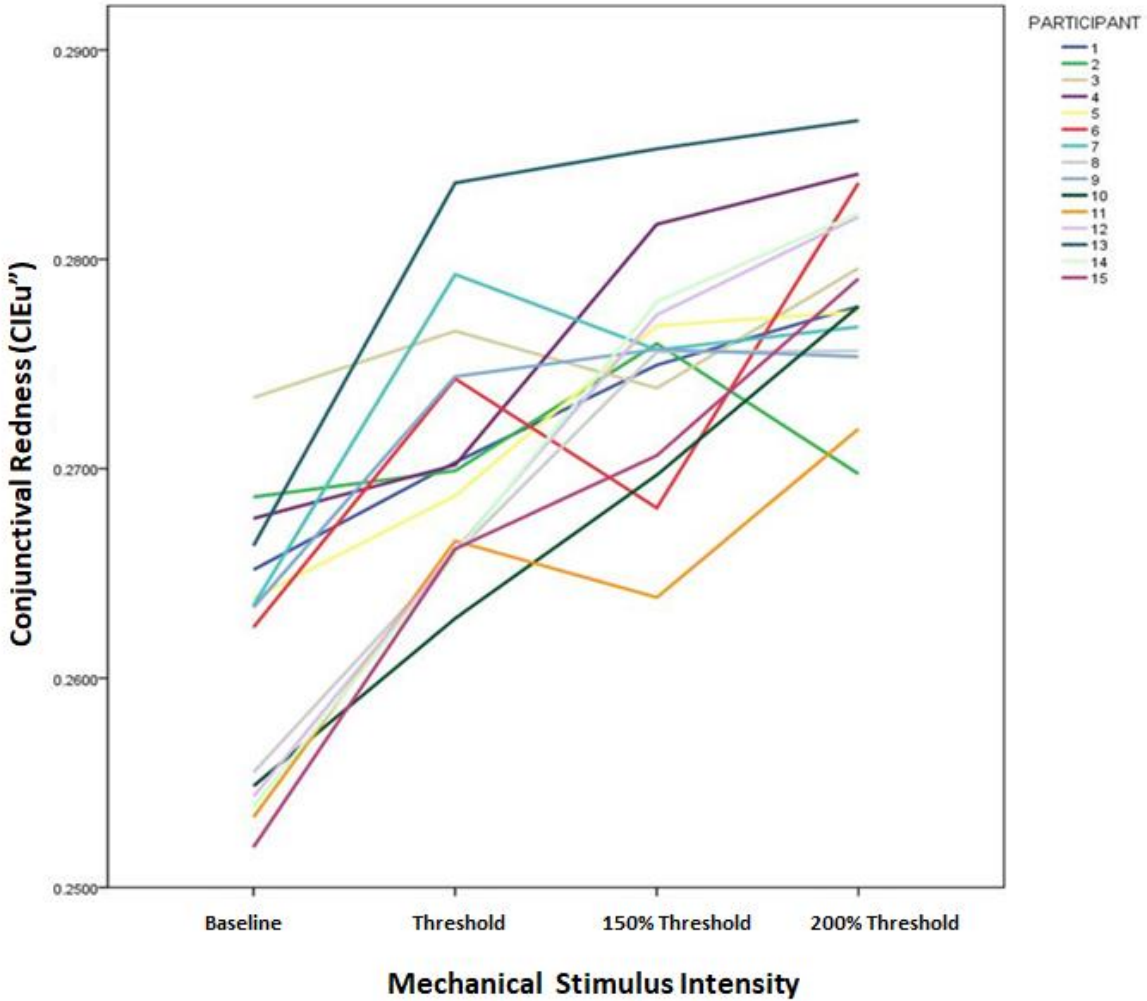


**Figure 6: The relationship between conjunctival redness and stimulus intensity during mechanical stimulation of the cornea. An average redness increase of 0.018 (CIEu') is expected from baseline to 200% threshold.**

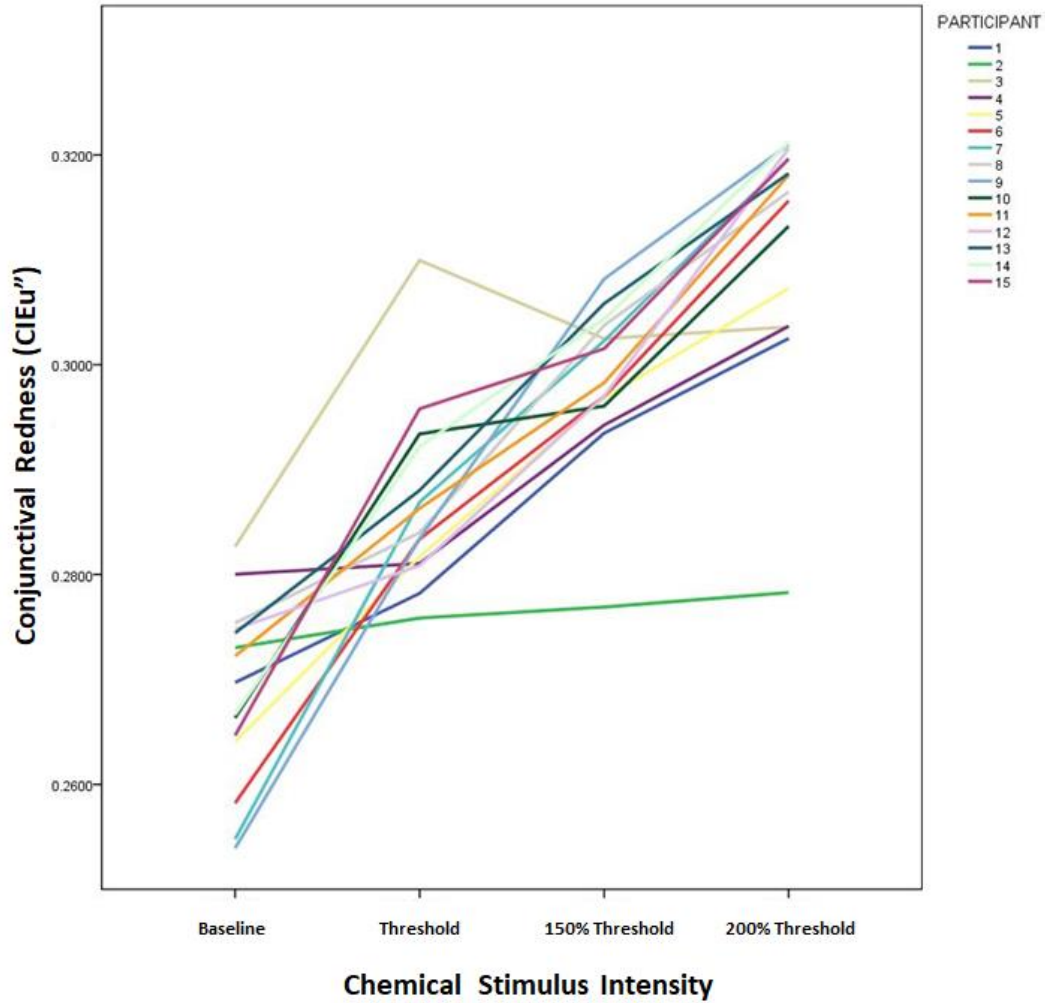


**Figure 7: The relationship between conjunctival redness and stimulus intensity during chemical stimulation of the cornea. An average redness increase of 0.043 (CIEu') is expected from baseline to 200% threshold.**

### **3.4 Discussion**

In this chapter, the effect of ocular surface stimulation on conjunctival blood flow was investigated. From the results of the study, mechanical and chemical suprathreshold stimulation of the cornea appear to produce an increase in conjunctival redness in a dose response-like manner. The stimulated (ipsilateral) eye appeared redder than the unstimulated (contralateral) eye after the delivery of suprathreshold mechanical and chemical corneal stimulation, and chemical stimulation of the cornea seems to produce greater conjunctival redness than mechanical corneal stimulation.

When suprathreshold mechanical or chemical stimuli are delivered to the cornea, the observed response of increased conjunctival redness suggests an increase in blood flow and thus blood volume in the region of interest (ROI). Similar findings have been observed in cats[18] and rats[19, 20] where there seems to be an increase in blood flow in the lips and tooth pulp as a result of noxious stimulation. Noxious stimulation in the facial skin and tooth pulp of humans was reported to produce an increase in the blood flow of the stimulated region[21, 22].

The increase in blood flow as a result of suprathreshold corneal stimulation, observed in my experiment may be due to an axon reflex mechanism, a central neuronal reflex mechanism or both. In support of the suggestion that an axon reflex mechanism may be responsible for the observed conjunctival blood flow increase in this study, some experiments using Doppler flowmetry proposed that antidromic activation of nociceptive afferent fibres may lead to increased peripheral blood flow[23-25]. An axon reflex between

the two ocular surface regions (cornea and conjunctiva) may be responsible for the blood flow increase.

Some research studies provide evidence to support that a central neuronal reflex mechanism may contribute to increased peripheral blood flow[18, 26-28]. Drummond[27], showed that noxious stimulation of the ocular surface caused vasodilation within the forehead and further argued that a centrally mediated parasympathetic reflex might be responsible for the vasodilation because he applied a sympathetic blockade in his experiment. Experiments in humans[22, 26, 28], cats[29, 30] and monkeys[22] demonstrate a central parasympathetic reflex mechanism that causes an increase in peripheral blood flow and, as such, it is possible that a similar central neuronal mechanism may contribute to increased conjunctival blood flow during noxious stimulation of the cornea.

Previous research by Situ and Simpson[31] investigating the interaction between suprathreshold corneal stimulation and ocular reflexes, found comparable results to that of this study; the researchers discovered that mechanical and chemical corneal stimulation evoked increased reflex tear secretion. In addition, Situ and Simpson[31] identified mechanical corneal stimulation to be responsible for the greatest amount of reflex tearing; however, in this ocular reflex study I discovered contrasting results.

The results of this study show that chemical stimulation of the cornea appears to evoke a greater conjunctival redness response than mechanical corneal stimulation. Evidence from electrophysiological experiments on cats and rabbits indicates that the cornea is innervated by fast conducting  $A\delta$  and slower conducting C fibres[32, 33]. There is expression of

epithelium Na<sup>+</sup> channels (ENaC), acid-sensitive ion (ASICs) and vanilloid receptor -1 channels (VR1) in the trigeminal ganglion and while ENaC mediates sensitivity to mechanical stimulation, ASICs and VR1 are responsible for sensitivity to acid stimulation[34-37].

The greater ocular redness observed with chemical stimulation of the cornea can be supported by Feng and Simpson's[14] postulation that chemical stimuli may excite slower conducting C fibers while mechanical stimuli excite fast conducting A $\delta$  fibers. When a chemical stimulus (CO<sub>2</sub> mixed with air) is applied to the cornea, CO<sub>2</sub> mixes with the tears on the surface of the eye resulting in a more acidic tear film[38]. This acidic mixture has been shown to have effects similar to that produced by tissue acidosis, resulting in inflammation, or infection, and appear to stimulate corneal C fibers through the mediation of ASICs and VR1 receptors[35, 36]. Since CO<sub>2</sub> remains in the tears even after stimulus delivery, the longer exposure may contribute to the greater ocular redness experienced in my experiment. It is also possible that a distinct C-fibre pathway, with greater gain, induces a more robust redness response than the equivalently intense (relative to threshold) mechanical stimulation.

In this experiment, delivery of a noxious stimulus in one eye caused an increase in conjunctival redness in both eyes but more so in the stimulated eye. Similar to this finding, ipsilateral electrical stimulation of the supraorbital branch of the trigeminal nerve elicits a facial nerve (blinking) response bilaterally[39]. Experiments involving pupillary responses to noxious corneal stimulation performed Chapter 4 of this thesis had similar findings with a bilateral pupillary reflex to ipsilateral nociceptive stimulation.

Bilateral ocular reflex mechanisms could possibly be due to a bilateral ascending afferent pathway, which in turn activates bilateral efferent motor fibers. In some brain imaging studies[40, 41], acute muscular and cutaneous noxious stimulation produced bilateral activation of both the primary and secondary somatosensory cortex which enabled the researchers to discover bilateral ascending trigeminothalamic pathways. Similar bilateral ascending trigeminothalamic pathways that exist for orofacial reflexes to noxious stimulation[40, 41] could mediate the conjunctival redness reflex to noxious corneal stimulation found in this study.

A shortcoming of this experiment is that there was a limitation to the stimulus intensity range as the highest stimulus intensity used was twice the threshold. Being able to go beyond 200% threshold for both mechanical and chemical corneal stimulation would be beneficial as information regarding what happens to the conjunctival vasculature at higher stimulus intensities is unknown. Determining at what levels saturation occurs, and characterising the 'complete' dose-effect relationship would allow fuller understanding of how painful corneal stimuli induce bulbar vessel dilation. Temporal effects of noxious corneal stimulation on conjunctival vasculature were not investigated. It would also be of interest to investigate how the initiation and duration of the ocular surface vasculature response (ie., temporal aspects).

A valuable addition to this study could have been the use of a visual analogue scale (VAS) to measure the degree of irritation at different stimulus intensities thus enabling us to investigate the relationship between a subjective and objective response to ocular surface stimulation.

To summarise, this set of experiments provides some support that stimulation of the central cornea by noxious corneal stimulation in the form of mechanical and chemical stimuli evokes a dose dependent autonomic direct and consensual conjunctival redness response. This study forms a foundation from which the characterization of the local stimulus-response neural circuitry relating nociceptive stimuli to autonomic responses can be developed and assessed in healthy patients and those with neurodegenerative conditions.

### **3.5 Conclusion**

In conclusion, this set of experiments provide some evidence that stimulation of the central cornea by noxious stimulation in the form of mechanical and chemical stimuli, evokes a dose dependent autonomic ipsi- and contralateral conjunctival redness response. The conjunctival blood flow response to the stimulated eye seems greater than that of the unstimulated eye, and chemical stimulation of the corneal appears to evoke a greater conjunctival redness response than mechanical stimulation of the cornea. This study serves as a basis for the characterization of the local stimulus-response neural circuitry relating nociceptive ocular surface stimuli to autonomic responses.

## Chapter 4

### Pupil Response to Noxious Ocular Surface Stimulation

#### 4.1 Introduction

The International Association for the Study of Pain defined pain as, “an unpleasant sensory and emotional experience associated with actual or potential tissue damage, or described in terms of such damage”[1]. The word “pain” has also been used to describe the experiences associated with discomfort and other unpleasant feelings[2, 3]. Pain is subjective and by definition it is experienced only when an individual is in a conscious state, yet the perception and modulation of pain induces brain activity that is largely driven by autonomic processes that operate below the level on consciousness[4-6]. Previous reports have proposed that autonomic nervous system (ANS) responses have a strong relationship to pain perception and as such, may be possible alternatives for the measurement of pain[7, 8].

Within the eye, the ANS controls two antagonistic iris muscles, namely the sphincter and dilator pupillae to bring about pupil size changes. The sphincter pupillae is innervated by parasympathetic fibers and constricts the pupil, and conversely, the dilator pupillae is innervated by sympathetic fibers and dilates the pupil[9]. Accommodation, luminance, attention, and alertness (among others) cause fluctuations in pupil size[10-12]. The change in the size of the pupils can also be due to the effect of noxious stimulation and in various places this has been termed pupillary reflex dilation[13], pupil dilation response[14], phasic pupil dilation[14, 15], reflex pupillary dilation[16], and ciliospinal reflex[17]. The

relationship between pupil size changes and pain perception has been looked into quantitatively[14, 15, 18, 19]. Chapman *et al*[14] delivered intra-cutaneous noxious fingertip stimulation to 20 subjects at four different intensities and observed a pupillary dilation response. The pupillary dilation response began 0.3 s after delivery of the stimulus and peaked at 1.25s. The researchers concluded that there was a consistent pupillary dilation response to painful stimulation in a dose-response manner. Ellermeier and Westphal[20] utilized both psychophysiological and psychophysical techniques to study pupil size changes during the noxious stimulation of the fingers of healthy subjects. The results of their experiments showed that there was a pupillary dilation response to painful fingertip stimulation, and they suggested that pupil dilation was an autonomic indicator to pain. Due to the existence of pupillary dilation responses to noxious stimulation in the fingertips and earlobes[14, 15, 18, 19], it is possible that a similar pupil dilation response may exist for noxious stimulation of the ocular surface.

The pain experience for men and women appear to be different[21, 22]. Ellermeier and Westphal[20] suggested females had greater pupil dilation responses than males when tonic pressure was applied to the fingers of subjects, and in the same study, females reported greater pain than males while experiencing the same amounts of noxious stimulation.

Corneal sensitivity has been shown to vary with age[23-25], time of day[26], and menstruation[27, 28] (among other factors); however, there is limited research on the effect of gender on corneal sensitivity[25, 29]. Acosta *et al*[25] reported that in comparison to men of similar age, premenopausal women had lower thresholds to both mechanical and

chemical corneal stimulation but, there was no difference between the overall corneal sensitivity of males and females.

Corneal nociceptors receive their innervation from the trigeminal ganglion, via the nasociliary branch of the ophthalmic division of the trigeminal nerve[30, 31] and respond to chemical, mechanical and thermal stimulation[32-39]. There are no experiments relating pupil size changes to noxious stimulation of the eye and the neuro-circuitry relating corneal nociceptive stimuli to the autonomic pupil reflex is unknown. The purpose of this exploratory study was to determine whether a pupil response exists for nociceptive corneal mechanical and chemical stimuli, and if so, whether the pupil response is intensity specific. In addition, we were interested in exploring whether the stimulation modality, ipsi- and contralateral effects and whether there were differences in the response between sexes

## **4.2 Methods**

### **4.2.1 Subjects**

Ethics clearance was obtained from the Office of Research Ethics at the University of Waterloo before the study began. Eligible subjects signed an informed consent document before enrolment in the study.

15 healthy subjects participated in this study. There were 8 male and 7 female volunteers ranging in age from 19 to 34. Subjects taking analgesic, anti-inflammatory or psychoactive medications were excluded from the study.

#### **4.2.2 Computer-controlled Belmonte Esthesiometer**

The calibrated computer-controlled Belmonte esthesiometer has been described in different experiments[33, 37, 40]. Our modified device used for the delivery of mechanical and chemical stimuli to the ocular surface consists of a control box that electronically regulates the mixture of air and carbon dioxide (CO<sub>2</sub>). The flow rates of air and concentration of CO<sub>2</sub> are separately controlled by two digital flow controllers. Within the nozzle assembly is a thermostat to control temperature. A calibrated video camera was used to ensure that the stimulus was orthogonal to, and the nozzle tip was 5mm from the ocular surface.

#### **4.2.3 Nociceptive Stimuli**

Mechanical stimuli consisted of a series of air pulses with varying flow rates from 0 to 200 ml/min and chemical stimulation was delivered by increasing the concentration of CO<sub>2</sub> in the air. An ascending methods of limits[41] was used to determine mechanical and chemical detection thresholds of the cornea.

The mechanical threshold, which is the lowest air flow rate (with CO<sub>2</sub> set at 0%) that the subject could detect, was first determined. The flow-rate steps were set at 10 mL/min, and the mechanical threshold was the average of three readings when the subject first reported the stimulus. For determining the chemical threshold, the flow rate of air was set at half the initially determined mechanical threshold, and CO<sub>2</sub> was added to the air in increments of 5% CO<sub>2</sub>. The chemical threshold was the average of three first reports of stimulus detection.

#### **4.2.4 Stimulus Delivery**

The subjects wore in-ear headphones with noise playing in the background. The stimulus was presented at the corneal apex of the left eye while subjects viewed a fixation target that was 3 meters away. The tip of the esthesiometer was rotated to ensure the stimulus was delivered perpendicular to the corneal surface during stimulus delivery. The temperature of the air was set to 50°C, this decreased to 33.4°C at the ocular surface at room temperature of 23°C. This was calibrated using a custom electronic thermometer positioned 5 mm from the probe tip (which corresponds to the position of the ocular surface in the experiments) [33, 34]. The duration of the stimulus was 2 seconds and it was delivered to the ocular surface immediately after a blink. The subject blinked freely between trials. The next stimulus was triggered after the sensation caused by the last stimulus had disappeared completely.

Once the mechanical and chemical thresholds were determined, a sham (no stimulus was delivered but the participant thought a stimulus was being delivered) and three stimuli were then delivered to the subject in random order, in both the mechanical and chemical stimulation experiments – stimuli at 0%, threshold (sham), stimulus at 150% threshold, and stimulus at 200% threshold. The pupil size prior to stimulus delivery (baseline) and after stimulus delivery were compared.

#### **4.2.5 Data Processing and Pupil Size Measurements**

Imaging of the stimulated and unstimulated eye was performed using two modified and calibrated Logitech c920 digital cameras (Logitech c920; Logitech International S.A.,

Newark, CA), for 4 seconds before (pre-stimulus capture) and 4 seconds after the delivery of the stimulus (post-stimulus capture). Calibration of the Logitech camera was done with dummy pupils of known diameters[39]. The data were processed with a custom segmentation algorithm to help identify the pupils. We then measured the pupil diameter (average of horizontal and vertical measures) using ImageJ software (NIH, Bethesda, MD), in every 15<sup>th</sup> frame (which corresponded to every 500 milliseconds in the pre/post stimulus captures) For each capture period, the total pupil diameters were averaged to extract a mean pupil diameter for pre/post stimulus capture and this represented the pupil size measurements. This method was selected because of my aim to provide a measurement approach that was quick, simple, robust, efficient and representative of the response of the pupils to corneal stimulation in the 4 post stimulus seconds.

#### **4.2.6 Analyses**

Pupil dilation response differences between the ipsi- and contralateral eye was analyzed using dependent T-tests. Non-linear regressions were performed to explore the relationship between time and stimulus intensities across males and females. Quantitative differences in pupil diameter, stimulus modality, sex of subject and stimulus intensity on pupil diameter were analyzed using repeated measures ANOVA. Tukey HSD tests were used for all post hoc analysis. SPSS for Windows, Version 16.0 (Chicago, SPSS Inc.) and Microsoft Excel for Windows (Redmond, WA, Microsoft Corp.) were used for data analysis procedures. A probability value of 0.05 or less was assumed to be significant.

### **4.3 Results**

Pupil diameters at baseline (before each measurement session), 0% threshold (the catch trials when the esthesiometer intensity setting was zero) and with mechanical and chemical stimulation of differing intensities stratified by modality are shown in Figure 10.

#### **4.3.1 Effects of Stimulus Intensity on Pupil Diameter**

On average, pupil diameter increased from baseline as the corneal apical stimulus intensity increased. This happened regardless of whether mechanical or chemical stimulation occurred (ANOVA  $F(4,224) = 356.6, p < 0.05$ ). At 200% threshold, pupil diameter was greater than all stimulus intensities (Tukey HSD, all  $p < 0.05$ ).

#### **4.3.2 Effects of Stimulus Modality and Stimulus Intensity on Pupil Diameter**

There was no difference between chemical and mechanical stimulation based on stimulus intensity (ANOVA  $F(4,224) = 0.1, p > 0.05$ ).

#### **4.3.3 Relationship Between Ipsi- and Contralateral Eye**

With mechanical stimulation of the cornea, there was no difference in pupil responses between the ipsilateral eye (stimulated eye [left eye]) and the contralateral (unstimulated) eye (dependent t-test  $t(14) = 0.6, p > 0.05$ ). A similar result occurred with chemical stimulation of the cornea (dependent t-test  $t(14) = 0.8, p > 0.05$ ).

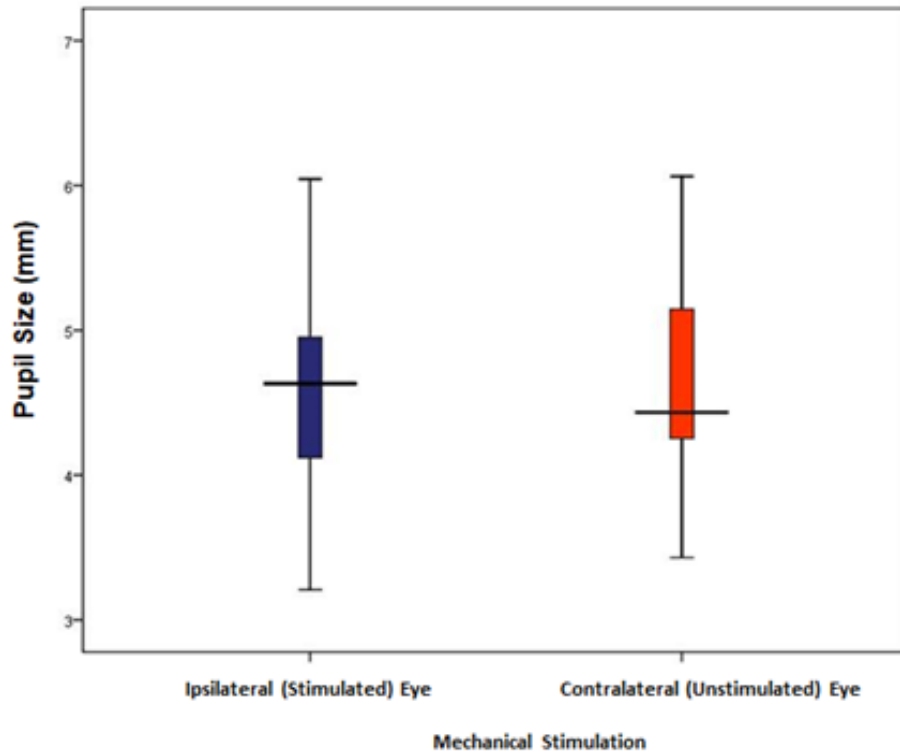


**Figure 8: Box-plot of pupil response between the ipsilateral (stimulated) and the contralateral (unstimulated) eye after corneal mechanical stimulation (error bars denote 95% confidence interval).**

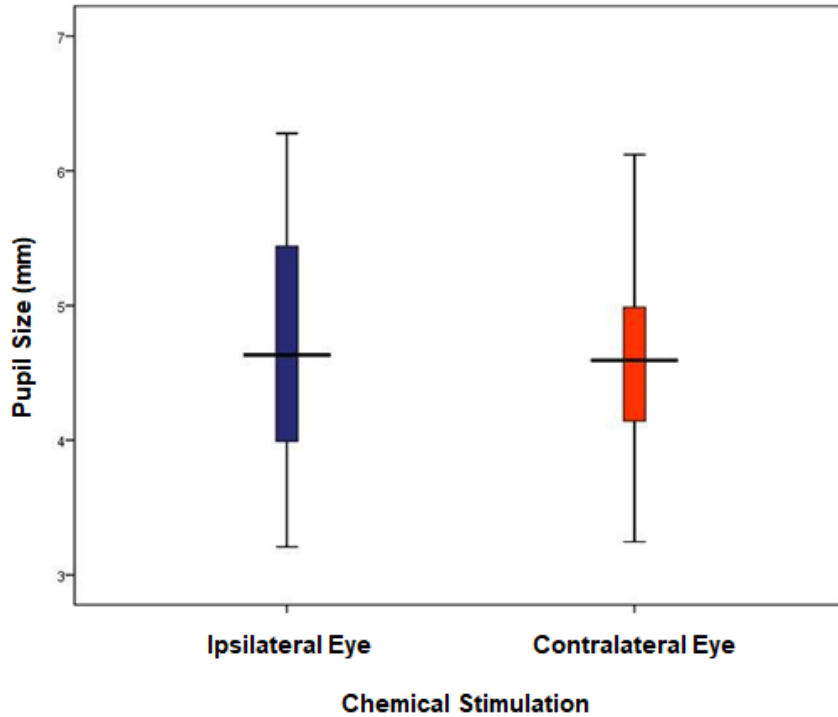
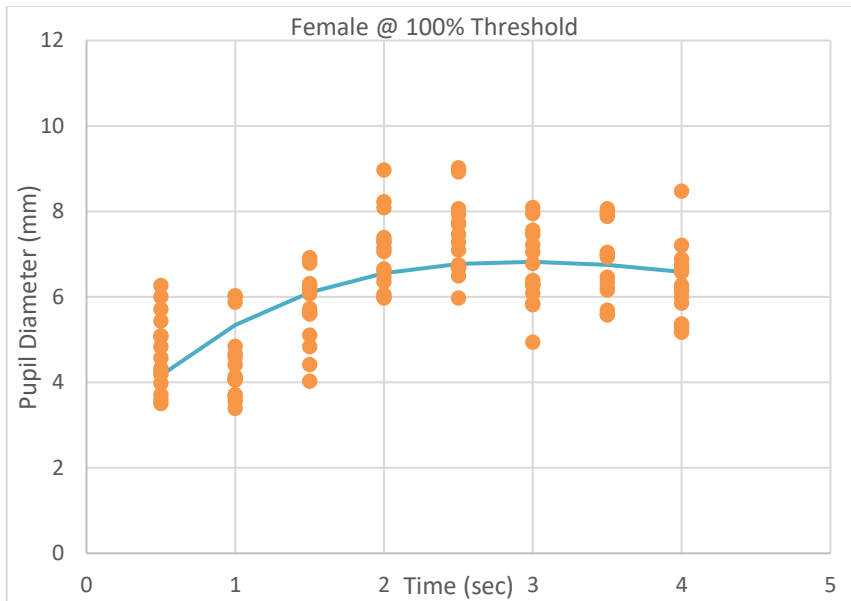
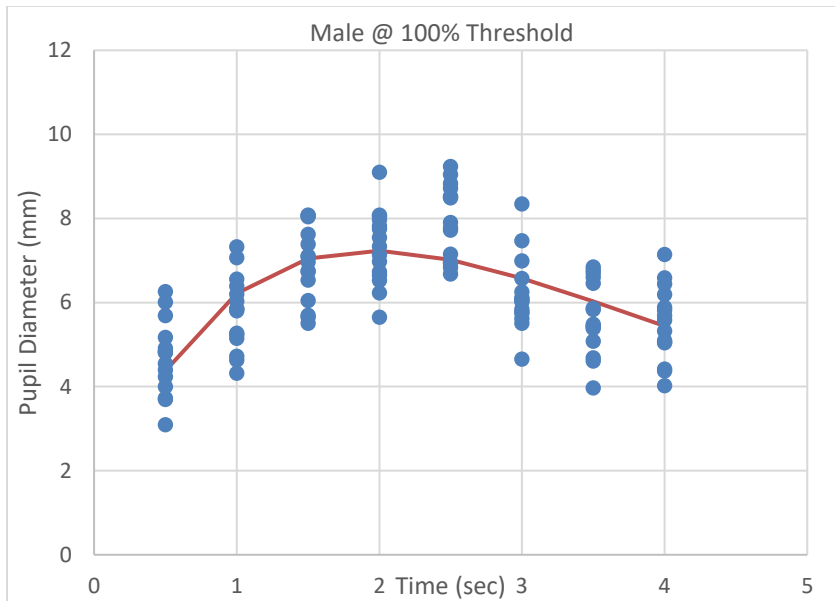
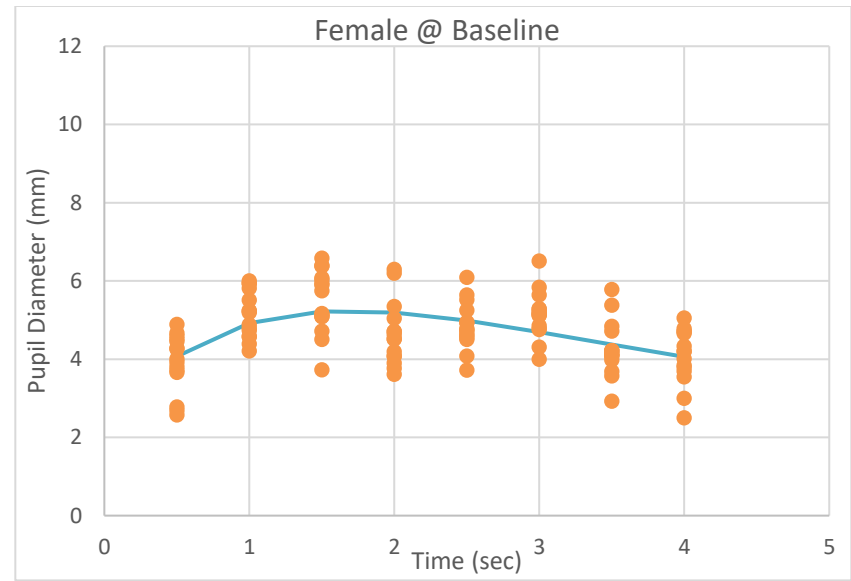
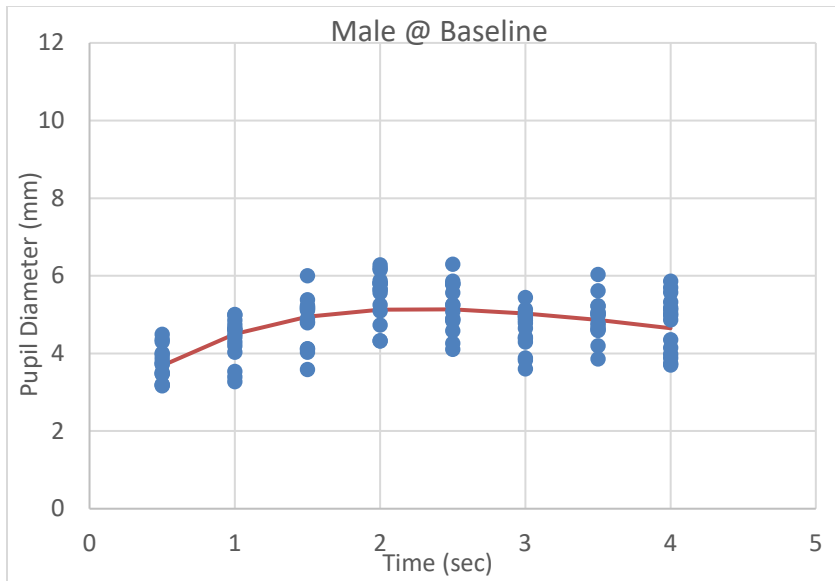


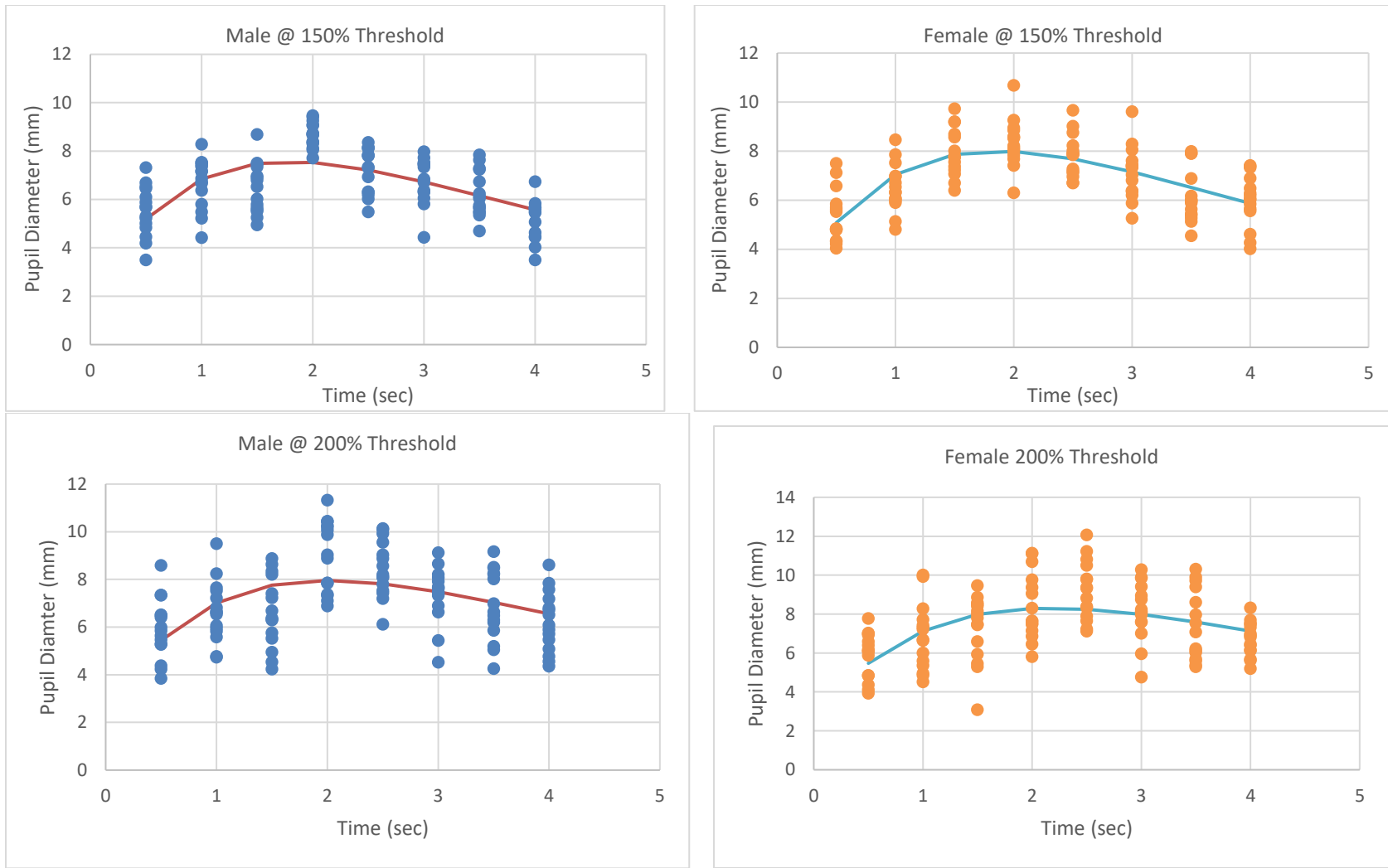
**Figure 9: Box-plot of pupil response between the ipsilateral (stimulated) and the contralateral (unstimulated) eye after corneal chemical stimulation (error bars denote 95% confidence interval).**

Non-linear regression was used to predict the pupil size based on time for male and female subjects at each stimulus intensity. A function  $y=C+(B*((A*time)/(EXP(A*time))))$  was used to fit all the data stratified by stimulus intensity. Below are the results of the non-linear modeling where y is the pupil size and A, B and C are constants. The values of A, B and C for the different stimulus modalities and intensities are displayed in Table 3. The pupil sizes at the different time points as determined by the model for both male and female subjects can also be found in Table 4.

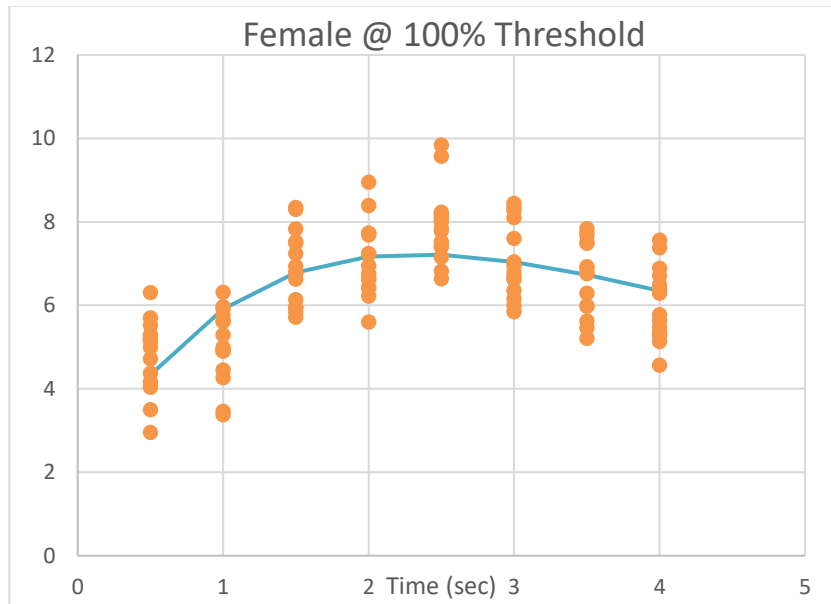
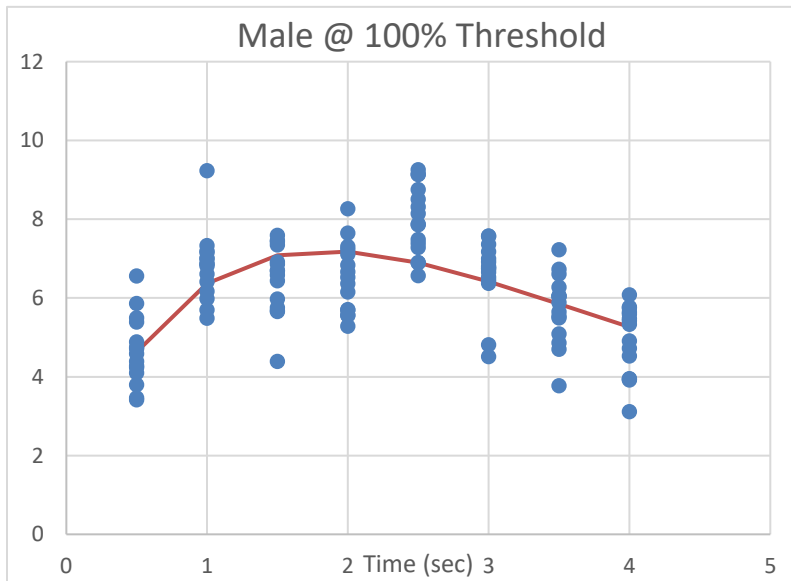
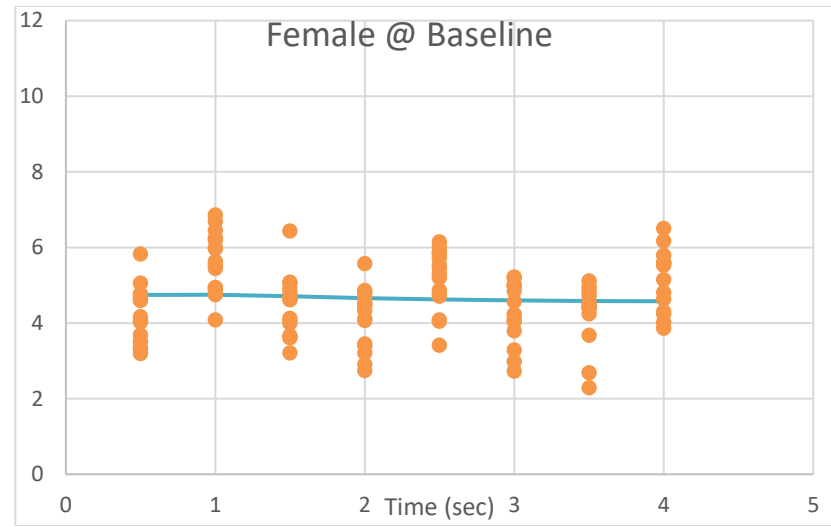
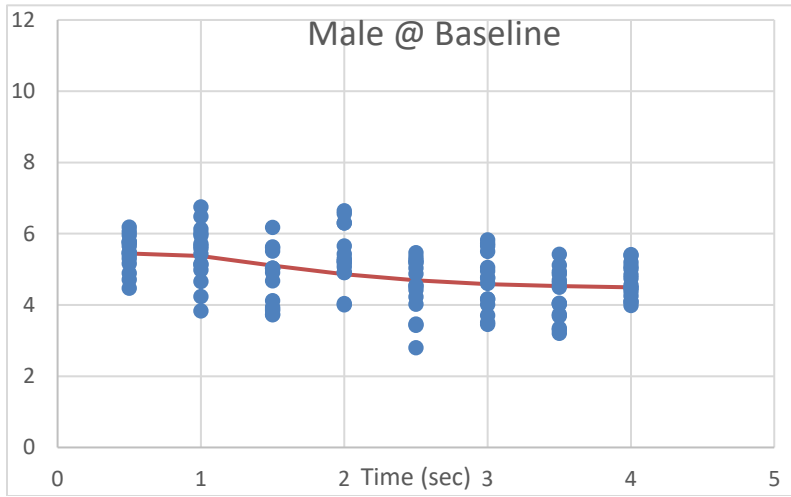
**Table 3: The values for the non-linear regression model for pupil response used mechanical and chemical corneal stimulation experiments.**

Stimulus Intensity	Value	Mechanical Stimulation		Chemical Stimulation	
		Male	Female	Male	Female
<b>Baseline</b>					
	A	0.440	0.595	1.525	1.341
	B	7.647	7.980	2.778	0.531
	C	2.335	2.303	4.457	4.564
<b>Sum of Squared Deviations</b>	SS	47.5	54.7	67.4	72.8
<b>100% Threshold</b>					
	A	0.516	0.343	0.544	0.429
	B	16.961	11.914	15.98	14.843
	C	0.996	2.440	1.320	1.766
<b>Sum of Squared Deviations</b>	SS	88.4	83.8	78.9	67.3
<b>150% Threshold</b>					
	A	0.562	0.540	0.562	0.427
	B	15.267	18.062	15.267	14.194
	C	1.954	1.364	1.954	2.643
<b>Sum of Squared Deviations</b>	SS	83.4	83.2	34.6	38.2
<b>200% Threshold</b>					
	A	0.499	0.462	0.516	0.486
	B	14.492	15.379	17.633	16.338
	C	2.626	2.652	1.773	2.621
<b>Sum of Squared Deviations</b>	SS	46.2	49.2	39.4	46.6





**Figure 10: Pre- and post-stimulus pupil diameter for mechanical corneal stimulation for male and female subjects.**



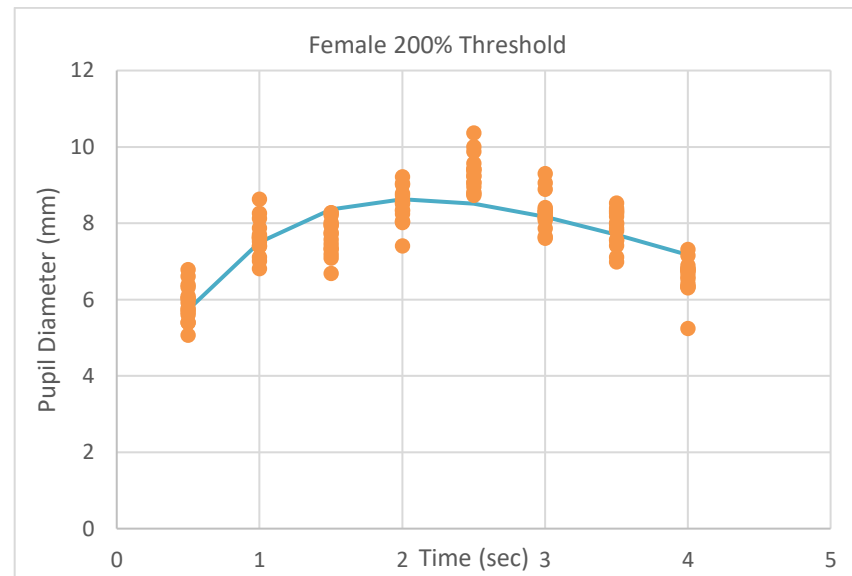
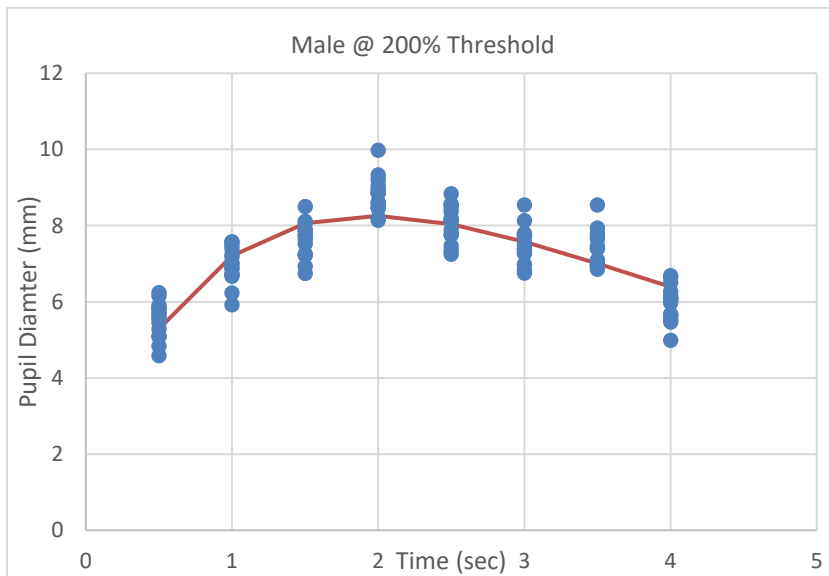
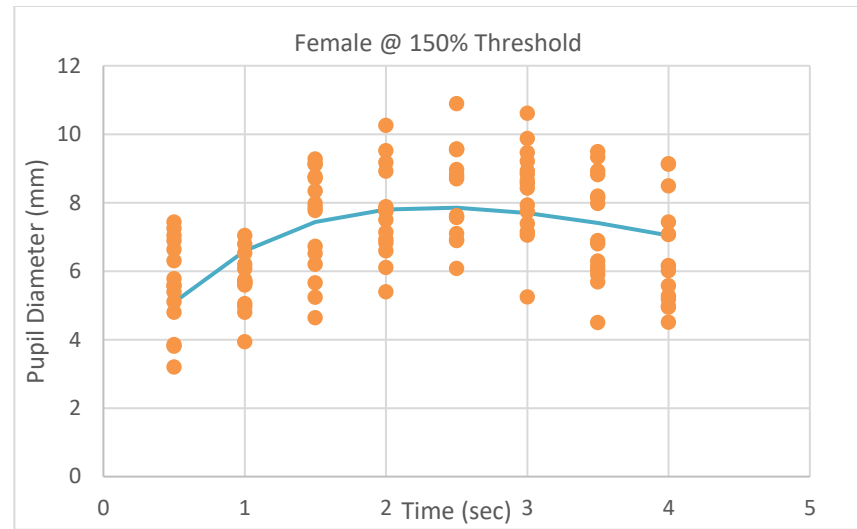
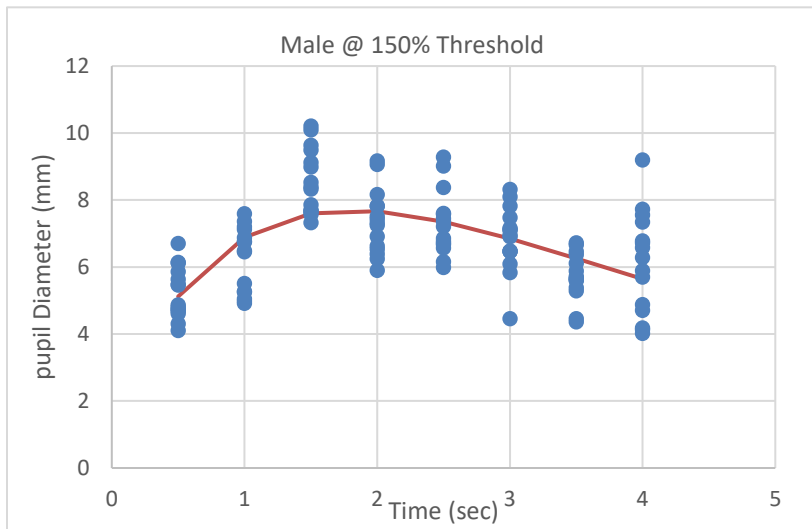


**Figure 11: Pre- and post-stimulus pupil diameter for chemical corneal stimulation for male and female subjects.**

**Table 4: Pupil sizes at the different time points as determined by the non-linear model  $y=C+(B*((A*time)/(EXP(A*time))))$  for male and female subjects.**

<b>Mechanical Stimulation</b>								
	Baseline		100% Threshold		150% Threshold		200% Threshold	
Time (sec)	Male	Female	Male	Female	Male	Female	Male	Female
0.5	3.64	4.07	4.38	4.16	5.19	5.09	5.44	5.47
1	4.40	4.92	6.22	5.34	6.85	7.05	7.02	7.13
1.5	4.84	5.22	7.05	6.11	7.49	7.87	7.76	7.98
2	5.05	5.19	7.23	6.56	7.53	7.99	7.96	8.29
2.5	5.10	4.98	7.02	6.77	7.22	7.69	7.82	8.25
3	5.04	4.69	6.58	6.82	6.72	7.16	7.48	7.98
3.5	4.91	4.37	6.03	6.75	6.15	6.52	7.04	7.59
4	4.74	4.06	5.44	6.59	5.58	5.87	6.56	7.13
<b>Chemical Stimulation</b>								
	Baseline		100% Threshold		150% Threshold		200% Threshold	
Time (sec)	Male	Female	Male	Female	Male	Female	Male	Female
0.5	5.45	4.75	4.63	4.33	5.19	5.09	5.29	5.73
1	5.38	4.75	6.37	5.91	6.85	6.60	7.20	7.50
1.5	5.10	4.71	7.09	6.78	7.49	7.43	8.07	8.36
2	4.86	4.66	7.18	7.17	7.53	7.80	8.26	8.63
2.5	4.69	4.63	6.90	7.21	7.22	7.85	8.03	8.51
3	4.59	4.60	6.42	7.04	6.72	7.70	7.58	8.17
3.5	4.53	4.59	5.85	6.73	6.15	7.40	7.01	7.70
4	4.50	4.58	5.27	6.35	5.58	7.04	6.39	7.17

**Table 5: Mean  $\pm$ (SD) pupil size between males and females for mechanical and chemical corneal stimulation experiments.**

			Mean Pupil Diameter (mm)	( $\pm$ ) Std. Deviation (mm)
		Sex		
Baseline	Mechanical Stimulus	Male	4.5	0.7
		Female	4.7	0.7
		Total	4.6	0.8
	Chemical Stimulus	Male	4.6	0.7
		Female	4.7	0.8
		Total	4.6	0.9
	Total	Male	4.5	0.7
		Female	4.7	0.8
		Total	4.6	0.8
0% Threshold	Mechanical Stimulus	Male	4.8	0.7
		Female	4.5	0.7
		Total	4.7	0.7
	Chemical Stimulus	Male	4.7	0.6
		Female	4.6	0.7
		Total	4.7	0.6
	Total	Male	4.8	0.6
		Female	4.6	0.7
		Total	4.7	0.7
100% Threshold	Mechanical Stimulus	Male	6.2	0.4
		Female	6.1	0.3
		Total	6.2	0.3
	Chemical Stimulus	Male	6.2	0.3
		Female	6.4	0.3
		Total	6.3	0.3
	Total	Male	6.2	0.3
		Female	6.3	0.4
		Total	6.3	0.3
150% Threshold	Mechanical Stimulus	Male	6.6	0.3
		Female	6.9	0.3
		Total	6.7	0.3
	Chemical Stimulus	Male	6.7	0.4
		Female	7.1	0.3
		Total	6.9	0.4
	Total	Male	6.6	0.3
		Female	7.0	0.3
		Total	6.8	0.4
200% Threshold	Mechanical Stimulus	Male	7.1	0.2
		Female	7.5	0.4
		Total	7.3	0.3
	Chemical Stimulus	Male	7.2	0.3
		Female	7.7	0.3
		Total	7.5	0.4
	Total	Male	7.2	0.2
		Female	7.6	0.4
		Total	7.4	0.4

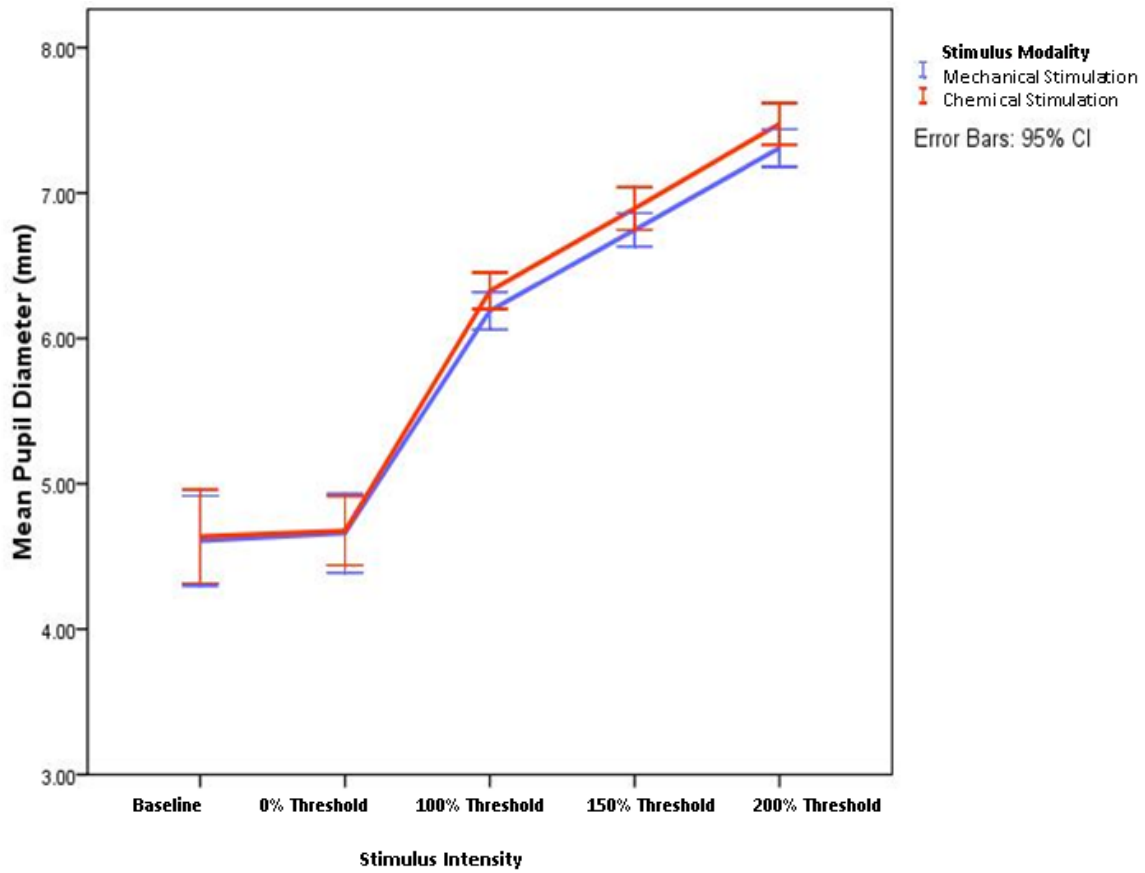


**Figure 12: Mean pupil diameter across different stimulus intensities for mechanical (blue) and chemical (red) corneal stimulation experiments (error bars denote 95% confidence interval).**

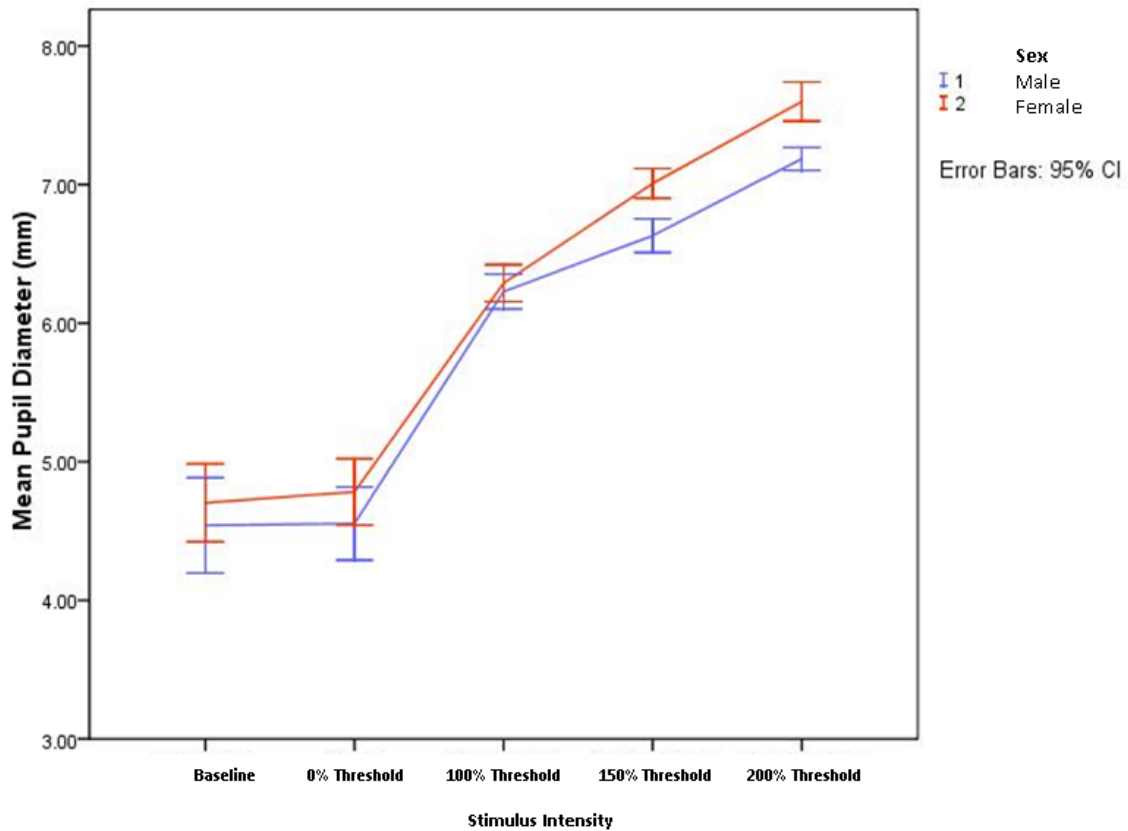


**Figure 13: Mean pupil diameter across different chemical stimulus intensities for male (blue) and female (red) subjects (error bars denote 95% confidence interval).**

#### **4.3.4 Effects of Sex and Stimulus Intensity on Pupil Diameter**

There was a difference in pupil diameter between male and female subjects based on stimulus intensity (ANOVA  $F(4,224) = 5.9, p < 0.05$ ). Females had greater pupil diameters than males at 150% threshold and 200% threshold (Tukey HSD  $p < 0.05$ ).

#### 4.4 Discussion

To my knowledge the set of experiments performed in this chapter is the first time the effect of noxious ocular surface stimulation on pupil response has been studied. From the results of this study, suprathreshold stimulation of the cornea appears to evoke an immediate dose-response like pupil size increase.

The dilator and sphincter pupillae muscles of the iris are innervated by sympathetic and parasympathetic neurons respectively. Together, these smooth muscles work antagonistically to control pupil size[9]. The Edinger-Westphal nucleus, located in the midbrain, controls circular fibers within the sphincter pupillae to cause constriction of the pupils, thereby mediating the pupillary light reflex[42]; it is however not involved in dilation. The hypothalamus controls radial muscles in the dilator pupillae to cause pupillary dilation[9]. The hypothalamus is also directly activated by ocular surface pain via the trigeminal pathway[30, 31], therefore the pupil dilation response to nociceptive corneal stimuli observed in this study may support the idea that a neural connection exists within the hypothalamus linking dilation response and corneal nociception.

In line with my experiment, other studies have also reported a similar increase in pupil size in response to noxious stimulation. Chapman *et al*[14] discovered that pupil diameter increased when the intensity of painful fingertip stimulation was increased and proposed that this pupil size change was a complex defensive response to nociception mediated by the brain, thus a good indicator of central processing of painful

stimuli. Larson *et al*[19], observed the effect of painful stimulation on physiological factors such as pupil size, heart rate and arterial blood pressure in anesthetized subjects. The researchers observed greater pupil sizes in subjects as painful stimulation increased and went on to conclude that in comparison to heart rate and arterial blood flow, pupil responses provide greater sensitivity as a measurement of noxious stimulation. Oka *et al*[15], studied the pupil dilation response to nociceptive stimuli and concluded that the increased pupil response to increasing noxious sensory input was not an artefact of cognitive effort, independent of painful experience, as some researchers had earlier suggested[43], but rather existed as part of a higher order defense response. In this experiment, I assessed the effect of the sex of subjects on the pupil dilation response to nociceptive corneal stimuli. From our results, there seems to be a difference in male and female pupil responses to noxious ocular surface stimulation. Females had a greater pupil size increase in comparison to males. Fillingim and Maixner[21] reviewed experiments conducted by others on gender differences in responses to noxious experimental stimuli using a ‘box-score’ or vote counting method and concluded that “females exhibit greater sensitivity to noxious stimulation than males”. Population based research by Unruh[22] shows that in comparison to men, there is a greater prevalence of back pain, arthritis and headaches among women. These findings may possibly be due to women having a tendency to honestly report pain (both acute and chronic) more often than men[44]. Hypotheses about sex differences include sex-role

expectations[45], hormones[46, 47], differences in skin thickness and body size[48] and sensory differences between men and women[49]. Ellermeier and Westphal[20] reported females had greater pupil dilation responses than males when high tonic pressure was applied to the fingers of subjects, and in that same study, females reported greater pain than males when the same amount of pressure was applied to the subjects' fingers. Since it is not possible for one to voluntarily control his/her pupil response to noxious stimulation, the gender differences found in this study may point to affective or sensory components of pain as opposed to subject bias in response[45] or attitudinal factors[50].

Some experimental limitations of this study include a restriction to the stimulus intensity range, a limit to the amount of time selected to observe the pupil response and not observing several autonomic responses simultaneously. The highest stimulus intensity used was twice the threshold. The potential to go beyond 200% threshold for both mechanical and chemical corneal stimulation would be beneficial because information regarding what happens to the pupil response at higher ocular surface stimulation intensities remains unknown.

The impact of the menstrual cycle on pain in women has been well documented [27, 28], in this study I did not collect data regarding the female participant's stage of menstruation and readily accept that it may have an impact on the results. Further studies

involving ocular surface stimulation and autonomic responses should factor in the effect of the female menstrual cycle.

In assessing the pupil response to noxious stimulation, I limited the measurements to a time frame of 4 seconds. This method was chosen because prior studies involving painful stimulation and pupil responses[14, 15, 20] identified the greatest pupil response within the first three seconds of the post stimulus period; however, the potential to observe the pupil response over a longer period of time would provide important information regarding the complete nature of the pupillary response to noxious stimulation.

A review of the Table 4 and Figures 10 - 11 above, shows a greater pupil dilation response for females than males across both modalities. Using a non-linear approach to identify the effect of stimulus intensity on pupil size over time is accurate (as every time point is considered) but very time consuming. The averaging procedure (similar to an area under the curve approach used in blood glucose studies[51]) described in the Analyses section of this chapter, presents a faster way to characterize the relationship between pupil size, sex and stimulus intensity. In addition, averaging over time appears to be a justifiable approach to analyzing pupil data because of the low temporal resolution that is characteristic of the sampling procedure applied to acquire pupil size and monotonic response of the pupils to stimulus intensity. It can be seen that similar results were obtained when either the non-linear regression or the averaging approach

was used to analyze the pupil response to ocular surface stimulation (see Tables 4,5 and Figures 10 – 13).

In this study, I only assessed the pupil dilation response to noxious stimulation. Research by Treister et al[52] suggests that a combination of several autonomic measures provides more accurate relationship information to pain in comparison to single measures, as such, other autonomic factors such as ocular surface blood flow could have been investigated simultaneously.

#### **4.5 Conclusion**

In summary, this study provides some evidence that stimulation of the central cornea by noxious stimulation in the form of mechanical and chemical stimuli, evokes a dose dependent autonomic pupil dilation response. There seems to be a sex difference in the pupil dilation response, with women having a greater response than men when experiencing greater amounts of noxious stimulation. This study, together with experiments from the previous chapter, serve as a basis for the characterization of the local stimulus-response neural circuitry relating nociceptive stimuli to autonomic responses.

## **Chapter 5**

### **Part A - Accommodative Response to Ocular Surface Stimulation**

#### **5.1 Introduction**

Accommodation or the eye's ability to focus and maintain clear vision when changing view from a distant to a near target, or vice versa, is a reflex mechanism driven by autonomic neuro-circuitry[1]. The autonomic nervous system innervation to accommodation is composed of both sympathetic (inhibitory) and para-sympathetic (excitatory) input[1-4]. In the unaccommodated eye, the ciliary muscle is relaxed and exerts tension on the zonular fibers which then flattens the lens thereby reducing the dioptric power.

Blur, proximity and retinal disparity are all factors that can stimulate accommodation[5-7]; however, blur is the main stimulus to accommodation[6]. The pathway for visual blur begins at the retinal cone receptors and from here, information is transmitted through the optic nerve and reaches the lateral geniculate body (LGB). The neural information is then transmitted to area V1 (visual cortex) for further processing. From V1, the neural signal is translated into a motor command at the Edinger-Westphal (EW) nucleus in the midbrain[8]. The pathway to the EW nucleus from the visual cortex remains unclear; however, the neural information can be derived from several areas in the cortex, midbrain and cerebellum[9-12]. The efferent pathway involves transmission

of the motor commands from the EW nucleus to the ciliary muscle in the eye via the third cranial (oculomotor) nerve[13, 14]. When the motor command reaches the ciliary muscle, it contracts and releases the tension on the zonules which causes the crystalline lens to increase its dioptric power by becoming steeper in shape. Changes in the vergence system and pupils, together with accommodation, ensures the maintenance of a clear and single image and the near triad is used to describe the synkinetic association between accommodation, vergence and constriction of pupil[15].

In the previous chapter, I investigated the response of the pupils to ocular surface stimulation. A pupil dilation response to corneal chemical and mechanical stimulation was discovered. In Chapter 3, the effect of ocular surface stimulation on conjunctival redness was evaluated and a dose-wise increase to conjunctival blood flow due to noxious corneal stimulation was found. Situ and Simpson[16] reported that chemical and mechanical corneal stimuli evoked measurable tear secretion, with central corneal mechanical stimulation producing the strongest lacrimation reflex. There are no studies evaluating the effect of noxious stimulation on accommodation. Therefore, the autonomic responses to corneal stimulation reported in the previous chapters led me to explore whether noxious corneal stimulation had an effect on the accommodative mechanism.

## **5.2 Methods**

This experiment was divided into two components (Part A and Part B), and data from the same subjects were used for Part A and Part B. Part A explored the effect of ocular surface stimulation on the accommodative response while Part B investigated the relationship between ocular surface stimulation and the pupil response while the eyes were accommodating.

### **5.2.1 Subjects**

Ethics clearance was obtained from the Office of Research Ethics at the University of Waterloo before commencement of the study. Eligible subjects signed an informed consent document before enrolment in the study.

Fifteen healthy emmetropic subjects participated in this study. There were 8 male and 7 female volunteers ranging in age from 19 to 27. Subjects with self-reported binocular vision anomalies were excluded from the study. One male subject dropped out of the experiment because he was unable to complete the study due to personal reasons.

### **5.2.2 Power Refractor**

In this study accommodative responses were measured with a validated eccentric infrared (IR) photorefractor[17], (Power Refractor, Multi-channel Systems, Reutlingen, Germany), shown in Figure 14. The power refractor can be used in the binocular mode to capture accommodative and pupil responses simultaneously at a sampling rate of

25hz in both eyes. The power refractor consists of a portable computer connected to a closed-circuit device (CCD) camera. Surrounding the CCD camera are six sets of nine infra-red (IR) light emitting diodes (LEDs) arranged in the shape of a triangle[17, 18].



**Figure 14: Image of the Power Refractor (Multi-channel Co, Reutlingen, Germany).**

### **5.2.3 Computer-controlled Belmonte Esthesiometer**

The computer-controlled Belmonte esthesiometer used in this study has been described in different experiments[19-21] and in Chapters 3 and 4. Briefly, the modified device used for the delivery of mechanical and chemical stimuli to the ocular surface consists of a control box that electronically regulates the mixture of air and carbon dioxide (CO<sub>2</sub>). The flow rates of air and concentration of CO<sub>2</sub> are separately controlled by two digital flow controllers. Within the nozzle assembly is a thermostat to control

temperature. A calibrated video camera was used to ensure that the stimulus was orthogonal to, and the nozzle tip was 5mm from, the ocular surface.

#### **5.2.4 Nociceptive Stimuli**

Mechanical stimuli consisted of a series of air pulses with varying flow rates from 0 to 200 ml/min and chemical stimulation was delivered by increasing the concentration of CO<sub>2</sub> in the air. An ascending methods of limits[22] was used to determine mechanical and chemical detection thresholds of the cornea. The flow-rate steps were set at 10 mL/min, and the mechanical threshold was the average of three readings when the subject first reported the stimulus. For the chemical threshold, the stimulus flow rate was set at half the initially determined mechanical threshold, and CO<sub>2</sub> was added to the air in increments of 5% CO<sub>2</sub>. The chemical threshold was the average of three first reports of stimulus detection.

#### **5.2.5 Stimulus Delivery**

The subjects wore in-ear headphones with noise playing in the background and room temperature, illumination and humidity were kept constant throughout the experimental procedure. The stimulus was presented at the corneal apex of the left eye while subjects viewed a fixation target that was 3 meters away the subjects then turned and looked at the photorefractor that was approximately 0.66 meters away. The tip of the esthesiometer was rotated to ensure the stimulus was delivered approximately

perpendicular to the corneal surface during stimulus delivery (the positioning was approximated with the help of the Logitech cameras and the experimenter's judgement). The temperature of the air was set to 50°C, this decreased to 33.4°C at the ocular surface at room temperature of 23°C. This was calibrated using a custom electronic thermometer positioned 5 mm from the probe tip (which corresponds to the position of the ocular surface in the experiments). The duration of the stimulus was 2 seconds and it was delivered to the ocular surface immediately after a blink. The subject blinked freely between trials. The next stimulus was triggered after the sensation caused by the last stimulus had disappeared completely.

Once the mechanical and chemical thresholds were determined, three stimuli and a catch trial (0% threshold – no stimulus was delivered, the esthesiometer intensity setting was zero) were then delivered to the subject in random order, in both the mechanical and chemical stimulation experiments – stimulus at 0% threshold, stimulus at 100% threshold, stimulus at 150% threshold, and stimulus at 200% threshold. The accommodative response at a sampling rate of 25Hz, over a 5 second period (while the subjects fixated on a single high contrast (85%) color cartoon frame at 66cm) prior to stimulus delivery (baseline) and after stimulus delivery were compared.

### **5.2.6 Analyses**

Measurement of accommodative response at 25 Hz for 5 seconds provided a total of 125 data points. Each data point was screened and accepted if the following criteria were met: the ocular alignment was less than 10 degrees and 5 degrees from the optical axis of the photorefractor in the horizontal and vertical axes respectively, the pupil size was above 3mm (as recommended by the manufacturer) and the responses were free of blinks. Each participant needed to have at least 113 rows of acceptable data after satisfying all the above criteria to be considered for further analysis (account for at least 90% of the acquired data). Each accommodative response value was then subtracted by 1.5D to account for the expected accommodation required at 66cm. The accommodative response for the left and right eye was averaged and all acceptable data points were used for the analysis. Data from one participant were excluded from the analysis because the pupil diameters were less than 3mm.

Non-linear regressions were performed to explore the relationship between time and accommodative response before and after stimulus delivery. Quantitative differences in accommodative response, stimulus modality and intensity were analyzed using repeated measures ANOVA. Tukey HSD tests were used for all post hoc analysis. SPSS for Windows, Version 16.0 (Chicago, IL, SPSS Inc.) and Microsoft Excel for Windows (Redmond, WA, Microsoft Corp.) were used for data analysis. An alpha value of 0.05 or less was assumed to be significant.

### 5.3 Results

Non-linear regression was used to predict the accommodative response based on time for all subjects at baseline and 200% threshold. A significant function (all  $p < 0.05$ ),  $y=C+(B*((A*time)/(EXP(A*time))))$  was used to fit all the data grouped by stimulus intensity. Below are the results of the non-linear modeling where  $y$  is the accommodative response and  $A$ ,  $B$  and  $C$  are constants. The values of  $A$ ,  $B$  and  $C$  for the different stimulus modalities and intensities are displayed in Table 5 and the corresponding plots are shown in Figure 15 and 16.

**Table 5: The best fit values for the non-linear regression model used for accommodative response in mechanical and chemical corneal stimulation experiments.**

Stimulus Intensity	Value	Mechanical Stimulation	Chemical Stimulation
<b>Baseline</b>			
	A	2.7E-03	0.7
	B	5.2	0
	C	0	0
<b>Sum of Squared Deviations</b>	SS	24.7	28.6
<b>200% Threshold</b>			
	A	2.7E-05	2.2E-05
	B	0	2766.9
	C	1.2	1.1
<b>Sum of Squared Deviations</b>	SS	34.5	32.4

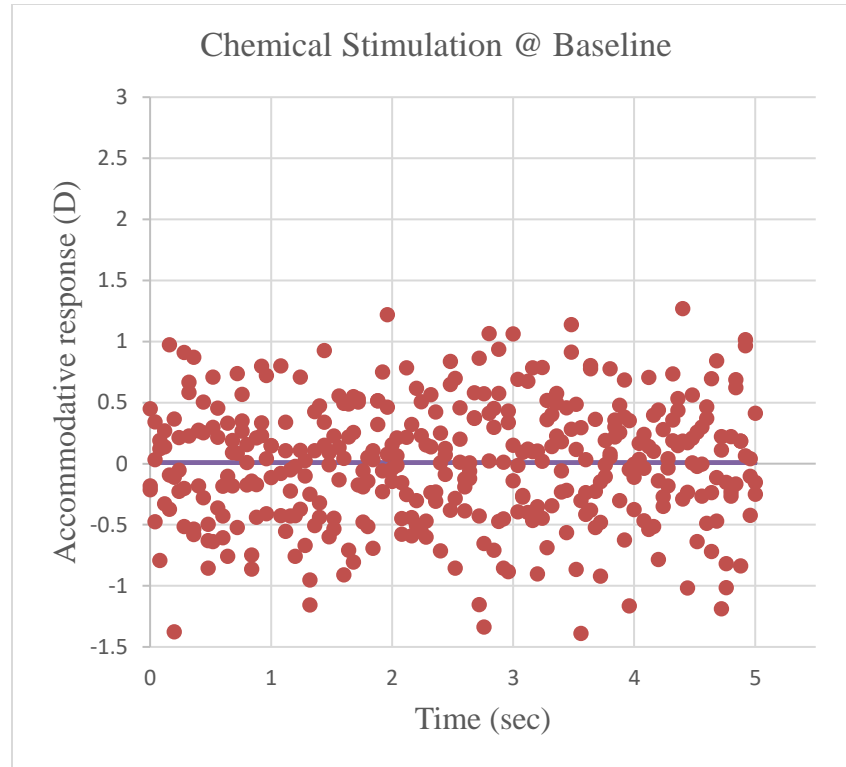
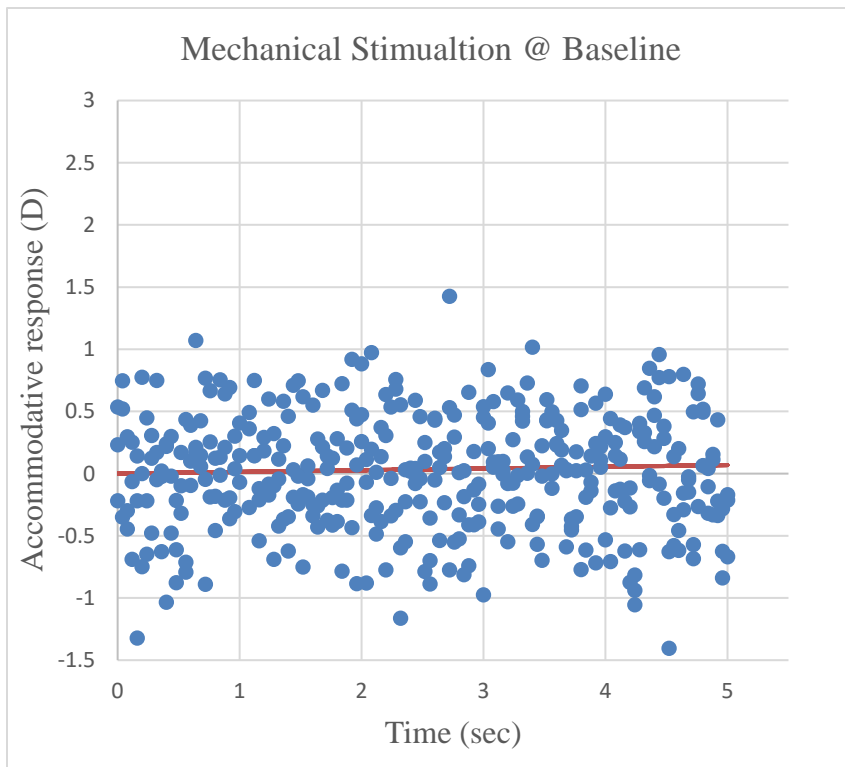


**Figure 15: Pre-stimulus accommodative response for all subjects in the mechanical (left) and chemical (right) corneal stimulation experiment**

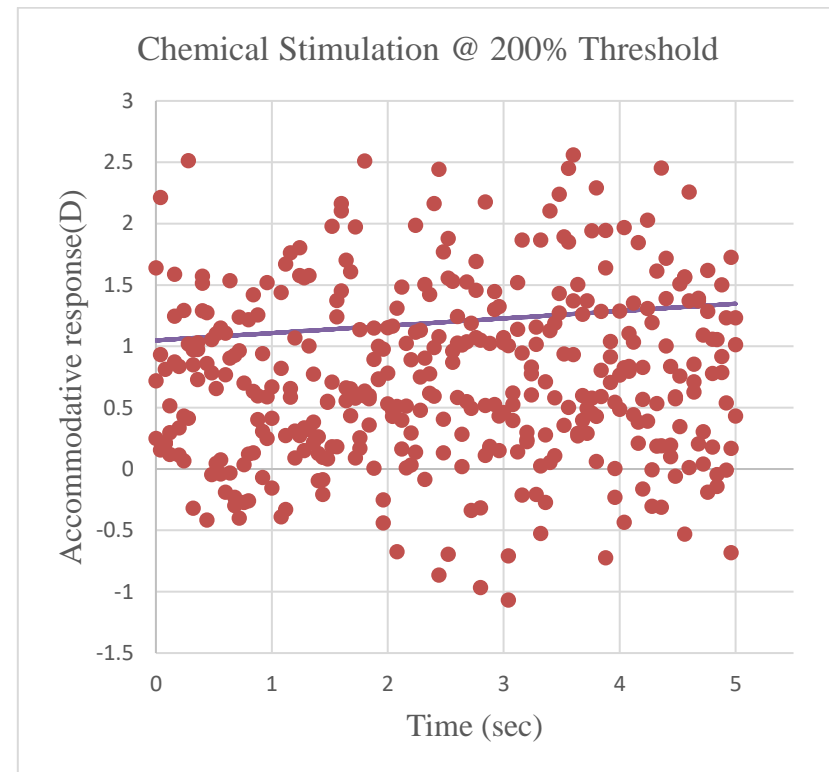
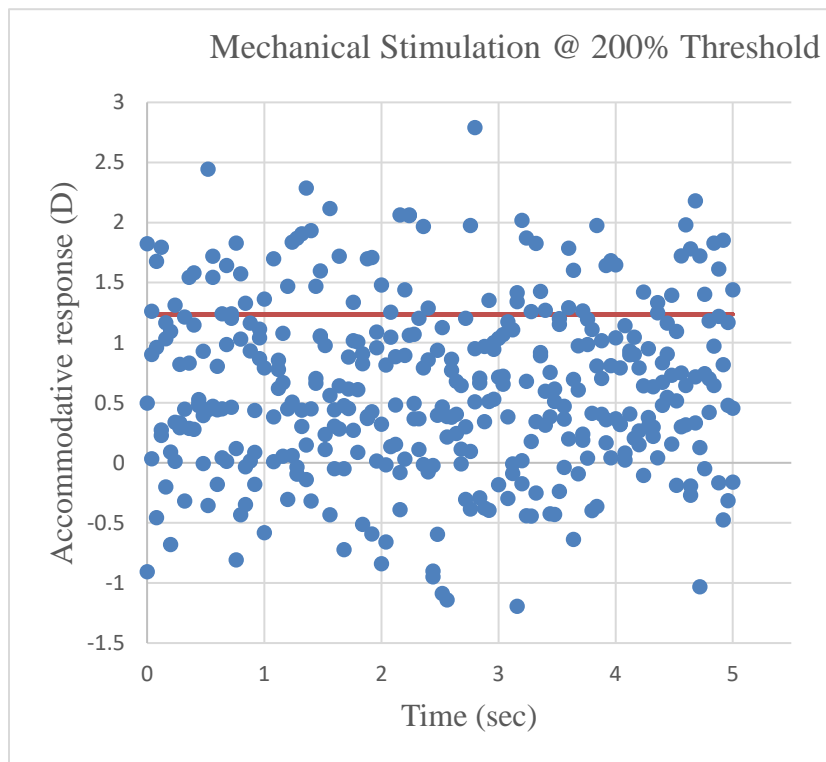


**Figure 16: Post-stimulus accommodative response for all subjects in the mechanical (left) and chemical (right) corneal stimulation experiments.**

A summary of the mean ( $\pm$  SD) accommodative response across the different stimulus intensities and modalities can be found in Table 6 below. Accommodative response at baseline (before each measurement session), and with mechanical and chemical stimulation of differing intensities grouped by modality are shown in Figure 17.

**Table 6: Mean ( $\pm$  SD) accommodative response across the different stimulus intensities in mechanical and chemical corneal stimulation experiments.**

	Stimulus Modality	Mean Accommodative Response	Std. Deviation
Baseline	Chemical	0.00	0.49
	Mechanical	0.00	0.46
	Total	0.00	0.48
0% threshold	Chemical	0.00	0.03
	Mechanical	0.01	0.04
	Total	0.00	0.04
Threshold	Chemical	0.23	0.49
	Mechanical	0.39	0.42
	Total	0.31	0.47
150% Threshold	Chemical	0.63	0.74
	Mechanical	0.63	0.63
	Total	0.63	0.68
200% Threshold	Chemical	0.81	0.84
	Mechanical	0.56	0.74
	Total	0.69	0.80

### **5.3.1.1 Effects of Stimulus Intensity on Accommodative Response**

Accommodation increased from baseline as the corneal apical stimulus intensity increased. This happened regardless of whether mechanical or chemical stimulation occurred (ANOVA  $F(4,2923) = 62.4, p < 0.05$ ). At 200% threshold, accommodative response was greater than all stimulus intensities (Tukey HSD, all  $p < 0.05$ ).

Baseline accommodative change for the chemical and mechanical stimulation experiments were not different from that at 0% threshold (Tukey HSD, all  $p > 0.05$  between baseline and 0% threshold).

### **5.3.1.2 Effects of Stimulus Modality and Stimulus Intensity on Accommodative Response**

There was no difference in accommodative response between chemical and mechanical stimulation based on stimulus intensity (ANOVA  $F(1,3248) = 2.9, p > 0.05$ ).

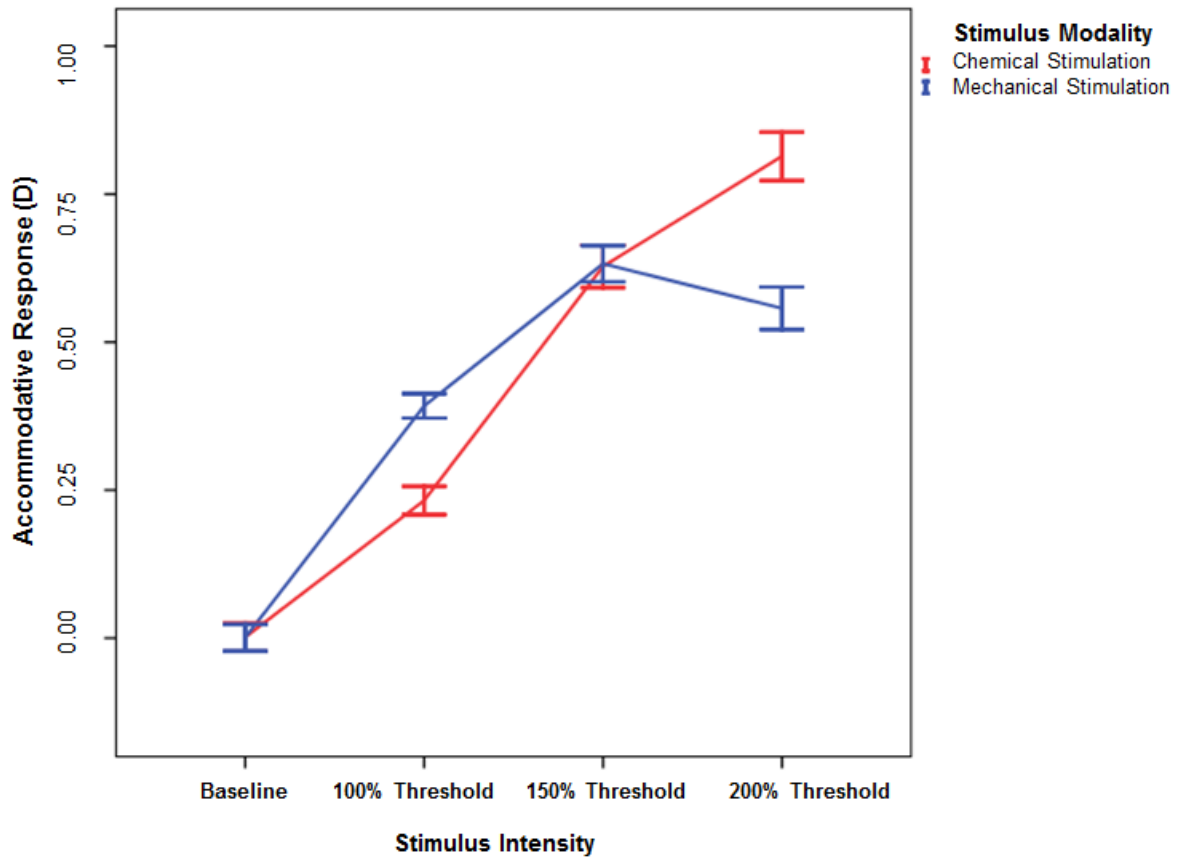


**Figure 17: Accommodative response across different stimulus intensities for mechanical (blue) and chemical (red) corneal stimulation experiments (error bars denote 95% confidence interval).**

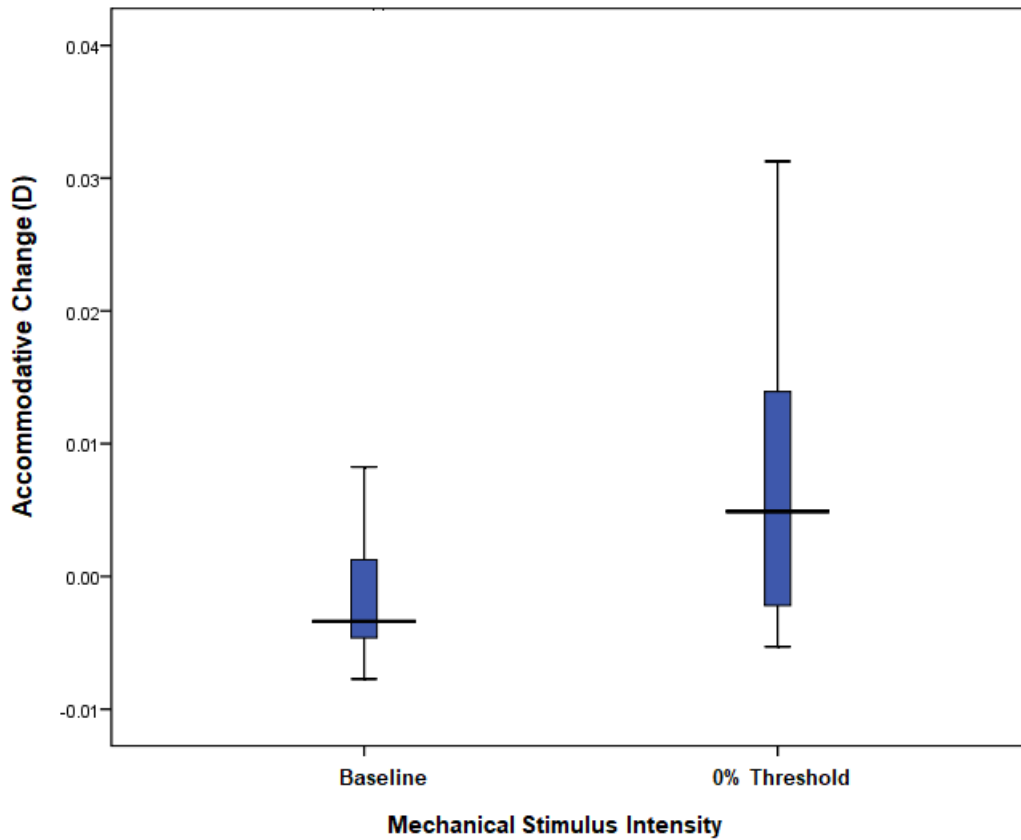


**Figure 18: Box-plot of accommodative response between baseline and 0% stimulus intensities for the mechanical corneal stimulation experiment (error bars denote 95% confidence interval).**

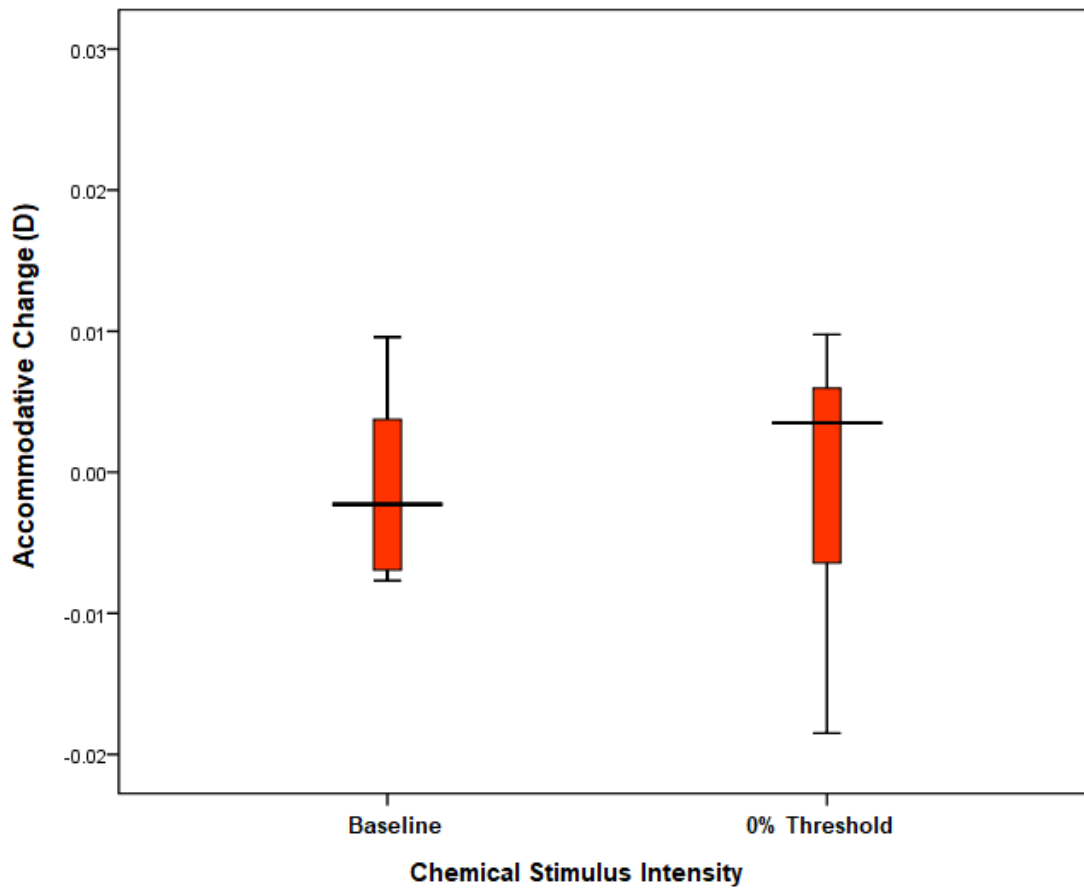


**Figure 19: Box-plot of accommodative response between baseline and 0% stimulus intensities for the chemical corneal stimulation experiment (error bars denote 95% confidence interval).**

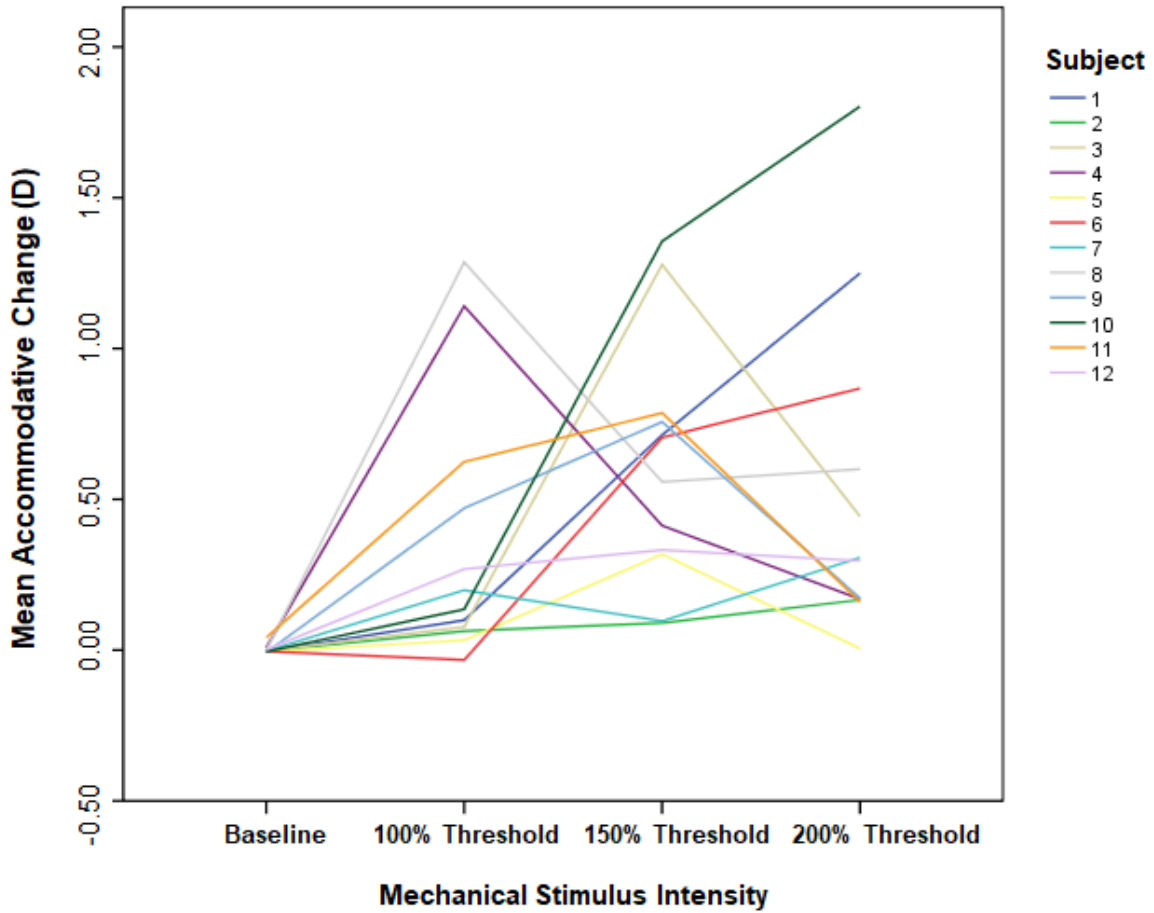


**Figure 20: The relationship between accommodation and stimulus intensity per subject during mechanical stimulation of the cornea.**

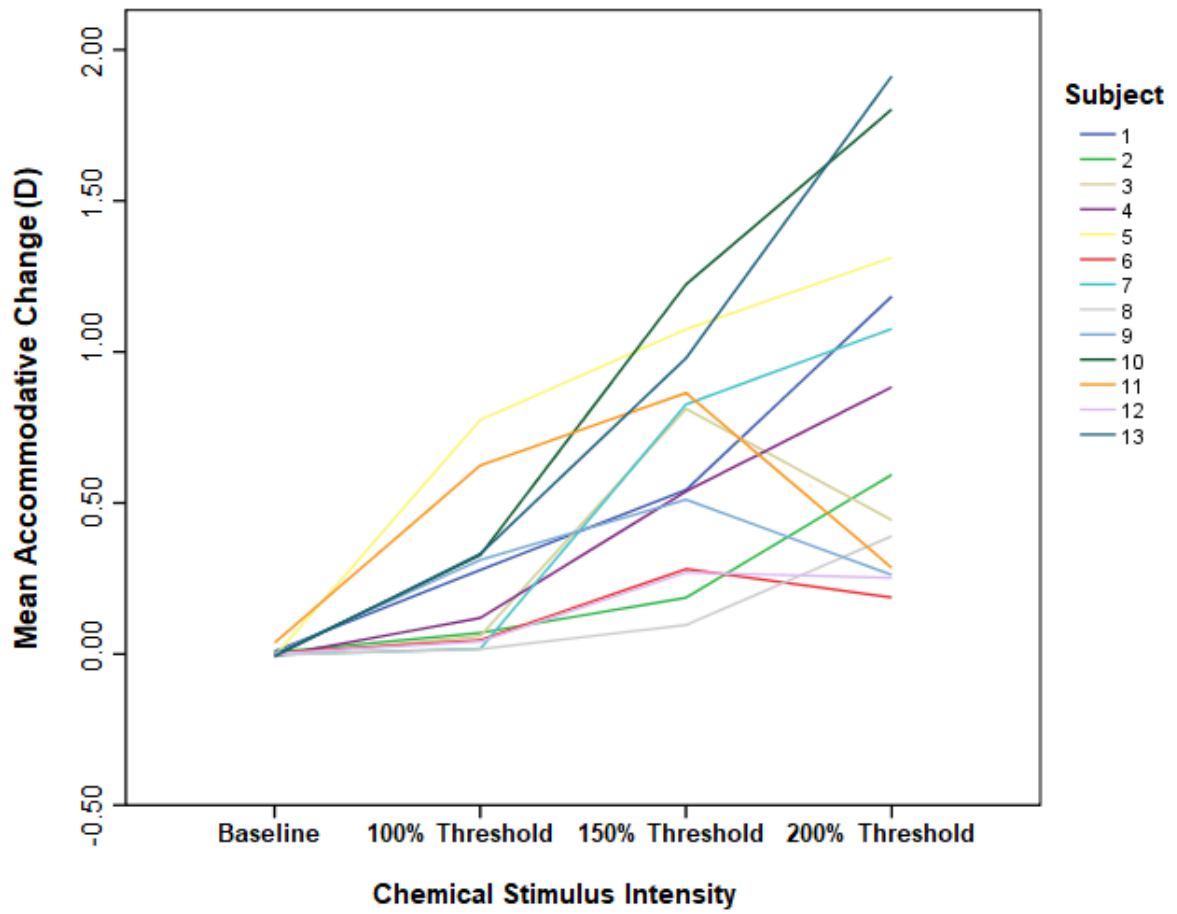


**Figure 21: The relationship between accommodation and stimulus intensity per subject during chemical stimulation of the cornea.**

## **5.4 Discussion**

### **5.4.1 Part A - Accommodative Response to Ocular Surface Stimulation**

To my knowledge, this is the first study to investigate the effect of ocular surface stimulation on accommodation. The results of this experiment indicate an increase in accommodation in relation to noxious corneal stimulation, and the increase in dioptric power of the eyes occurred regardless of whether chemical or mechanical stimulation was used.

Accommodation is the eye's ability to focus and maintain clear vision when changing view from a distant to a near target, or vice versa, and in the accommodated eye, the ciliary muscle contracts thereby releasing the tension on the zonules which causes the crystalline lens to increase its dioptric power[1]. The experiments in Chapters 3 and 4 of this thesis have demonstrated a dose-wise autonomic response to ocular surface stimulation similar to that which has been observed in this chapter.

Suggestions have been made that small changes in the mean accommodative response could be related to mechanical characteristics of the ciliary body[23] and a possible explanation for the resultant accommodative increase from noxious stimulation could be because the blood supply of the ciliary body (ciliary muscle and ciliary processes) and that of the conjunctiva are from the same source[24]. In Chapter 3 of this thesis an increase in conjunctival blood flow was reported because of noxious corneal stimulation. Branches of the anterior ciliary arteries supply the conjunctiva, limbus,

ciliary body and iris[25]. There are about seven anterior ciliary arteries and are distributed as follows: three arteries supply the rectus muscles, after passing over the muscle tendons of the rectus muscles, the arteries bifurcate and one set (major perforating branches) penetrates the sclera to arrive at the ciliary body while the other set of branches (episcleral arteries) continues on the surface of the eye[24]. Based on the interconnectivity between the vasculature of the conjunctiva and ciliary body, I propose that the resultant increase in blood flow in the conjunctiva from nociceptive corneal stimulation causes a corresponding increase in blood flow to the ciliary body which then contracts to bring about the accommodative change found in this experiment. However, Dr Maria Costa stated that the blood flow increase on the ocular surface may be insufficient to impact accommodation (personal communication Maria Carmen Acosta).

The increase in accommodation might also be in response to blur. From Chapter 4, a pupil dilation response to nociceptive corneal stimulation was observed, this dilation can result in blurred vision which will trigger the accommodative mechanism to increase the optical power of the eyes.

There is another possible cause of changes in optical power of the eyes that might contribute in an artefactual way to provide a dose-related effect of pneumatic stimulation. The esthesiometer blows onto the eye, disrupting the tear film. Until the tear film is reformed (depending on many tear physical chemical factors and the

participants' blink-responses to stimulation [26, 27]), it can be assumed that the stronger the flow of the stimulus, the greater the disruption of the tear film, so it might not be surprising if a dose-related effect were found after pneumatic stimulation. There are 2 major problems with this argument to account for the results. The first is that the tear film would be 'indented' to a greater extent as the stimulus intensity increased, resulting in negative power change, and this is exactly the opposite of what was found: as the stimulus intensity increased, the eye appeared to accommodate, not relax accommodation (the ocular power increased). A second flaw with the argument that there are 'simple' mechanical dose-related effects that alter the tear film in predictable ways to account for the optical changes measured, is with chemical stimulation: for chemical stimulation, flow does not increase as stimulus intensity increases. For each subject, flow is selected to be 50% of their mechanical threshold flow rate and that is fixed at this flow (and so constant physical effects on the tear film surface are experienced). Only the percentage of CO<sub>2</sub> is systematically increased as stimulus intensity in the stimulus column increases, so there is no physical difference in tear film morphology and a dose related effect cannot be ascribed to simple physical changes in the tear film induced by the stimulus air column (conversation with Trefford L. Simpson).

Two important components that impact the result of this experiment are the influence of time on accommodation and the tendency for accommodation to occur in different

directions (positive and negative accommodation). These factors led me to analyse the data using a non-linear approach. The non-linear model used considers the effect of time and ocular surface stimulation on accommodation at each data point and displays the relationship between time, accommodation and stimulus intensity for all the subjects. It can be seen from Figures 15 and 16 that for both mechanical and chemical stimulation experiments, the model predicted a greater accommodative response when 200% threshold stimulus intensity was applied to the eyes in comparison to the pre-stimulus baseline condition. Interestingly from visual inspection of Figure 16, the accommodative response appears to be at approximately the same amplitude while time increases for mechanical stimulation, but for chemical stimulation, the accommodative response seems to increase over time. This difference in accommodative response, though not statistically significant, may have been brought about because of the differences between mechanical and chemical stimulation that accounted for stimulus modality induced conjunctival redness disparity discussed in Chapter 3 of this thesis. The accommodative system appears to respond to noxious mechanical and chemical stimulation of the cornea. This finding could possibly be due to the possible influence of pupil size, an artefact in the experimental design, and/or instrumentation, or an actual response of the accommodative system to pain. Further investigation is required to rule out the possibility of an artefact causing this resultant accommodative response to noxious stimulation identified in this study.

## **Part B – Pupil Response to Ocular Surface Stimulation in the Accommodating Eye**

In Part A of this chapter, I looked at the response of the accommodative system to mechanical and chemical stimulation of the cornea. There appeared to be an increase in accommodation as a response to noxious corneal stimulation. Accommodation is characterised by three major processes, otherwise known as the near triad – a change in pupil size, vergence and shape of the lens[15]. In the accommodated state (when focusing from far to near), the pupils constrict but research suggests that this constriction is negligible when it is below or equal to 1D of accommodation[28, 29]

In Chapter 4 of this thesis the effect of ocular surface stimulation on the pupils was investigated and there appeared to be a pupil dilation response to corneal stimulation consistent with pupil dilation responses from other experiments[17, 18, 30-32]. Based on the previous experiments and results of this thesis, I investigated the pupil response to ocular surface stimulation (under the influence of accommodation) as a control study, to rule out the influence of pupil size on the accommodative response detected by the Power Refractor (Multi-channel Systems, Reutlingen, Germany) in Part A.

### **5.4.2 Subjects**

Ethics clearance was obtained from the Office of Research Ethics at the University of Waterloo before commencement of the study. Eligible subjects signed an informed consent document before enrolment in the study.

Data from the same subjects in Part A of this thesis were used for this control study. As a recap, fifteen healthy emmetropic subjects participated in this study. There were 8 male and 7 female volunteers ranging in age from 19 to 27. Subjects with self-reported binocular vision anomalies were excluded from the study. Two male subjects were excluded from the experiment because one was unable to complete the study due to personal reasons and the data from the other male participant did not meet the manufacturer's recommendation (the ocular alignment being less than 10 degrees and 5 degrees from the optical axis of the photorefractor in the horizontal and vertical axes respectively).

### **5.4.3 Power Refractor**

The Power Refractor (Multi-channel Systems, Reutlingen, Germany) was used to capture the pupil response to ocular surface stimulation in the accommodated eye. The binocular measurement setting was used, which provides information on the accommodative response along the vertical ocular meridian coupled with measurement of pupil diameter. Measurements of pupil size are made using a contrast detection

algorithm to locate the pupils and the first Purkinje image (personal communication with Vivek Labishietey).

#### **5.4.4 Computer-controlled Belmonte Esthesiometer**

The computer-controlled Belmonte esthesiometer from the experiments of Chapters 3 and 4 (and described in other studies [19-21]) was used for this set of experiments. Briefly, the modified device used for the delivery of mechanical and chemical stimuli to the ocular surface consists of a control box that electronically regulates the mixture of air and carbon dioxide (CO<sub>2</sub>). The flow rates of air and concentration of CO<sub>2</sub> are separately controlled by two digital flow controllers. Within the nozzle assembly is a thermostat to control temperature. A calibrated video camera was used to ensure that the stimulus was orthogonal to, and the nozzle tip was 5mm from the ocular surface.

#### **5.4.5 Nociceptive Stimuli**

Mechanical stimuli consisted of a series of air pulses with varying flow rates from 0 to 200 ml/min and chemical stimulation was delivered by increasing the concentration of CO<sub>2</sub> in the air while the subjects looked at a target 4 meters away. An ascending methods of limits[22] was used to determine mechanical and chemical detection thresholds of the cornea.

The mechanical threshold, which is the lowest air flow rate (with CO<sub>2</sub> set at 0%) that the subject could detect, was first determined. The flow-rate steps were set at 10

mL/min, and the mechanical threshold was the average of three readings when the subject first reported the stimulus. For determining the chemical threshold, the flow rate of air was set at half the initially determined mechanical threshold, and CO<sub>2</sub> was added to the air in increments of 5% CO<sub>2</sub>. The chemical threshold was the average of three first reports of stimulus detection.

#### **5.4.6 Stimulus Delivery**

Subjects wore in-ear headphones with noise playing in the background. The stimulus was presented at the corneal apex of the left eye while subjects viewed a fixation target that was 3 meters away. The tip of the esthesiometer was rotated to ensure the stimulus was delivered perpendicular to the corneal surface during stimulus delivery. The temperature of the air was set to 50°C, this decreased to 33.4°C at the ocular surface at room temperature of 23°C. This was calibrated using a custom electronic thermometer positioned 5 mm from the probe tip (which corresponds to the position of the ocular surface in the experiments). The duration of the stimulus was 2 seconds and it was delivered to the ocular surface immediately after a blink. The subject blinked freely between trials. The next stimulus was triggered after the sensation caused by the last stimulus had disappeared completely.

Once the mechanical and chemical thresholds were determined, three stimuli were then delivered to the subject in random order in both the mechanical and chemical

stimulation experiments – stimulus at 100% threshold, stimulus at 150% threshold, and stimulus at 200% threshold. Pupil size was captured simultaneously every 0.04 seconds by the Power Refractor (Multi-channel Systems, Reutlingen, Germany), while the subjects fixated on a single high contrast (85%) colour cartoon frame at 66cm for a period of 5 seconds prior to stimulus delivery (baseline) and after stimulus delivery.

## **5.5 Analyses**

Measurement of the pupil response at 25 Hz for 5 seconds provided a total of 125 data points. Each data point was screened and accepted if the following criteria were met: ocular alignment was less than 10 degrees and 5 degrees from the optical axis of the photorefractor in the horizontal and vertical axes respectively (as recommended by the manufacturer), and the responses were free of blinks. Each participant needed to have at least 113 rows of acceptable data after satisfying all the above criteria to be considered for further analysis. The pupil response for the left and right eye was averaged and all acceptable data points were used for the analysis.

Quantitative differences in pupil response, stimulus modality and intensity were analyzed using repeated measures ANOVA. Tukey HSD tests were used for all post hoc analysis. SPSS for Windows, Version 16.0 (Chicago, IL, SPSS Inc.) and Microsoft Excel for Windows (Redmond, WA, Microsoft Corp.) were used for data analysis. An alpha value of 0.05 or less was assumed to be significant.

## 5.6 Results

A summary of the mean ( $\pm$  SD) pupil response across the different stimulus intensities and modalities can be found in Table 7 below. Pupil response at baseline (before each measurement session), and with mechanical and chemical stimulation of differing intensities grouped by modality are shown in Figure 22.

**Table 7: Mean ( $\pm$  SD) pupil response across the different stimulus intensities in mechanical and chemical corneal stimulation experiments.**

	Stimulus Modality	Mean pupil Response	Std. Deviation
Baseline	Chemical	4.14	0.65
	Mechanical	4.13	0.73
	Total	4.14	0.69
100% Threshold	Chemical	3.97	0.55
	Mechanical	3.97	0.51
	Total	3.97	0.53
150% Threshold	Chemical	3.94	0.67
	Mechanical	3.98	0.64
	Total	3.96	0.65
200% Threshold	Chemical	3.94	0.72
	Mechanical	3.93	0.73
	Total	3.93	0.72

### **5.6.1.1 Effects of Stimulus Intensity on Pupil Response**

Pupil response increased between baseline and the maximum stimulus intensity (200% threshold) but there was no difference in pupil response between the stimulation intensities (100%, 150% and 200% threshold). This happened regardless of whether mechanical or chemical stimulation occurred (ANOVA  $F(3,9537) = 330.8, p < 0.05$ ; Tukey HSD, all  $p > 0.05$  except at 200% threshold).

### **5.6.1.2 Effects of Stimulus Modality and Stimulus Intensity on Pupil Response**

There was no difference in pupil response between chemical and mechanical stimulation based on stimulus intensity (ANOVA  $F(1,3179) = 0.03, p > 0.05$ ).

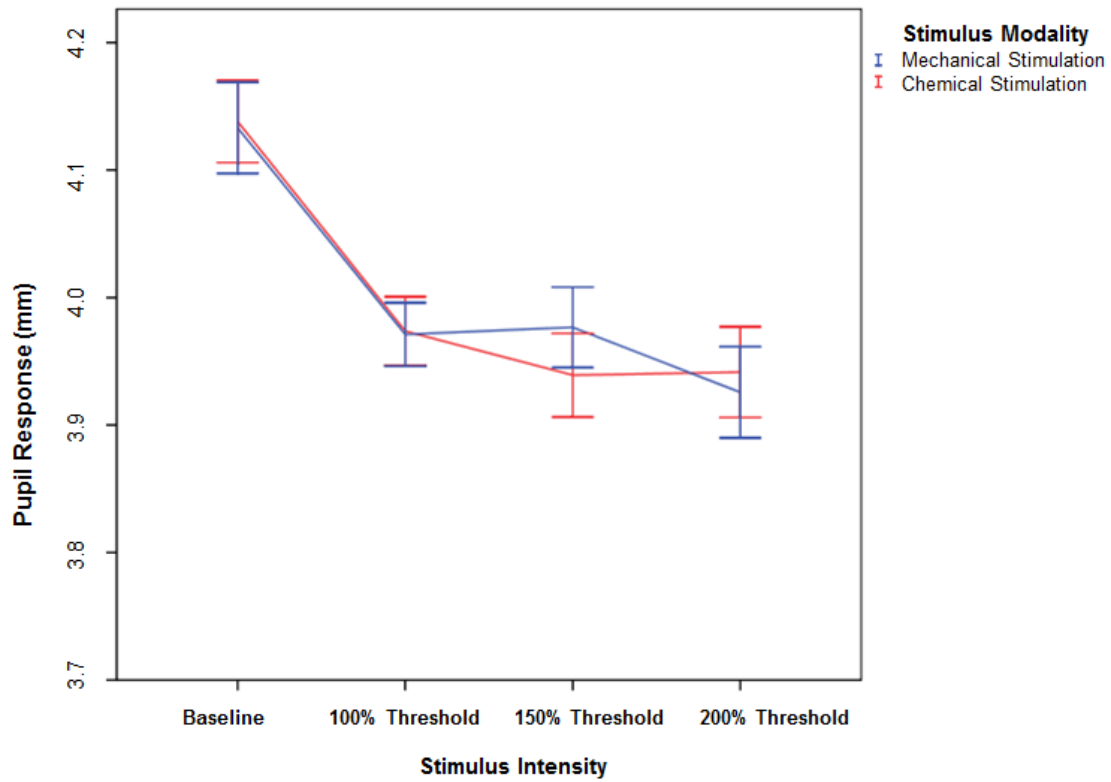


**Figure 22: Pupil response (in the accommodating eye) across different stimulus intensities for mechanical (blue) and chemical (red) corneal stimulation experiments (error bars denote 95% confidence interval).**

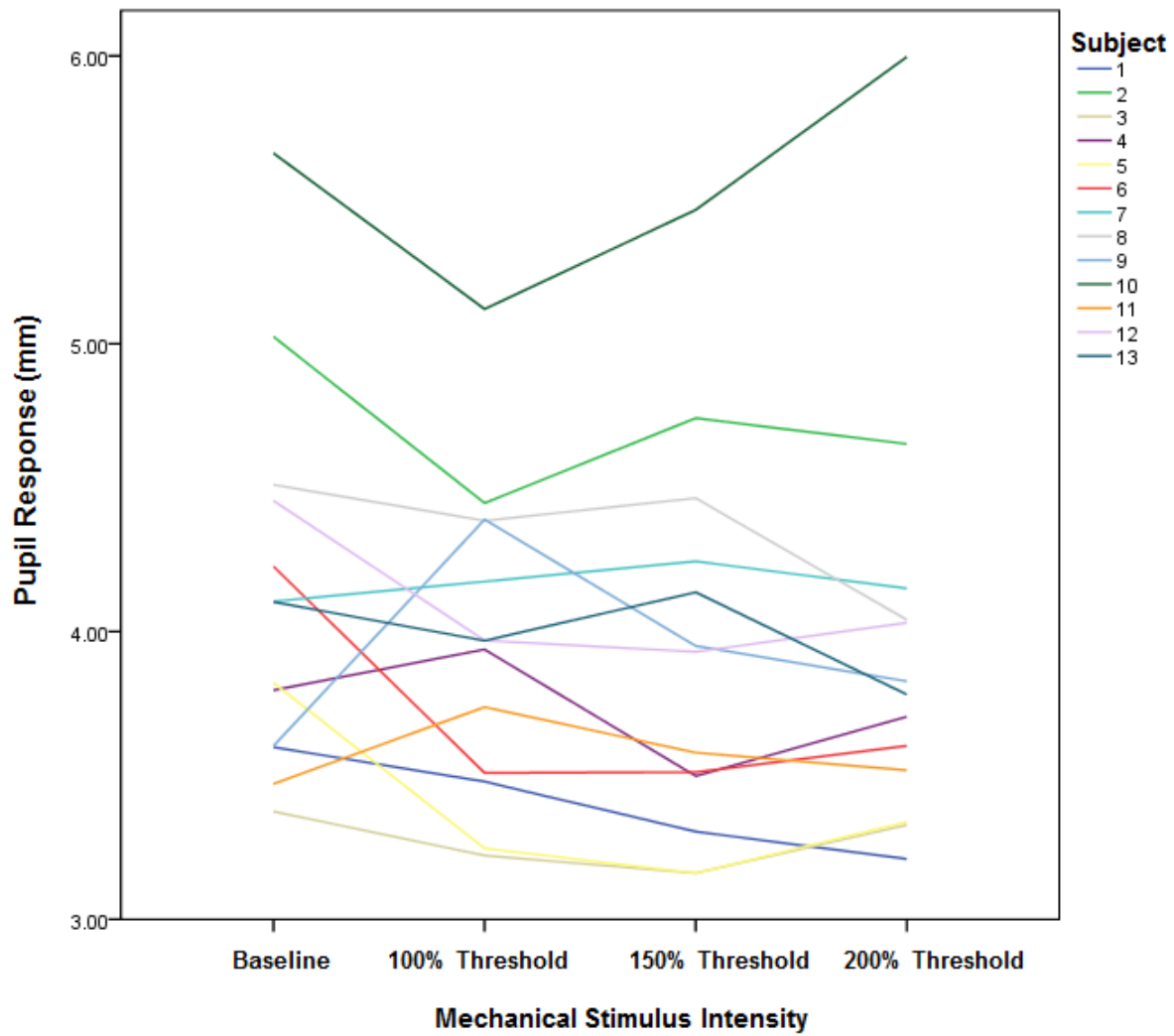


**Figure 23: The relationship between pupil response and stimulus intensity per subject during mechanical stimulation of the cornea.**

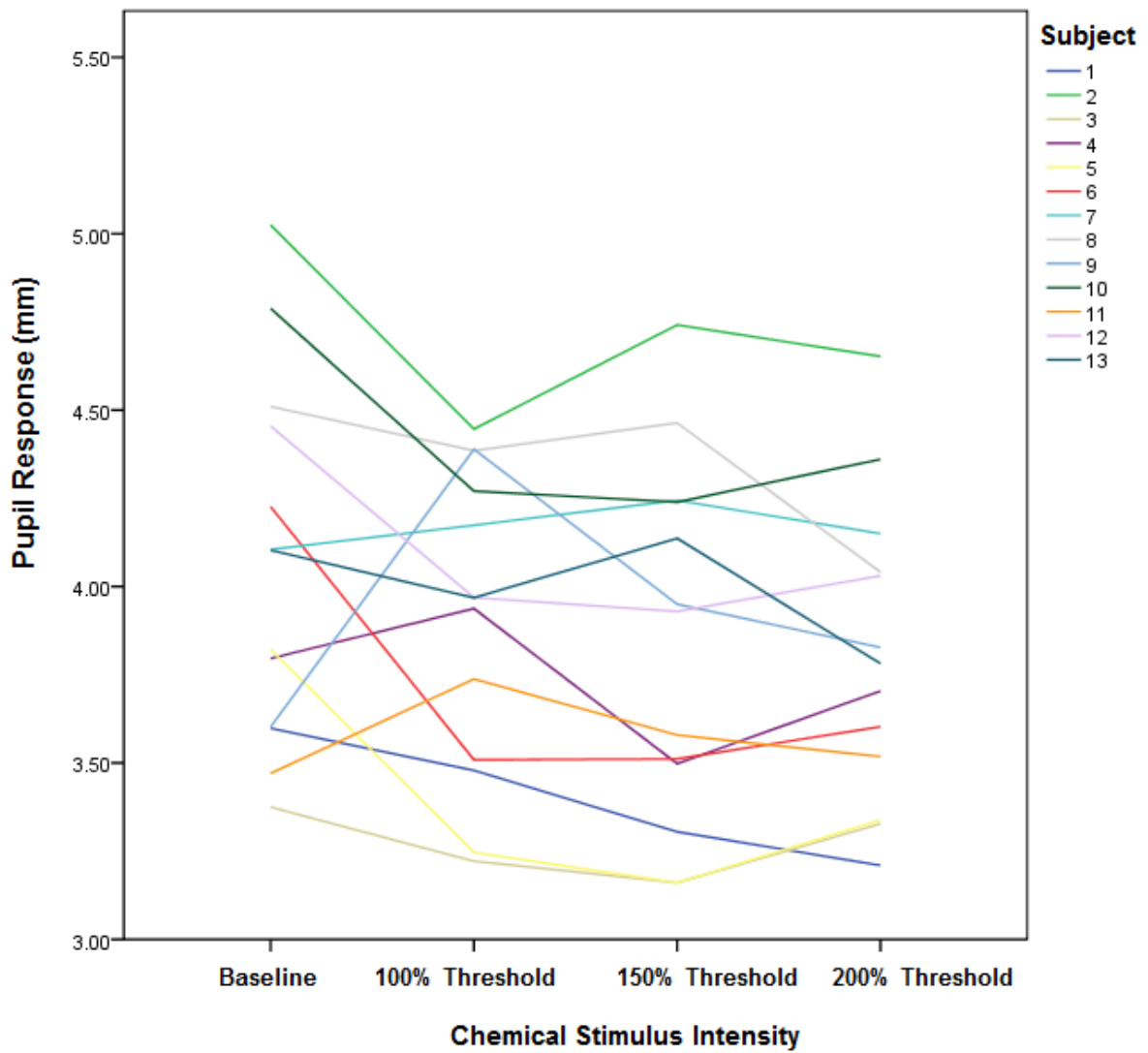


**Figure 24: The relationship between pupil response and stimulus intensity per subject during chemical stimulation of the cornea.**

## **5.7 Discussion**

In Part B of this chapter, I investigated the effect of ocular surface stimulation on the pupil response while the eyes were accommodating to a target at 66cm. The results of this control experiment suggest that there was no dose-dependent pupil response to chemical and mechanical noxious stimulation of the cornea, and provide support to rule out the suggestion that the increased accommodative response to ocular surface stimulation (Part A), was due to an artefact of the effect of pupil size on the accommodative response.

The pupil response to accommodation when viewing a visual stimulus has been studied extensively[29, 33-39] with findings that indicate that small pupils lead to increased low frequency fluctuations in accommodation which are independent of the mean accommodative response level. The experiment in Part B is different from other studies assessing the pupillary response to accommodation because of the introduction of noxious corneal stimulation. From the previous experiments in Chapter 4 of this thesis, (and from previous experiments assessing the pupil response to noxious stimulation[40-43]) there is an expectation that the pupils will dilate in response to ocular surface stimulation in a dose dependent manner but in the experiments of this chapter, the pupil response data is collected while the eyes are viewing an accommodative target and this may account for the smaller pupils observed in the results of Part B.

The results of Part A suggested an increase in the optical power of the eye after ocular surface stimulation. An increase in accommodation is associated with three key processes (convergence, pupillary constriction and an increase in dioptric power of the eye[15]), so I believe the increased accommodation (and convergence associated with accommodation) may be responsible for the pupil constriction in Experiment B. Both accommodation and pupillary constriction are mediated by the parasympathetic division of the ANS, and the association between these two parasympathetic responses can be traced to the EW nucleus[8, 44, 45]. Blur is the main stimulus to accommodation[6] and the pathway for visual blur starts at retina where information is transmitted through the optic nerve and reaches the lateral geniculate body (LGB). From the LGB, neural information is then transmitted to the visual cortex (V1) for further processing. From V1, the neural signal is translated into a motor command at the EW nucleus in the midbrain[8]. The efferent pathway involves transmission of the motor commands from the EW nucleus to the ciliary muscle in the eye via the third cranial nerve[13, 14]. When the motor command reaches the ciliary muscle, it contracts and releases the tension on the zonules which causes the crystalline lens to increase its optical power by becoming steeper in shape. The midbrain EW nucleus also controls circular fibres in the iris sphincter pupillae muscle to cause constriction of the pupils[45].

The explanation that increase in accommodation could be responsible for the pupil constriction response to ocular surface stimulation is questionable as research suggests that blur-driven accommodation on its own is not adequate to drive pupillary constriction[46, 47]. During experimentation, subjects switch from looking at a target 4 meters away (during stimulation with the esthesiometer) to viewing a near target at 0.66 meters (during pupil response acquisition with the photorefractor), and this is accompanied by a considerable amount of convergence. The effect of convergence on pupillary constriction is well documented[34, 47-49] and because of this association, I agree that the influence of both convergence and accommodation may be responsible for the pupil constriction response of the experiments in this chapter.

There are some limitations to the experiments in this chapter. Many questions remain unanswered as I was unable to use a stimulation intensity of more than 200% of the threshold. Does the accommodative/pupil constriction response increase as the stimulus intensity increases? Are there ceiling effects in the accommodative/pupil response? These questions could have been addressed with greater simulation intensity levels.

An accommodative target at 66cm was used to stimulate accommodation in the participants during experimentation. Varying the distance of this target can provide information as to the nature of the accommodative/pupil response that occurs including whether there is an increase or decrease in the accommodative/pupil response (associated to noxious stimulation) when viewing a closer target (more accommodative

demand). Finally, the effect of ocular surface stimulation on vergence can also be evaluated in a bid to either confirm or deny the notion that convergence and accommodation are responsible for the pupil constriction response observed in the experiments of this chapter.

## **5.8 Conclusion**

In summary, noxious stimulation of the cornea seems to produce a dose-dependent increase in the optical power of the eyes but not a dose-dependent pupil response and since there is no pupil effect with different doses different accommodative responses (from Part A) are not a pupil artefact but rather a dose dependent effect from the noxious stimulation. The behavior of the accommodative system when the cornea is stimulated can be due to mechanical effects of the ciliary body or artefacts introduced through the experimental design and/or instrumentation. Further investigation is required to characterise and quantify the relationship between accommodation, pupil response and noxious ocular surface stimulation.

## **Chapter 6**

### **General Discussion**

This thesis is the first of its kind to investigate the functional response of the autonomic nervous system (ANS) to ocular surface stimulation by measuring pupil size, ocular vascular variations and changes in the accommodative state of the eye after the delivery of noxious corneal stimuli. The results of the experiments contained in this thesis suggest that the ANS actively responds to ocular surface stimulation in a dose-response manner, so the amount of suprathreshold corneal stimulation causes a predictable increase in each autonomic measure (that is conjunctival blood flow, pupil size and accommodation).

The ANS is important to human functioning as it acts below the level of consciousness to regulate the organs of the body thus controlling secretory cells, smooth muscle and cardiac muscle[1]. In the eye, the ANS is responsible for the control of pupillary reflexes, accommodation and regulation of blood flow[2-4] among other functions. Monitoring the impact of sensory stimulation of the ocular surface on these autonomic reflex mechanisms has provided novel information about ANS functionality in healthy individuals.

This thesis has demonstrated that the physiological measures that represent the ANS response to ocular surface pain (namely pupil size, conjunctival redness and

accommodation), are accessible, quick to capture and cost effective to obtain. Take for example the experiments involving the pupillary response to corneal stimulation: two Logitech c920 cameras (Logitech International S.A., Newark, CA) each costing less than \$100 were used to capture the pupil dilation response to corneal pain.

There is literature to support that acquiring several measures of the ANS in its response to pain and combining these measures will provide better characterisation of the relationship that exists between the ANS and pain[5]. Therefore, the proof of concept that these autonomic responses do exist and are easily obtainable (as demonstrated by this thesis) will perhaps prove beneficial in the creation of innovative pain metrics.

The results of the experiments in this thesis showed that with increasing stimulation of the cornea, there were corresponding increases in conjunctival blood flow, pupil size and accommodation. Belmonte et al (2015) describe nociceptors as “peripheral sensory fibers acting as specific detectors for injurious stimuli”; however, the collective responses of the different components of the ANS evoked by ocular surface stimulation may provide some support to the idea that corneal nociceptors might have additional roles other than the detection of pain. Probable explanations for why each autonomic response occurs in the first place might provide us with some insight into the auxiliary functional roles corneal nociceptors may play in addition to its primary role of sensation.

In Chapter 3, the stimulated eye appeared redder than the unstimulated eye, which suggests that corneal nociceptors may be involved in some form of local blood flow regulation on the ocular surface. Research supports the idea that both an axon reflex mechanism and a central neuronal reflex mechanism may drive the increase in conjunctival blood flow that occurs with ocular surface stimulation, thus highlighting possible vascular regulatory roles corneal nociceptors may be involved in[6-10]. Further investigation is needed into the auxiliary role corneal nociceptors may play in conjunctival blood flow regulation during suprathreshold ocular surface stimulation. Pupil dilation has been linked to an increase in concentration[11, 12] and attention[11, 13, 14], therefore the pupil dilation response experienced with suprathreshold corneal stimulation may be indicative of a warning mechanism initiated by corneal nociceptors to increase an individual's alertness and prepare for impending danger. The exact mechanism through which corneal nociceptors may cause pupil changes is unknown and further investigation is required to elucidate this; however, based on literature, I propose a neural connection between the corneal nociceptors and the locus coeruleus (LC). The LC modulates pupil dilation by releasing norepinephrine which results in an inhibitory effect on the parasympathetic oculomotor complex[15]. With the exception of the basal ganglia, the LC (which is a brainstem nucleus found in the rostral pons) sends noradrenergic projections to all other regions of the brain[16]. The greatest projections from the LC are towards the parietal cortex, superior colliculus and the

thalamus[17, 18]. While the parietal cortex and superior colliculus play a role in attentional processing[17], the thalamus is involved in pain processing including that which occurs at the ocular surface[19]. It is therefore feasible to hypothesize that a link between ocular surface pain processing, pupil dilation and attentional processing is likely to exist and may be modulated by the LC.

In Chapter 5 of this thesis, there was an increase in accommodation in response to ocular surface stimulation. A possible explanation for the increase in accommodation due to corneal stimulation could be because minor changes in the mechanical characteristics of the ciliary body cause small shifts in accommodation[20]. Chapter 3 of this thesis suggests that there is increased blood flow to the ocular surface when the cornea is stimulated. The increase in conjunctival blood flow may bring about the slight changes in accommodation observed in Chapter 5 because the ciliary body and conjunctival vessels are supplied by the same vascular source[21]. Simultaneously imaging the ciliary body and crystalline lens (perhaps using anterior segment optical coherence tomography) while delivering nociceptive stimuli to the cornea could provide information regarding what exactly occurs to the accommodative mechanism during ocular surface stimulation.

The association between ocular surface pain and increase in accommodation can perhaps be supported by the use of cycloplegia to treat ocular pain in ophthalmology. Cycloplegia (the temporary paralysis of the ciliary muscle which causes a loss of

accommodation and also induces pupillary mydriasis) has been used to treat ocular surface pain[22-24], uveitis [25] and post photorefractive surgery pain [26]. It is possible that minor changes in the mechanical characteristics of the ciliary body brought about by ocular surface stimulation contribute to increased ciliary spasms that lead to ocular pain therefore, paralysing the ciliary muscle reduces mechanical influence on the ciliary body brought about by the conjunctival vasculature and leads to a greater reduction of ocular pain. A simple experiment involving the instillation of a topical vasoconstrictor followed by delivery of ocular surface stimulation while observing the pre- and post-stimulus accommodative response can help identify the true impact of conjunctival blood flow on the accommodative mechanism.

Temporal effects were a major influence in the studies conducted in this thesis. For the experiments in Chapter 4 and 5, a nonlinear regression model was adopted to describe the influence of time on the pupil response and accommodation. Using a non-linear approach to identify the effect of stimulus intensity on pupil size and accommodation over time is accurate because every time point is considered. The accommodative/pupil response to ocular surface stimulation is not monotonic, therefore, an analysis using an averaging procedure is problematic as a positive accommodative response can be canceled out by a negative accommodative response. Similarly, pupil dilation can be cancelled out by pupil constriction.

Two stimulus modalities were used in all the experiments of this thesis (mechanical and chemical stimulation). For the experiments of Chapter 3, there was a difference in effect of chemical and mechanical stimulation on conjunctival redness. In the pupil response experiments, there was no statistical difference in the effect of chemical and mechanical stimulation on pupil size; however, visual inspection of the effect of stimulus intensity on pupil diameter chart (Figure 12) will reveal that the pupil diameters associated with chemical stimulation are marginally greater than that associated with mechanical stimulation at the greatest stimulus intensities. A similar observation can be made in the results of the experiments involving accommodative response. These observations may be attributed to the greater amount of time a chemical stimulus has on the surface of the eye in comparison to a mechanical stimulus.

When a chemical stimulus (CO<sub>2</sub> mixed with air) is applied to the cornea, CO<sub>2</sub> mixes with the tears on the surface of the eye resulting in a more acidic tear film[27]. This acidic mixture has been shown to have effects similar to that produced by tissue acidosis resulting inflammation or infection, and appear to stimulate corneal C fibers through the mediation of ASICs and VR1 receptors[28, 29]. CO<sub>2</sub> remains in the tears even after stimulus delivery and the longer exposure may contribute to the greater autonomic responses experienced when a chemical stimulus is applied to the cornea, as opposed to mechanical corneal stimulation.

The experimental design used in this thesis was susceptible to sequential and timing effects. It is not uncommon that (because of superstitious behavior or the inappropriate linking of a stimulus presentation with consequences) participants can identify hidden patterns when stimuli are presented in a genuinely random manner[30, 31]. Research shows that subjects' responses are biased if stimulus delivery is associated with a pattern[32]. As an example, in the detection threshold component of the experiments of this thesis, stimuli were presented to all subjects using an ascending method of limits, depending on the number of stimulus presentations required to detect the threshold, a subject may have identified the ascending nature of the stimulus delivery and provided a response well below/above his/her threshold, which would in turn influence the suprathreshold stimulus delivery component of the experiments.

Time was a factor that played a significant role in all the trials. Apart for the temporal effects associated with autonomic responses (explained above), the amount of time that subjects kept their eyes open could have impacted the autonomic responses. Take for example the experiments of Chapter 3 (conjunctival redness response to ocular surface stimulation). The subject's eyes remained open at different stages throughout threshold detection as well as suprathreshold stimulus delivery. The increasing amount of time that the eyes remain open causes ocular surface irritation which may cause an increase in conjunctival blood flow (redness)[33-36]. Increased conjunctival blood flow can

impact the ciliary body vasculature which may affect accommodation and influence the experiments of Chapter 5.

The impact time has on the experiments in this thesis can only be controlled to a certain extent. One way to limit this impact was to ensure that all the subjects within each set of experiments experienced suprathreshold delivery and autonomic response data acquisition within the same period. Clearly this was not possible during threshold detection as the exposure would be based on how high or low a subject's detection threshold was for a stimulus. The impact of time is a shortcoming that needs to be addressed in future ocular reflex studies.

This thesis has demonstrated that dose dependent relationships exist between ocular surface stimulation and autonomic responses. The autonomic responses to noxious stimulation are accessible and relatively easy to measure with the use of simple, cost-effective instruments. Jointly, the autonomic response measures (namely conjunctival blood flow, pupil size changes and accommodation) and their relationship with corneal stimulation enable us, for the first time, to characterise the local stimulus-response neural circuitry, relating nociceptive stimuli to autonomic responses. This in and of itself is important, and sets the foundation to enable us to develop novel objective metrics of ocular surface pain, something very important in non-communicative patients and in infants.

## **Chapter 7**

### **Future Work**

In this thesis, single autonomic responses were evaluated before and after noxious stimulation to the cornea. Treister et al[1] suggest that combining several autonomic measures would provide more accurate relationship information to pain in comparison to single measures, so for future work, I hope to monitor multiple autonomic measures simultaneously before and after stimulus delivery. For example, the experiment can be modified to measure the conjunctival redness, accommodative and pupillary response to noxious stimulation at the same time.

The corneal stimulus modalities used in the experiments in this thesis were mechanical and chemical; however, the cornea responds to thermal stimulation[2, 3] as well so future studies should be designed to assess the effect of thermal corneal stimulation on autonomic measures.

Neuroimaging is the use of imaging techniques to directly or indirectly capture the structure function of the nervous system, and includes brain imaging techniques such as magnetic resonance imaging (MRI), cranial ultrasound, and positron emission tomography, among others[4]. Information regarding activation areas of the brain during the interaction between autonomic responses and noxious corneal stimulation can be acquired by incorporating neuroimaging to the experiments performed in this

thesis. In an attempt to predict pain from autonomic responses, subjective pain ratings can be incorporated for each stimulus intensity, the relationship between stimulus intensity, autonomic response and pain rating can then be analyzed in a parametric way[5].

The experiments of this thesis used noxious corneal stimulation and for future work I would like to incorporate other noxious stimulation techniques such as pressure to the finger tips and tooth pulp while observing the ocular responses (if any) to the different stimulation methods.

# Letter of Copyright Permission

## ELSEVIER LICENSE TERMS AND CONDITIONS

Nov 23, 2017

This Agreement between University of Waterloo ("You") and Elsevier ("Elsevier") consists of your license details and the terms and conditions provided by Elsevier and Copyright Clearance Center.

License Number	4234960140896
License date	Nov 23, 2017
Licensed Content Publisher	Elsevier
Licensed Content Publication	The Ocular Surface
Licensed Content Title	TFOS DEWS II Report Executive Summary
Licensed Content Author	Jennifer P. Craig, J. Daniel Nelson, Dimitri T. Azar, Carlos Belmonte, Anthony J. Bron, Sunil K. Chauhan, Cintia S. de Paiva, José A. P. Gomes, Katherine M. Hammitt, Lyndon Jones, Jason J. Nichols, Kelly K. Nichols, Gary D. Novack, Fiona J. Stapleton et al.
Licensed Content Date	Oct 1, 2017
Licensed Content Volume	15
Licensed Content Issue	4
Licensed Content Pages	11
Start Page	802
End Page	812
Type of Use	reuse in a thesis/dissertation
Portion	figures/tables/illustrations
Number of figures/tables/illustrations	1
Format	both print and electronic
Are you the author of this Elsevier article?	No
Will you be translating?	No
Original figure numbers	Figure 2
Title of your thesis/dissertation	Autonomic Responses to Ocular Surface Stimuli
Expected completion date	Dec 2017
Estimated size (number of pages)	180
Requestor Location	University of Waterloo 200 university ave w  waterloo, ON n2l3g1 Canada Attn: University of Waterloo

## **Bibliography**

### Chapter 1

1. Knop E, Knop N. Anatomy and immunology of the ocular surface. *Immune Response and the Eye*. 92: Karger Publishers; 2007. p. 36-49.
2. Kaufman PL, Adler FH, Levin LA, Alm A. *Adler's Physiology of the Eye*: Elsevier Health Sciences; 2011.
3. Feng Y, Simpson TL. Corneal, limbal, and conjunctival epithelial thickness from optical coherence tomography. *Optometry & Vision Science*. 2008;85(9):E880-E3.
4. Reinstein DZ, Archer TJ, Gobbe M, Coleman DJ, Silverman RH. Epithelial thickness in the normal cornea: three-dimensional display with Artemis very high-frequency digital ultrasound. *Journal of Refractive Surgery*. 2008;24(6):571-81.
5. Oyster CW. *The human eye: structure and function*: Sinauer Associates; 1999.
6. Jacobsen IE, Jensen O, Prause J. Structure and composition of Bowman's membrane. *Acta Ophthalmologica*. 1984;62(1):39-53.
7. Tao A, Wang J, Chen Q, Shen M, Lu F, Dubovy SR. Topographic thickness of Bowman's layer determined by ultra-high resolution spectral domain–optical coherence tomography. *Investigative Ophthalmology & Visual Science*. 2011;52(6):3901-7.

8. Reinstein DZ, Archer TJ, Gobbe M, Silverman RH, Coleman DJ. Stromal thickness in the normal cornea: three-dimensional display with Artemis very high-frequency digital ultrasound. *Journal of Refractive Surgery*. 2009;25(9):776-86.
9. Hanlon SD, Behzad AR, Sakai LY, Burns AR. Corneal stroma microfibrils. *Experimental Eye Research*. 2015;132:198-207.
10. Eghrari AO, Riazuddin SA, Gottsch JD. Chapter two-overview of the cornea: structure, function, and development. *Progress in Molecular Biology and Translational Science*. 2015;134:7-23.
11. Bourne WM, Nelson LR, Hodge DO. Central corneal endothelial cell changes over a ten-year period. *Investigative Ophthalmology & Visual Science*. 1997;38(3):779-82.
12. Waring GO, Bourne WM, Edelhauser HF, Kenyon KR. The corneal endothelium: normal and pathologic structure and function. *Ophthalmology*. 1982;89(6):531-90.
13. Bourne WM, McLaren JW. Clinical responses of the corneal endothelium. *Experimental Eye Research*. 2004;78(3):561-72.

14. Zavala J, Jaime GL, Barrientos CR, Valdez-Garcia J. Corneal endothelium: developmental strategies for regeneration. *Eye*. 2013;27(5):579.
15. Galloway NR, Amoaku WM, Galloway PH, Browning AC. Basic anatomy and physiology of the eye. *Common Eye Diseases and their Management*: Springer; 2016. p. 7-16.
16. Davson H. *Physiology of the Eye*: Elsevier; 2012.
17. Zhang X, Li Q, Xiang M, Zou H, Liu B, Zhou H. Bulbar conjunctival thickness measurements with optical coherence tomography in healthy chinese subjects. *Investigative Ophthalmology & Visual Science*. 2013;54(7):4705-9.
18. Ueta M, Kinoshita S. Ocular surface inflammation is regulated by innate immunity. *Progress in Retinal and Eye research*. 2012;31(6):551-75.
19. Kobayashi A, Yoshita T, Sugiyama K. In vivo findings of the bulbar/palpebral conjunctiva and presumed meibomian glands by laser scanning confocal microscopy. *Cornea*. 2005;24(8):985-8.
20. Efron N, Al-Dossari M, Pritchard N. Confocal microscopy of the bulbar conjunctiva in contact lens wear. *Cornea*. 2010;29(1):43-52.

21. Stevenson W, Chauhan SK, Dana R. Dry eye disease: an immune-mediated ocular surface disorder. *Archives of Ophthalmology*. 2012;130(1):90-100.
22. Bizheva K, Hutchings N, Sorbara L, Moayed AA, Simpson T. In vivo volumetric imaging of the human corneo-scleral limbus with spectral domain OCT. *Biomedical Optics Express*. 2011;2(7):1794-802.
23. Sweeney DF, Millar TJ, Raju SR. Tear film stability: a review. *Experimental Eye Research*. 2013;117:28-38.
24. Hong J, Sun X, Wei A, Cui X, Li Y, Qian T. Assessment of tear film stability in dry eye with a newly developed keratograph. *Cornea*. 2013;32(5):716-21.
25. Fukuda R, Usui T, Miyai T, Yamagami S, Amano S. Tear meniscus evaluation by anterior segment swept-source optical coherence tomography. *American Journal of Ophthalmology*. 2013;155(4):620-4. e2.
26. Holly FJ. Tear film physiology. *Optometry and Vision Science*. 1980;57(4):252-7.

27. Lemke BN, Lucarelli MJ. Anatomy of the ocular adnexa, orbit, and related facial structures. *Smith and Nesi's Ophthalmic Plastic and Reconstructive Surgery*: Springer; 2012. p. 3-58.
28. Whitney JB. The anatomy of the ocular adnexa. *Archives of Ophthalmology*. 1975;93(11):1226-.
29. Broekhuysen R. Lactoferrin and the protective function of the lacrimal fluid. *Ophthalmologica*. 1976;173(3-4):268-70.
30. Craig J, Blades K, Patel S. Tear lipid layer structure and stability following expression of the meibomian glands. *Ophthalmic and Physiological Optics*. 1995;15(6):569-74.
31. Stern ME, Beuerman RW, Fox RI, Gao J, Mircheff AK, Pflugfelder SC. A unified theory of the role of the ocular surface in dry eye. *Lacrimal Gland, Tear Film, and Dry Eye Syndromes 2*: Springer; 1998. p. 643-51.
32. Shaheen BS, Bakir M, Jain S. Corneal nerves in health and disease. *Survey of Ophthalmology*. 2014;59(3):263-85.

33. MacIver MB, Tanelian DL. Free nerve ending terminal morphology is fiber type specific for A delta and C fibers innervating rabbit corneal epithelium. *Journal of Neurophysiology*. 1993;69(5):1779-83.
34. Conrady CD, Joos ZP, Patel BC. The lacrimal gland and its role in dry eye. *Journal of Ophthalmology*. 2016;32(7):177-83.
35. Scott G, Balsiger H, Kluckman M, Fan J, Gest T. Patterns of innervation of the lacrimal gland with clinical application. *Clinical Anatomy*. 2014;27(8):1174-7.
36. Sabatino F, Di Zazzo A, De Simone L, Bonini S. The intriguing role of neuropeptides at the ocular surface. *The Ocular Surface*. 2017;15(1):2-14.
37. Ruskell G. Ocular fibres of the maxillary nerve in monkeys. *Journal of Anatomy*. 1974;118(Pt 2):195.
38. Belmonte C, Acosta MC, Merayo-Llodes J, Gallar J. What causes eye pain? *Current Ophthalmology Reports*. 2015;3(2):111-21.
39. Belmonte C, Nichols JJ, Cox SM, Brock JA, Begley CG, Bereiter DA. TFOS DEWS II Pain and sensation report. *The Ocular Surface*. 2017.

40. Müller L, Vrensen G, Pels L, Cardozo BN, Willekens B. Architecture of human corneal nerves. *Investigative Ophthalmology & Visual Science*. 1997;38(5):985-94.
41. González-González O, Bech F, Gallar J, Merayo-Llodes J, Belmonte C. Functional properties of sensory nerve terminals of the mouse. *Investigative Ophthalmology & Visual Science*. 2017;58(1):404-15.
42. Belmonte C, Aracil A, Acosta MC, Luna C, Gallar J. Nerves and sensations from the eye surface. *The Ocular Surface*. 2004;2(4):248-53.
43. Belmonte C, Garcia-Hirschfeld J, Gallar J. Neurobiology of ocular pain. *Progress in Retinal and Eye Research*. 1997;16(1):117-56.
44. Feng Y, Simpson TL. Nociceptive sensation and sensitivity evoked from human cornea and conjunctiva stimulated by CO<sub>2</sub>. *Investigative Ophthalmology & Visual Science*. 2003;44(2):529-32.
45. Acosta MC, Tan ME, Belmonte C, Gallar J. Sensations evoked by selective mechanical, chemical, and thermal stimulation of the conjunctiva and cornea. *Investigative Ophthalmology & Visual Science*. 2001;42(9):2063-7.

46. Adriaensen H, Gybels J, Handwerker H, Van Hees J. Response properties of thin myelinated (A-delta) fibers in human skin nerves. *Journal of Neurophysiology*. 1983;49(1):111-22.
47. Ahlquist M, Franzén O. Pulpal ischemia in man: effects on detection threshold, A-delta neural response and sharp dental pain. *Dental Traumatology*. 1999;15(1):6-16.
48. Belmonte C, Acosta MC, Schmelz M, Gallar J. Measurement of corneal sensitivity to mechanical and chemical stimulation with a CO<sub>2</sub> esthesiometer. *Investigative Ophthalmology & Visual Science*. 1999;40(2):513-9.
49. Belmonte C, Brock JA, Viana F. Converting cold into pain. *Experimental Brain Research*. 2009;196(1):13-30.
50. Acosta MC, Belmonte C, Gallar J. Sensory experiences in humans and single-unit activity in cats evoked by polymodal stimulation of the cornea. *The Journal of Physiology*. 2001;534(2):511-25.
51. Gallar J, Santiago B, Acosta MC, Belmonte C. In vivo functional characterization of trigeminal neurons innervating the eye and periocular tissues. *Investigative Ophthalmology & Visual Science*. 2014;55(13):3645-.

52. Brock J, Acosta MC, Al Abed A, Pianova S, Belmonte C. Barium ions inhibit the dynamic response of guinea-pig corneal cold receptors to heating but not to cooling. *The Journal of Physiology*. 2006;575(2):573-81.
53. Carr RW, Pianova S, Fernandez J, Fallon JB, Belmonte C, Brock JA. Effects of heating and cooling on nerve terminal impulses recorded from cold-sensitive receptors in the guinea-pig cornea. *The Journal of General Physiology*. 2003;121(5):427-39.
54. Sauer SK, Weidner C, Carr RW, Averbeck B, Nesnidal U, Reeh PW. Can receptor potentials be detected with threshold tracking in rat cutaneous nociceptive terminals? *Journal of Neurophysiology*. 2005;94(1):219-25.
55. Belmonte C, Gallar J. Cold thermoreceptors, unexpected players in tear production and ocular dryness sensations. *Investigative Ophthalmology & Visual Science*. 2011;52(6):3888-92.
56. Madrid R, Donovan-Rodríguez T, Meseguer V, Acosta MC, Belmonte C, Viana F. Contribution of TRPM8 channels to cold transduction in primary sensory neurons and peripheral nerve terminals. *Journal of Neuroscience*. 2006;26(48):12512-25.

57. Gallar J, Acosta MC, Belmonte C. Activation of scleral cold thermoreceptors by temperature and blood flow changes. *Investigative Ophthalmology & Visual Science*. 2003;44(2):697-705.
58. Parra A, Madrid R, Echevarria D, Del Olmo S, Morenilla-Palao C, Acosta MC, et al. Ocular surface wetness is regulated by TRPM8-dependent cold thermoreceptors of the cornea. *Nature Medicine*. 2010;16(12):1396-9.
59. MacIver M, Tanelian DL. Structural and functional specialization of A delta and C fiber free nerve endings innervating rabbit corneal epithelium. *Journal of Neuroscience*. 1993;13(10):4511-24.
60. Tanelian D, Beuerman R. Responses of rabbit corneal nociceptors to mechanical and thermal stimulation. *Experimental Neurology*. 1984;84(1):165-78.
61. Belmonte C, Acosta MC, Gallar J. Neural basis of sensation in intact and injured corneas. *Experimental Eye Research*. 2004;78(3):513-25.
62. Chen X, Gallar J, Pozo MA, Baeza M, Belmonte C. CO<sub>2</sub> stimulation of the cornea: a comparison between human sensation and nerve activity in polymodal nociceptive afferents of the cat. *European Journal of Neuroscience*. 1995;7(6):1154-63.

63. Murphy PJ, Patel S, Marshall J. A new non-contact corneal aesthesiometer (NCCA). *Ophthalmic and Physiological Optics*. 1996;16(2):101-7.
64. Chen J, Feng Y, Simpson TL. Human corneal adaptation to mechanical, cooling, and chemical stimuli. *Investigative Ophthalmology & Visual Science*. 2010;51(2):876-81.
65. Hagan CE, Bolon B, Keene CD. Nervous system. *Nucleus*. 2012;6(S1):S2-S4.
66. Chiel HJ, Beer RD. The brain has a body: adaptive behavior emerges from interactions of nervous system, body and environment. *Trends in Neurosciences*. 1997;20(12):553-7.
67. Lovallo W, Sollers J. *Autonomic nervous system*. 2000.
68. Gabella G. *Autonomic nervous system: Wiley Online Library*; 2001.
69. Goyal RK, Hirano I. The enteric nervous system. *New England Journal of Medicine*. 1996;334(17):1106-15.
70. Low PA. Autonomic nervous system function. *Journal of Clinical Neurophysiology*. 1993;10(1):14-27.

71. Neuhuber W, Schrödl F. Autonomic control of the eye and the iris. *Autonomic Neuroscience*. 2011;165(1):67-79.
72. Davies LN, Wolffsohn JS, Gilmartin B. Autonomic correlates of ocular accommodation and cardiovascular function. *Ophthalmic and Physiological Optics*. 2009;29(4):427-35.
73. Hoeks B, Levelt WJ. Pupillary dilation as a measure of attention: A quantitative system analysis. *Behavior Research Methods*. 1993;25(1):16-26.
74. Steinhauer SR, Siegle GJ, Condray R, Pless M. Sympathetic and parasympathetic innervation of pupillary dilation during sustained processing. *International Journal of Psychophysiology*. 2004;52(1):77-86.
75. Geuter S, Gamer M, Onat S, Büchel C. Parametric trial-by-trial prediction of pain by easily available physiological measures. *Pain*. 2014;155(5):994-1001.
76. Barvais L, Engelman E, Eba J, Coussaert E, Cantraine F, Kenny G. Effect site concentrations of remifentanyl and pupil response to noxious stimulation. *British Journal of Anaesthesia*. 2003;91(3):347-52.

77. Chapman CR, Oka S, Bradshaw DH, Jacobson RC, Donaldson GW. Phasic pupil dilation response to noxious stimulation in normal volunteers: relationship to brain evoked potentials and pain report. *Psychophysiology*. 1999;36(1):44-52.
78. Daluwatte C, Miles J, Sun J, Yao G. Association between pupillary light reflex and sensory behaviors in children with autism spectrum disorders. *Research in developmental disabilities*. 2015;37:209-15.
79. Harle DE, Wolffsohn JS, Evans BJ. The pupillary light reflex in migraine. *Ophthalmic and Physiological Optics*. 2005;25(3):240-5.
80. Kase M, Nagata R, Yoshida A, Hanada I. Pupillary light reflex in amblyopia. *Investigative Ophthalmology & Visual Science*. 1984;25(4):467-71.
81. Rukmini A, Milea D, Aung T, Gooley JJ. Pupillary responses to short-wavelength light are preserved in aging. *Scientific Reports*. 2017;7.
82. Do MTH, Yau K-W. Intrinsically photosensitive retinal ganglion cells. *Physiological Reviews*. 2010;90(4):1547-81.
83. Ellis C. The pupillary light reflex in normal subjects. *British Journal of Ophthalmology*. 1981;65(11):754-9.

84. Lucas RJ, Douglas RH, Foster RG. Characterization of an ocular photopigment capable of driving pupillary constriction in mice. *Nature Neuroscience*. 2001;4(6):621.
85. Panda S, Provencio I, Tu DC, Pires SS, Rollag MD, Castrucci AM, et al. Melanopsin is required for non-image-forming photic responses in blind mice. *Science*. 2003;301(5632):525-7.
86. Joo HR, Peterson BB, Dacey DM, Hattar S, Chen S-K. Recurrent axon collaterals of intrinsically photosensitive retinal ganglion cells. *Visual Neuroscience*. 2013;30(4):175-82.
87. Sun F, Tauchi P, Stark L. Dynamic pupillary response controlled by the pupil size effect. *Experimental neurology*. 1983;82(2):313-24.
88. Werner L, Trindade F, Pereira F, Werner L. Physiology of accommodation and presbyopia. *Arquivos Brasileiros de Oftalmologia*. 2000;63(6):487-93.
89. Croft MA, Glasser A, Kaufman PL. Accommodation and presbyopia. *International Ophthalmology Clinics*. 2001;41(2):33-46.

90. Lütjen-Drecoll E, Kaufman PL, Wasielewski R, Ting-Li L, Croft MA. Morphology and accommodative function of the vitreous zonule in human and monkey eyes. *Investigative Ophthalmology & Visual Science*. 2010;51(3):1554-64.
91. Chen JC, Schmid KL, Brown B. The autonomic control of accommodation and implications for human myopia development: a review. *Ophthalmic and Physiological Optics*. 2003;23(5):401-22.
92. Shinoe T, Matsui M, Taketo MM, Manabe T. Modulation of synaptic plasticity by physiological activation of M1 muscarinic acetylcholine receptors in the mouse hippocampus. *Journal of Neuroscience*. 2005;25(48):11194-200.
93. Jiang Y, Li YR, Tian H, Ma M, Matsunami H. Muscarinic acetylcholine receptor M3 modulates odorant receptor activity via inhibition of  $\beta$ -arrestin-2 recruitment. *Nature Communications*. 2015;6:6448.
94. Gilmartin B, Mallen E, Wolffsohn J. Sympathetic control of accommodation: evidence for inter-subject variation. *Ophthalmic and Physiological Optics*. 2002;22(5):366-71.

95. Merskey H, Bogduk N. Classification of chronic pain, IASP Task Force on Taxonomy. Seattle, WA: International Association for the Study of Pain Press (Also available online at [www.iasp-pain.org](http://www.iasp-pain.org)). 1994.
96. Williams ACdC, Craig KD. Updating the definition of pain. *Pain*. 2016;157(11):2420-3.
97. Dallenbach KM. Pain: history and present status. *The American Journal of Psychology*. 1939;52(3):331-47.
98. Gruner OC. *A Treatise on the Canon of Medicine of Avicenna. Incorporating a Translation of the First Book*. 1984.
99. Keele K. *Anatomies of Pain*, Charles C. Thomas, Springfield, Illinois. 1957.
100. Sherrington C. *The integrative action of the nervous system*: CUP Archive; 1910.
101. Hardy JD, Wolff HG, Goodell H. *Pain sensations and reactions*. 1952.
102. Tursky B. The development of a pain perception profile: a psychophysical approach. *Pain: New Perspectives in Therapy and Research*. 1976:171-94.

103. Melzack R, Casey KL. Sensory, motivational and central control determinants of pain: a new conceptual model. *The Skin Senses*. 1968;1.
104. Patel NB. Physiology of pain. *Guide to pain management in low-resource settings*. 2010:13.
105. Edmeads J. The physiology of pain: a review. *Progress in Neuro-Psychopharmacology and Biological Psychiatry*. 1983;7(4):413-9.
106. Engel GL. “Psychogenic” pain and the pain-prone patient. *The American Journal of Medicine*. 1959;26(6):899-918.
107. Boyce-Rustay JM, Jarvis MF. Neuropathic pain: models and mechanisms. *Current Pharmaceutical Design*. 2009;15(15):1711-6.
108. Diatchenko L, Nackley AG, Slade GD, Fillingim RB, Maixner W. Idiopathic pain disorders—pathways of vulnerability. *Pain*. 2006;123(3):226-30.
109. Baron R, Binder A. How neuropathic is sciatica? The mixed pain concept. *Der Orthopade*. 2004;33(5):568-75.

110. Kanerva L, Tarvainen K, Pinola A, Leino T, Granlund H, Estlander T, et al. A single accidental exposure may result in a chemical burn, primary sensitization and allergic contact dermatitis. *Contact Dermatitis*. 1994;31(4):229-35.
111. Pasero C, Paice JA, McCaffery M. Basic mechanisms underlying the causes and effects of pain. *Pain: Clinical Manual 2nd Edition* St Louis: Mosby. 1999:15-34.
112. Farquhar-Smith WP. Anatomy, physiology and pharmacology of pain. *Anaesthesia and Intensive Care Medicine*. 2008;9(1):3-7.
113. Dickenson A. Spinal cord pharmacology of pain. *British Journal of Anaesthesia*. 1995;75(2):193-200.
114. Fechner G. *Elements of psychophysics* (Vol. 1), 1860. Translated and edited by HE Adler, DH Howes, & EG Boring. New York: Holt, Rinehart, & Winston; 1966.
115. Norton TT, Corliss DA. *The psychophysical measurement of visual function*: Butterworth-Heinemann; 2002.
116. Gescheider GA. *Psychophysical measurement of thresholds: differential sensitivity. Psychophysics: the fundamentals*. 1997:1-15.

117. Engen T. Psychophysics II. scaling methods. Woodworth and Schlosberg's Experimental Psychology. 1971;1:47-86.
118. Gescheider G. The measurement of sensory attributes and discrimination scales. Psychophysics: The Fundamentals. 1997.
119. Gescheider G. Psychophysics: The Fundamentals. Lawrence Erlbaum Associates. Inc, Publishers. 1997:1-71.
120. Draeger J. Corneal sensitivity: measurement and clinical importance: Springer Science & Business Media; 2012.
121. Boberg-Ans J. On the corneal sensitivity. Acta Ophthalmologica. 1956;34(3):149-62.
122. Cochet P, Bonnet R. Corneal esthesiometry. Performance and practical importance. Bulletin des Sociétés d'ophtalmologie de France. 1961;6:541.
123. Murphy PJ, Lawrenson JG, Patel S, Marshall J. Reliability of the Non-Contact Corneal Aesthesiometer and its comparison with the Cochet–Bonnet aesthesiometer. Ophthalmic and Physiological Optics. 1998;18(6):532-9.

124. Larson WL. Electro-mechanical corneal aesthesiometer. *The British Journal of Ophthalmology*. 1970;54(5):342.
125. Millodot M. A review of research on the sensitivity of the cornea. *Ophthalmic and Physiological Optics*. 1984;4(4):305-18.
126. Golebiowski B, Papas E, Stapleton F. Assessing the sensory function of the ocular surface: implications of use of a non-contact air jet aesthesiometer versus the Cochet–Bonnet aesthesiometer. *Experimental Eye Research*. 2011;92(5):408-13.
127. Millodot M, Larson W. Effect of bending the nylon thread of the Cochet Bonnet aesthesiometer upon the recorded pressure. *Contact Lens*. 1967;1:5-7.
128. Millodot M, O'Leary DJ. Corneal fragility and its relationship to sensitivity. *Acta Ophthalmologica*. 1981;59(6):820-6.
129. Stapleton F, Tan M, Papas E, Ehrmann K, Golebiowski B, Vega J. Corneal and conjunctival sensitivity to air stimuli. *British Journal of Ophthalmology*. 2004;88(12):1547-51.
130. Feng Y, Simpson TL. Characteristics of human corneal psychophysical channels. *Investigative Ophthalmology & Visual Science*. 2004;45(9):3005-10.

131. Vega JA, Simpson TL, Fonn D. A noncontact pneumatic esthesiometer for measurement of ocular sensitivity: a preliminary report. *Cornea*. 1999;18(6):675-81.
132. Marks LE, Gescheider GA. Psychophysical scaling. *Stevens' Handbook of Experimental Psychology*. 2002.
133. Gescheider GA. Psychophysical scaling. *Annual Review of Psychology*. 1988;39(1):169-200.
134. Stevens SS. On the psychophysical law. *Psychological Review*. 1957;64(3):153.
135. Millodot M. Psychophysical scaling of corneal sensitivity. *Psychonomic Science*. 1968;12(8):401-2.
136. Stevens S, Greenbaum HB. Regression effect in psychophysical judgment. *Perception & Psychophysics*. 1966;1(12):439-46.
137. Feng Y, Simpson TL. The inhibitory interaction between human corneal and conjunctival sensory channels. *Investigative Ophthalmology & Visual Science*. 2005;46(4):1251-5.

138. Situ P, Simpson T, Fonn D. Eccentric variation of corneal sensitivity to pneumatic stimulation at different temperatures and with CO<sub>2</sub>. *Experimental Eye Research*. 2007;85(3):400-5.
139. Hunt RWG, Pointer MR. *Measuring colour*: John Wiley & Sons; 2011.
140. Malacara D, *Color vision and colorimetry: theory and applications*. 2011: SPIE Washington.
141. Smith T, Guild J. The CIE colorimetric standards and their use. *Transactions of the Optical Society*. 1931;33(3):73.
142. Duench S, Simpson T, Jones LW, Flanagan JG, Fonn D. Assessment of variation in bulbar conjunctival redness, temperature, and blood flow. *Optometry & Vision Science*. 2007;84(6):511-6.
143. Schulze MM, Jones DA, Simpson TL. The development of validated bulbar redness grading scales. *Optometry & Vision Science*. 2007;84(10):976-83.
144. Sorbara L, Simpson T, Duench S, Schulze M, Fonn D. Comparison of an objective method of measuring bulbar redness to the use of traditional grading scales. *Contact Lens and Anterior Eye*. 2007;30(1):53-9.

145. Fieguth P, Simpson T. Automated measurement of bulbar redness. *Investigative Ophthalmology & Visual Science*. 2002;43(2):340-7.

146. Schulze MM, Hutchings N, Simpson TL. The use of fractal analysis and photometry to estimate the accuracy of bulbar redness grading scales. *Investigative Ophthalmology & Visual Science*. 2008;49(4):1398-406.

## Chapter 2

1. Gabella G. Autonomic nervous system: Wiley Online Library; 2001.
2. Neuhuber W, Schrödl F. Autonomic control of the eye and the iris. *Autonomic Neuroscience*. 2011;165(1):67-79.
3. Davies LN, Wolffsohn JS, Gilmartin B. Autonomic correlates of ocular accommodation and cardiovascular function. *Ophthalmic and Physiological Optics*. 2009;29(4):427-35.
4. Bill A. Autonomic nervous control of uveal blood flow. *Acta Physiologica*. 1962;56(1):70-81.
5. Ruskell G. Innervation of the conjunctiva. *Transactions of the Ophthalmological Societies of the United Kingdom*. 1984;104:390-5.
6. Duke-Elder S. Textbook of ophthalmology. *British Medical Journal*. 1961;1(5231):1015.
7. Schaser K-D, Settmacher U, Puhl G, Zhang L, Mittlmeier T, Stover J. Noninvasive analysis of conjunctival microcirculation during carotid artery surgery

reveals microvascular evidence of collateral compensation and stenosis-dependent adaptation. *Journal of Vascular Surgery*. 2003;37(4):789-97.

8. Ohtani N. Laser Doppler flowmetry of the bulbar conjunctiva as a monitor of the cerebral blood flow. *Zasshi Journal*. 1996;44(9):1721-8.

9. Alnæs D, Sneve MH, Espeseth T, Endestad T, van de Pavert SHP, Laeng B. Pupil size signals mental effort deployed during multiple object tracking and predicts brain activity in the dorsal attention network and the locus coeruleus. *Journal of Vision*. 2014;14(4):1-.

10. Harrison NA, Wilson CE, Critchley HD. Processing of observed pupil size modulates perception of sadness and predicts empathy. *Emotion*. 2007;7(4):724.

11. Stern ME, Beuerman RW, Fox RI, Gao J, Mircheff AK, Pflugfelder SC. A unified theory of the role of the ocular surface in dry eye. *Lacrimal Gland, Tear Film, and Dry Eye Syndromes 2*: Springer; 1998. p. 643-51.

12. Belmonte C, Aracil A, Acosta MC, Luna C, Gallar J. Nerves and sensations from the eye surface. *The Ocular Surface*. 2004;2(4):248-53.

13. Chen JC, Schmid KL, Brown B. The autonomic control of accommodation and implications for human myopia development: a review. *Ophthalmic and Physiological Optics*. 2003;23(5):401-22.

### Chapter 3

1. Duke-Elder S. Textbook of ophthalmology. British Medical Journal. 1961;1(5231):1015.
2. Duench S, Simpson T, Jones LW, Flanagan JG, Fonn D. Assessment of variation in bulbar conjunctival redness, temperature, and blood flow. Optometry & Vision Science. 2007;84(6):511-6.
3. Mayrovitz HN, Larnard D, Duda G. Blood velocity measurement in human conjunctival vessels. Cardiovascular Diseases. 1981;8(4):509.
4. Piovella C. In vivo observations of the microcirculation of the bulbar conjunctiva in migraineurs. International Migraine-Headache Symposium; 1972: Karger Publishers.
5. Bloch EH. Microscopic observations of the circulating blood in the bulbar conjunctiva in man in health and disease. Ergebnisse der Anatomie und Entwicklungsgeschichte. 1956;35:1-98.
6. Schaser K-D, Settmacher U, Puhl G, Zhang L, Mittlmeier T, Stover J. Noninvasive analysis of conjunctival microcirculation during carotid artery surgery

reveals microvascular evidence of collateral compensation and stenosis-dependent adaptation. *Journal of Vascular Surgery*. 2003;37(4):789-97.

7. Ohtani N. Laser Doppler flowmetry of the bulbar conjunctiva as a monitor of the cerebral blood flow. *Zasshi Journal*. 1996;44(9):1721-8.

8. Efron N, Brennan NA, More J, Rieper K. Temperature of the hyperemic bulbar conjunctiva. *Current Eye Research*. 1988;7(6):615-8.

9. Papas E. On the relationship between soft contact lens oxygen transmissibility and induced limbal hyperaemia. *Experimental Eye Research*. 1998;67(2):125-31.

10. Solomon A, Dursun D, Liu Z, Xie Y, Macri A, Pflugfelder SC. Pro-and anti-inflammatory forms of interleukin-1 in the tear fluid and conjunctiva of patients with dry-eye disease. *Investigative Ophthalmology & Visual Science*. 2001;42(10):2283-92.

11. Van der Werf F, Baljet B, Prins M, Ruskell G, Otto J. Innervation of the palpebral conjunctiva and the superior tarsal muscle in the cynomolgous monkey: a retrograde fluorescent tracing study. *Journal of Anatomy*. 1996;189(Pt 2):285.

12. Ruskell G. Innervation of the conjunctiva. *Transactions of the Ophthalmological Societies of the United Kingdom*. 1984;104:390-5.

13. Kobayashi A, Yoshita T, Sugiyama K. In vivo findings of the bulbar/palpebral conjunctiva and presumed meibomian glands by laser scanning confocal microscopy. *Cornea*. 2005;24(8):985-8.
14. Feng Y, Simpson TL. Nociceptive sensation and sensitivity evoked from human cornea and conjunctiva stimulated by CO<sub>2</sub>. *Investigative Ophthalmology & Visual Science*. 2003;44(2):529-32.
15. Acosta MC, Tan ME, Belmonte C, Gallar J. Sensations evoked by selective mechanical, chemical, and thermal stimulation of the conjunctiva and cornea. *Investigative Ophthalmology & Visual Science*. 2001;42(9):2063-7.
16. Belmonte C, Acosta MC, Schmelz M, Gallar J. Measurement of corneal sensitivity to mechanical and chemical stimulation with a CO<sub>2</sub> esthesiometer. . *Investigative Ophthalmology & Visual Science*. 1999;40(2):513-9.
17. Gescheider GA. Psychophysical measurement of thresholds: differential sensitivity. *Psychophysics: the fundamentals*. 1997:1-15.
18. Karita K, Izumi H. Somatosensory afferents in the parasympathetic vasodilator reflex in cat lip. *Journal of the Autonomic Nervous System*. 1992;39(3):229-34.

19. Matthews B, Vongsavan N. Axon reflex vasodilatation in cat tooth-pulp. Society for Neuroscience Abstract Archive; 1991; (Vol. 17), p. 1368.
20. Olgart L, Edwall L, Gazelius B. Involvement of afferent nerves in pulpal blood-flow reactions in response to clinical and experimental procedures in the cat. Archives of Oral Biology. 1991;36(8):575-81.
21. Kemppainen P, Forster C, Handwerker H. The importance of stimulus site and intensity in differences of pain-induced vascular reflexes in human orofacial regions. Pain. 2001;91(3):331-8.
22. Kemppainen P, Leppänen H, Jyväsjärvi E, Pertovaara A. Blood flow increase in the orofacial area of humans induced by painful stimulation. Brain Research Bulletin. 1994;33(6):655-62.
23. Schmelz M, Michael K, Weidner C, Schmidt R, Handwerker HO. Which nerve fibers mediate the axon reflex flare in human skin? Neuroreport. 2000;11(3):645-8.
24. Szolcsanyi J. Antidromic vasodilatation and neurogenic inflammation. Inflammation Research. 1988;23(1):4-11.

25. Wårdell K, Naver H, Nilsson G, Wallin B. The cutaneous vascular axon reflex in humans characterized by laser Doppler perfusion imaging. *The Journal of Physiology*. 1993;460(1):185-99.
26. Aars H, Gazelius B, Edwall L, Olgart L. Effects of autonomic reflexes on tooth pulp blood flow in man. *Acta Physiologica*. 1992;146(4):423-9.
27. Drummond PD. The effect of sympathetic blockade on facial sweating and cutaneous vascular responses to painful stimulation of the eye. *Brain*. 1993;116(1):233-41.
28. Goadsby P, Macdonald G. Extracranial vasodilatation mediated by vasoactive intestinal polypeptide (VIP). *Brain Research*. 1985;329(1):285-8.
29. Gonzalez G, Onofrio BM, Kerr FW. Vasodilator system for the face. *Journal of Neurosurgery*. 1975;42(6):696-703.
30. Izumi H, Karita K. Selective excitation of parasympathetic nerve fibers to elicit the vasodilatation in cat lip. *Journal of the Autonomic Nervous System*. 1992;37(2):99-107.

31. Situ P, Simpson TL. Interaction of corneal nociceptive stimulation and lacrimal secretion. *Investigative Ophthalmology & Visual Science*. 2010;51(11):5640-5.
32. Müller L, Pels L, Vrensen G. Ultrastructural organization of human corneal nerves. *Investigative ophthalmology & visual science*. 1996;37(4):476-88.
33. Müller L, Vrensen G, Pels L, Cardozo BN, Willekens B. Architecture of human corneal nerves. . *Investigative Ophthalmology & Visual Science*. 1997;38(5):985-94.
34. Caterina MJ, Rosen TA, Tominaga M, Brake AJ, Julius D. A capsaicin-receptor homologue with a high threshold for noxious heat. *Nature*. 1999;398(6726):436-41.
35. Waldmann R, Champigny G, Bassilana F, Heurteaux C, Lazdunski M. A proton-gated cation channel involved in acid-sensing. *Nature*. 1997;386(6621):173.
36. Ugawa S, Ueda T, Takahashi E, Hirabayashi Y, Yoneda T, Komai S. Cloning and functional expression of ASIC- $\beta$ 2, a splice variant of ASIC- $\beta$ . *Neuroreport*. 2001;12(13):2865-9.
37. Fricke B, Lints R, Stewart G, Drummond H, Dodt G, Driscoll M, et al. Epithelial Na<sup>+</sup> channels and stomatin are expressed in rat trigeminal mechanosensory neurons. *Cell and Tissue Research*. 2000;299(3):327-34.

38. Chen X, Gallar J, Pozo MA, Baeza M, Belmonte C. CO<sub>2</sub> stimulation of the cornea: a comparison between human sensation and nerve activity in polymodal nociceptive afferents of the cat. *European Journal of Neuroscience*. 1995;7(6):1154-63.
39. Berardelli A, Rothwell J, Day B, Marsden C. Pathophysiology of blepharospasm and oromandibular dystonia. *Brain*. 1985;108(3):593-608.
40. Nash PG, Macefield VG, Klineberg IJ, Gustin SM, Murray GM, Henderson LA. Bilateral activation of the trigeminothalamic tract by acute orofacial cutaneous and muscle pain in humans. *Pain*. 2010;151(2):384-93.
41. Nash PG, Macefield VG, Klineberg IJ, Murray GM, Henderson LA. Differential activation of the human trigeminal nuclear complex by noxious and non-noxious orofacial stimulation. *Human Brain Mapping*. 2009;30(11):3772-82.

## Chapter 4

1. Merskey H, Bogduk N. Classification of chronic pain, IASP Task Force on Taxonomy. Seattle, WA: International Association for the Study of Pain Press (Also available online at [www.iasp-pain.org](http://www.iasp-pain.org)). 1994.
2. Rosenthal P, Borsook D. The corneal pain system. Part I: the missing piece of the dry eye puzzle. *The Ocular Surface*. 2012;10(1):2-14.
3. Jensen MP, Karoly P, Harris P. Assessing the affective component of chronic pain: development of the Pain Discomfort Scale. *Journal of Psychosomatic Research*. 1991;35(2):149-54.
4. Casey KL, Minoshima S, Berger KL, Koeppe RA, Morrow TJ, Frey KA. Positron emission tomographic analysis of cerebral structures activated specifically by repetitive noxious heat stimuli. *Journal of Neurophysiology*. 1994;71(2):802-7.
5. Chen AC. Human brain measures of clinical pain: a review I. Topographic mappings. *Pain*. 1993;54(2):115-32.

6. Coghill RC, Talbot JD, Evans AC, Meyer E, Gjedde A, Bushnell MC, et al. Distributed processing of pain and vibration by the human brain. *Journal of Neuroscience*. 1994;14(7):4095-108.
7. Donaldson GW, Chapman CR, Nakamura Y, Bradshaw DH, Jacobson RC, Chapman CN. Pain and the defense response: structural equation modeling reveals a coordinated psychophysiological response to increasing painful stimulation. *Pain*. 2003;102(1):97-108.
8. Colloca L, Benedetti F, Pollo A. Repeatability of autonomic responses to pain anticipation and pain stimulation. *European Journal of Pain*. 2006;10(7):659-.
9. Beatty J, Lucero-Wagoner B. The pupillary system. *Handbook of Psychophysiology*. 2000;2:142-62.
10. Wierda SM, van Rijn H, Taatgen NA, Martens S. Pupil dilation deconvolution reveals the dynamics of attention at high temporal resolution. *Proceedings of the National Academy of Sciences*. 2012;109(22):8456-60.
11. Hoeks B, Levelt WJ. Pupillary dilation as a measure of attention: A quantitative system analysis. *Behavior Research Methods*. 1993;25(1):16-26.

12. Iriki A, Tanaka M, Iwamura Y. Attention-induced neuronal activity in the monkey somatosensory cortex revealed by pupillometrics. *Neuroscience Research*. 1996;25(2):173-81.
13. Yang LL, Niemann CU, Larson MD. Mechanism of pupillary reflex dilation in awake volunteers and in organ donors. *Anesthesiology: The Journal of the American Society of Anesthesiologists*. 2003;99(6):1281-6.
14. Chapman CR, Oka S, Bradshaw DH, Jacobson RC, Donaldson GW. Phasic pupil dilation response to noxious stimulation in normal volunteers: relationship to brain evoked potentials and pain report. *Psychophysiology*. 1999;36(1):44-52.
15. Oka S, Chapman CR, Jacobson RC. Phasic pupil dilation response to noxious stimulation: Effects of conduction distance, sex, and age. *Journal of Psychophysiology*. 2000;14(2):97.
16. Loewenfeld IE. Mechanisms of reflex dilatation of the pupil. *Documenta Ophthalmologica*. 1958;12(1):185-448.
17. Reeves AG, Posner JB. The ciliospinal response in man. *Neurology*. 1969;19(12):1145-.

18. Geuter S, Gamer M, Onat S, Büchel C. Parametric trial-by-trial prediction of pain by easily available physiological measures. *Pain*. 2014;155(5):994-1001.
19. Larson MD, Sessler DI, Washington DE, Merrifield BR, Hynson JA, McGuire J. Pupillary response to noxious stimulation during isoflurane and propofol anesthesia. *Anesthesia & Analgesia*. 1993;76(5):1072-8.
20. Ellermeier W, Westphal W. Gender differences in pain ratings and pupil reactions to painful pressure stimuli. *Pain*. 1995;61(3):435-9.
21. Fillingim RB, Maixner W. Gender differences in the responses to noxious stimuli. *Pain Forum* 1995 Dec 1 (Vol. 4, No. 4, pp. 209-221). Churchill Livingstone.
22. Unruh AM. Gender variations in clinical pain experience. *Pain*. 1996;65(2-3):123-67.
23. Lawrenson J, Ruskell G. Investigation of limbal touch sensitivity using a Cochet-Bonnet aesthesiometer. *British Journal of Ophthalmology*. 1993;77(6):339-43.
24. Millodot M, Owens H. The influence of age on the fragility of the cornea. *Acta ophthalmologica*. 1984;62(5):819-24.

25. Acosta MC, Alfaro ML, Borrás F, Belmonte C, Gallar J. Influence of age, gender and iris color on mechanical and chemical sensitivity of the cornea and conjunctiva. *Experimental Eye Research*. 2006;83(4):932-8.
26. Millodot M. Diurnal variation of corneal sensitivity. *The British Journal of Ophthalmology*. 1972;56(11):844.
27. Riss B, Binder S, Riss P, Kemeter P. Corneal sensitivity during the menstrual cycle. *The British Journal of Ophthalmology*. 1982;66(2):123-6.
28. Millodot M, Lamont A. Influence of menstruation on corneal sensitivity. *The British Journal of Ophthalmology*. 1974;58(8):752.
29. Millodot M. Do blue-eyed people have more sensitive corneas than brown-eyed people? *Nature*. 1975;255(5504):151-2.
30. Marfurt C, Kingsley R, Echtenkamp S. Sensory and sympathetic innervation of the mammalian cornea. A retrograde tracing study. *Investigative Ophthalmology & Visual Science*. 1989;30(3):461-72.

31. Van der Werf F, Baljet B, Prins M, Ruskell G, Otto J. Innervation of the palpebral conjunctiva and the superior tarsal muscle in the cynomolgous monkey: a retrograde fluorescent tracing study. *Journal of Anatomy*. 1996;189(Pt 2):285.
32. Vega JA, Simpson TL, Fonn D. A noncontact pneumatic esthesiometer for measurement of ocular sensitivity: a preliminary report. *Cornea*. 1999;18(6):675-81.
33. Feng Y, Simpson TL. Nociceptive sensation and sensitivity evoked from human cornea and conjunctiva stimulated by CO<sub>2</sub> *Investigative Ophthalmology & Visual Science*. 2003;44(2):529-32.
34. Chen J, Feng Y, Simpson TL. Human corneal adaptation to mechanical, cooling, and chemical stimuli. *Investigative Ophthalmology & Visual Science*. 2010;51(2):876-81.
35. Rao SBS, Simpson TL. Measurement of difference thresholds on the ocular surface. *Investigative Ophthalmology & Visual Science*. 2014;55(2):1095-100.
36. Chen X, Gallar J, Pozo MA, Baeza M, Belmonte C. CO<sub>2</sub> stimulation of the cornea: a comparison between human sensation and nerve activity in polymodal nociceptive afferents of the cat. *European Journal of Neuroscience*. 1995;7(6):1154-63.

37. Belmonte C, Acosta MC, Schmelz M, Gallar J. Measurement of corneal sensitivity to mechanical and chemical stimulation with a CO<sub>2</sub> esthesiometer. *Investigative Ophthalmology & Visual Science*. 1999;40(2):513-9.
38. Acosta MC, Tan ME, Belmonte C, Gallar J. Sensations evoked by selective mechanical, chemical, and thermal stimulation of the conjunctiva and cornea. *Investigative Ophthalmology & Visual Science*. 2001;42(9):2063-7.
39. Belmonte C, Aracil A, Acosta MC, Luna C, Gallar J. Nerves and sensations from the eye surface. *The Ocular Surface*. 2004;2(4):248-53.
40. Situ P, Simpson T, Fonn D. Eccentric variation of corneal sensitivity to pneumatic stimulation at different temperatures and with CO<sub>2</sub>. *Experimental Eye Research*. 2007;85(3):400-5.
41. Gescheider GA. Psychophysical measurement of thresholds: differential sensitivity. *Psychophysics: the fundamentals*. 1997:1-15.
42. Kardon R. Pupillary light reflex. *Current Opinion in Ophthalmology*. 1995;6(6):20-6.

43. Beatty J. Phasic not tonic pupillary responses vary with auditory vigilance performance. *Psychophysiology*. 1982;19(2):167-72.
44. Bingefors K, Isacson D. Epidemiology, co-morbidity, and impact on health-related quality of life of self-reported headache and musculoskeletal pain—a gender perspective. *European Journal of Pain*. 2004;8(5):435-50.
45. Levine FM, De Simone LL. The effects of experimenter gender on pain report in male and female subjects. *Pain*. 1991;44(1):69-72.
46. Velle W. Sex differences in sensory functions. *Perspectives in Biology and Medicine*. 1987;30(4):490-522.
47. Craft RM, Mogil JS, Aloisi AM. Sex differences in pain and analgesia: the role of gonadal hormones. *European Journal of Pain*. 2004;8(5):397-411.
48. Lautenbacher S, Strian F. Sex differences in pain and thermal sensitivity: the role of body size. *Attention, Perception, & Psychophysics*. 1991;50(2):179-83.
49. Feine JS, Bushnell MC, Miron D, Duncan GH. Sex differences in the perception of noxious heat stimuli. *Pain*. 1991;44(3):255-62.

50. Otto MW, Dougher MJ. Sex differences and personality factors in responsivity to pain. *Perceptual and Motor Skills*. 1985;61(2):383-90.
51. Le Floch J-P, Escuyer P, Baudin E, Baudon D, Perlemuter L. Blood glucose area under the curve: methodological aspects. *Diabetes Care*. 1990;13(2):172-5.
52. Treister R, Kliger M, Zuckerman G, Aryeh IG, Eisenberg E. Differentiating between heat pain intensities: the combined effect of multiple autonomic parameters. *Pain*. 2012;153(9):1807-14.

## Chapter 5

1. Chen JC, Schmid KL, Brown B. The autonomic control of accommodation and implications for human myopia development: a review. *Ophthalmic and Physiological Optics*. 2003;23(5):401-22.
2. Culhane HM, Winn B, Gilmartin B. Human dynamic closed-loop accommodation augmented by sympathetic inhibition. *Investigative Ophthalmology & Visual Science*. 1999;40(6):1137-43.
3. Gilmartin B, Mallen E, Wolffsohn J. Sympathetic control of accommodation: evidence for inter-subject variation. *Ophthalmic and Physiological Optics*. 2002;22(5):366-71.
4. Mallen EA, Gilmartin B, Wolffsohn JS. Sympathetic innervation of ciliary muscle and oculomotor function in emmetropic and myopic young adults. *Vision Research*. 2005;45(13):1641-51.
5. Morgan MW. Accommodation and vergence. *Optometry & Vision Science*. 1968;45(7):417-54.

6. Phillips S, Stark L. Blur: a sufficient accommodative stimulus. *Documenta Ophthalmologica*. 1977;43(1):65-89.
7. Fincham EF, Walton J. The reciprocal actions of accommodation and convergence. *The Journal of Physiology*. 1957;137(3):488-508.
8. Gamlin P, Zhang Y, Clendaniel RA, Mays LE. Behavior of identified Edinger-Westphal neurons during ocular accommodation. *Journal of Neurophysiology*. 1994;72(5):2368-82.
9. Mays LE, Gamlin PD. Neuronal circuitry controlling the near response. *Current Opinion in Neurobiology*. 1995;5(6):763-8.
10. Zhang Y, Mays L, Gamlin P. Characteristics of near response cells projecting to the oculomotor nucleus. *Journal of Neurophysiology*. 1992;67(4):944-60.
11. Gamlin P, Clarke RJ. Single-unit activity in the primate nucleus reticularis tegmenti pontis related to vergence and ocular accommodation. *Journal of Neurophysiology*. 1995;73(5):2115-9.

12. Judge S, Cumming B. Neurons in the monkey midbrain with activity related to vergence eye movement and accommodation. *Journal of Neurophysiology*. 1986;55(5):915-30.
13. Ruskell G. Accommodation and the nerve pathway to the ciliary muscle: a review. *Ophthalmic and Physiological Optics*. 1990;10(3):239-42.
14. Ruskell G, Griffiths T. Peripheral nerve pathway to the ciliary muscle. *Experimental Eye Research*. 1979;28(3):277-84.
15. Semmlow JL, Zuber B. Oculomotor responses to near stimuli: the near triad. *Models of oculomotor behavior and control*. 1981:162-91.
16. Situ P, Simpson TL. Interaction of corneal nociceptive stimulation and lacrimal secretion. *Investigative Ophthalmology & Visual Science*. 2010;51(11):5640-5.
17. Blade PJ, Candy TR. Validation of the PowerRefractor for measuring human infant refraction. *Optometry and Vision Science*. 2006;83(6):346.
18. Choi M, Weiss S, Schaeffel F, Seidemann A, Howland HC, Wilhelm B, et al. Laboratory, clinical, and kindergarten test of a new eccentric infrared photorefractor (PowerRefractor). *Optometry & Vision Science*. 2000;77(10):537-48.

19. Belmonte C, Acosta MC, Schmelz M, Gallar J. Measurement of corneal sensitivity to mechanical and chemical stimulation with a CO<sub>2</sub> esthesiometer. *Investigative ophthalmology & visual science*. 1999;40(2):513-9.
20. Situ P, Simpson T, Fonn D. Eccentric variation of corneal sensitivity to pneumatic stimulation at different temperatures and with CO<sub>2</sub>. *Experimental Eye Research*. 2007;85(3):400-5.
21. Feng Y, Simpson TL. Nociceptive sensation and sensitivity evoked from human cornea and conjunctiva stimulated by CO<sub>2</sub>. *Investigative Ophthalmology & Visual Science*. 2003;44(2):529-32.
22. Gescheider GA. Psychophysical measurement of thresholds: differential sensitivity. *Psychophysics: the fundamentals*. 1997:1-15.
23. Kotulak JC, Schor CM. Temporal variations in accommodation during steady-state conditions. *Journal of the Optical Society of America*. 1986;3(2):223-7.
24. Oyster CW. *The human eye: structure and function*: Sinauer Associates; 1999.

25. Wilcox LM, Keough EM, Connolly RJ, Hotte CE. The contribution of blood flow by the anterior ciliary arteries to the anterior segment in the primate eye. *Experimental Eye Research*. 1980;30(2):167-74.
26. Stapleton F, Tan M, Papas E, Ehrmann K, Golebiowski B, Vega J, et al. Corneal and conjunctival sensitivity to air stimuli. *British Journal of Ophthalmology*. 2004;88(12):1547-51.
27. Belmonte C, Gallar J. Cold thermoreceptors, unexpected players in tear production and ocular dryness sensations. *Investigative Ophthalmology & Visual Science*. 2011;52(6):3888-92.
28. Marg E, Morgan MW. The pupillary near reflex: the relation of pupillary diameter to accommodation and the various components of convergence. *Optometry & Vision Science*. 1949;26(5):183-98.
29. Alpern M, Mason GL, Jardinico RE. Vergence and accommodation: V. Pupil size changes associated with changes in accommodative vergence. *American Journal of Ophthalmology*. 1961;52(5):762-7.

30. Sreenivasan V. Near addition lenses as a tool to investigate vergence adaptation in myopic children. 2011.
31. Sreenivasan V, Irving EL, Bobier WR. Binocular adaptation to near addition lenses in emmetropic adults. *Vision Research*. 2008;48(10):1262-9.
32. Allen PM, Radhakrishnan H, O'leary DJ. Repeatability and validity of the PowerRefractor and the Nidek AR600-A in an adult population with healthy eyes. *Optometry & Vision Science*. 2003;80(3):245-51.
33. Hennessy RT, Iida T, Shiina K, Leibowitz H. The effect of pupil size on accommodation. *Vision Research*. 1976;16(6):587-9.
34. Ripps H, Chin NB, SIEGEL IM, Breinin GM. The effect of pupil size on accommodation, convergence, and the AC/A ratio. *Investigative Ophthalmology & Visual Science*. 1962;1(1):127-35.
35. Stark LR, Atchison DA. Pupil size, mean accommodation response and the fluctuations of accommodation. *Ophthalmic and Physiological Optics*. 1997;17(4):316-23.

36. Ward P, Charman W. Effect of pupil size on steady state accommodation. *Vision Research*. 1985;25(9):1317-26.
37. Wolffsohn JS, Gilmartin B, Mallen EAH, Tsujimura S-i. Continuous recording of accommodation and pupil size using the Shin-Nippon SRW-5000 autorefractor. *Ophthalmic and Physiological Optics*. 2001;21(2):108-13.
38. Winn B, Pugh J, Gilmartin B, Owens H. The effect of pupil size on static and dynamic measurements of accommodation using an infra-red optometer. *Ophthalmic and Physiological Optics*. 1989;9(3):277-83.
39. Gray L, Gilmartin B, Winn B. Accommodation microfluctuations and pupil size during sustained viewing of visual display terminals. *Ophthalmic and Physiological Optics*. 2000;20(1):5-10.
40. Beatty J. Phasic not tonic pupillary responses vary with auditory vigilance performance. *Psychophysiology*. 1982;19(2):167-72.
41. Chapman CR, Oka S, Bradshaw DH, Jacobson RC, Donaldson GW. Phasic pupil dilation response to noxious stimulation in normal volunteers: relationship to brain evoked potentials and pain report. *Psychophysiology*. 1999;36(1):44-52.

42. Ellermeier W, Westphal W. Gender differences in pain ratings and pupil reactions to painful pressure stimuli. *Pain*. 1995;61(3):435-9.
43. Oka S, Chapman CR, Jacobson RC. Phasic pupil dilation response to noxious stimulation: Effects of conduction distance, sex, and age. *Journal of Psychophysiology*. 2000;14(2):97.
44. Beatty J, Lucero-Wagoner B. The pupillary system. *Handbook of Psychophysiology*. 2000;2:142-62.
45. Kardon R. Pupillary light reflex. *Current Opinion in Ophthalmology*. 1995;6(6):20-6.
46. Stakenburg M. Accommodation without pupillary constriction. *Vision Research*. 1991;31(2):267-73.
47. Phillips N, Winn B, Gilmartin B. Absence of pupil response to blur-driven accommodation. *Vision Research*. 1992;32(9):1775-9.
48. Jaschinski W, Bonacker M, Alshuth E. Accommodation, convergence, pupil diameter and eye blinks at a CRT display flickering near fusion limit. *Ergonomics*. 1996;39(1):152-64.

49. Campbell F, Westheimer G. Dynamics of accommodation responses of the human eye. *The Journal of Physiology*. 1960;151(2):285-95.

## Chapter 6

1. Gabella G. Autonomic nervous system: Wiley Online Library; 2001.
2. Neuhuber W, Schrödl F. Autonomic control of the eye and the iris. *Autonomic Neuroscience*. 2011;165(1):67-79.
3. Davies LN, Wolffsohn JS, Gilmartin B. Autonomic correlates of ocular accommodation and cardiovascular function. *Ophthalmic and Physiological Optics*. 2009;29(4):427-35.
4. Bill A. Autonomic nervous control of uveal blood flow. *Acta Physiologica*. 1962;56(1):70-81.
5. Treister R, Kliger M, Zuckerman G, Aryeh IG, Eisenberg E. Differentiating between heat pain intensities: the combined effect of multiple autonomic parameters. *Pain*. 2012;153(9):1807-14.
6. Wårdell K, Naver H, Nilsson G, Wallin B. The cutaneous vascular axon reflex in humans characterized by laser Doppler perfusion imaging. *The Journal of Physiology*. 1993;460(1):185-99.

7. Schmelz M, Michael K, Weidner C, Schmidt R, Handwerker HO. Which nerve fibers mediate the axon reflex flare in human skin? *Neuroreport*. 2000;11(3):645-8.
8. Aars H, Gazelius B, Edwall L, Olgart L. Effects of autonomic reflexes on tooth pulp blood flow in man. *Acta Physiologica*. 1992;146(4):423-9.
9. Goadsby P, Macdonald G. Extracranial vasodilatation mediated by vasoactive intestinal polypeptide (VIP). *Brain Research*. 1985;329(1):285-8.
10. Kemppainen P, Leppänen H, Jyväsjärvi E, Pertovaara A. Blood flow increase in the orofacial area of humans induced by painful stimulation. *Brain Research Bulletin*. 1994;33(6):655-62.
11. Alnæs D, Sneve MH, Espeseth T, Endestad T, van de Pavert SHP, Laeng B. Pupil size signals mental effort deployed during multiple object tracking and predicts brain activity in the dorsal attention network and the locus coeruleus. *Journal of Vision*. 2014;14(4):1-.
12. Hyönä J, Tommola J, Alaja A-M. Pupil dilation as a measure of processing load in simultaneous interpretation and other language tasks. *The Quarterly Journal of Experimental Psychology*. 1995;48(3):598-612.

13. Gabay S, Pertzov Y, Henik A. Orienting of attention, pupil size, and the norepinephrine system. *Attention, Perception, & Psychophysics*. 2011;73(1):123-9.
14. Goldwater BC. Psychological significance of pupillary movements. *Psychological Bulletin*. 1972;77(5):340.
15. Wilhelm B, Wilhelm H, Lüdtke H. Pupillography: Principles and applications in basic and clinical research. *Pupillography: Principles, methods and applications*. 1999:1-11.
16. Sara SJ. The locus coeruleus and noradrenergic modulation of cognition. *Nature Reviews Neuroscience*. 2009;10(3):211-23.
17. Schneider KA, Kastner S. Effects of sustained spatial attention in the human lateral geniculate nucleus and superior colliculus. *Journal of Neuroscience*. 2009;29(6):1784-95.
18. Foote SL, Morrison JH. Extrathalamic modulation of cortical function. *Annual Review of Neuroscience*. 1987;10(1):67-95.
19. Belmonte C, Garcia-Hirschfeld J, Gallar J. Neurobiology of ocular pain. *Progress in Retinal and Eye Research*. 1997;16(1):117-56.

20. Kotulak JC, Schor CM. Temporal variations in accommodation during steady-state conditions. *Journal of the Optical Society of America*. 1986;3(2):223-7.
21. Oyster CW. *The human eye: structure and function*: Sinauer Associates; 1999.
22. Janda AM. Ocular trauma: triage and treatment. *Postgraduate Medicine*. 1991;90(7):51-60.
23. Torok P, Mader T. Corneal abrasions: diagnosis and management. *American Family Physician*. 1996;53(8):2521-9, 32.
24. Wilson SA, Last A. Management of corneal abrasions. *American Family Physician*. 2004;70:123-32.
25. Nishimoto JY. Iritis. How to recognize and manage a potentially sight-threatening disease. *Postgraduate Medicine*. 1996;99(2):255-7, 61-2.
26. Joshaghani M, Nazari H, Falavarjani KG, Shokrollahi S, Ghaempanah MJ, Aghdam KA, et al. Effect of Homatropine eye drops on pain after photorefractive keratectomy: A pilot study. *Saudi Journal of Ophthalmology*. 2013;27(2):83-5.

27. Chen X, Gallar J, Pozo MA, Baeza M, Belmonte C. CO<sub>2</sub> stimulation of the cornea: a comparison between human sensation and nerve activity in polymodal nociceptive afferents of the cat. *European Journal of Neuroscience*. 1995;7(6):1154-63.
28. Ugawa S, Ueda T, Takahashi E, Hirabayashi Y, Yoneda T, Komai S, et al. Cloning and functional expression of ASIC- $\beta$ 2, a splice variant of ASIC- $\beta$ . *Neuroreport*. 2001;12(13):2865-9.
29. Waldmann R, Champigny G, Bassilana F, Heurteaux C, Lazdunski M. A proton-gated cation channel involved in acid-sensing. *Nature*. 1997;386(6621):173.
30. Angela JY, Cohen JD, editors. Sequential effects: superstition or rational behavior? *Advances in Neural Information Processing Systems*; 2009.
31. Ecott CL, Critchfield TS. Noncontingent reinforcement, alternative reinforcement, and the matching law: A laboratory demonstration. *Journal of Applied Behavior Analysis*. 2004;37(3):249-65.
32. Laming DRJ. Information theory of choice-reaction times. 1968.
33. Tsubota K, Nakamori K. Effects of ocular surface area and blink rate on tear dynamics. *Archives of Ophthalmology*. 1995;113(2):155-8.

34. Tsubota K, Yamada M. Tear evaporation from the ocular surface. *Investigative Ophthalmology & Visual Science*. 1992;33(10):2942-50.
35. Mathers W. Evaporation from the ocular surface. *Experimental Eye Research*. 2004;78(3):389-94.
36. Serin D, Karsloglu S, Kyan A, Alagöz G. A simple approach to the repeatability of the Schirmer test without anesthesia: eyes open or closed? *Cornea*. 2007;26(8):903-6.

## Chapter 7

1. Treister R, Kliger M, Zuckerman G, Aryeh IG, Eisenberg E. Differentiating between heat pain intensities: the combined effect of multiple autonomic parameters. *Pain*. 2012;153(9):1807-14.
2. Acosta MC, Tan ME, Belmonte C, Gallar J. Sensations evoked by selective mechanical, chemical, and thermal stimulation of the conjunctiva and cornea. *Investigative Ophthalmology & Visual Science*. 2001;42(9):2063-7.
3. Situ P, Simpson T, Fonn D. Eccentric variation of corneal sensitivity to pneumatic stimulation at different temperatures and with CO<sub>2</sub>. *Experimental Eye Research*. 2007;85(3):400-5.
4. Filler AG. The history, development and impact of computed imaging in neurological diagnosis and neurosurgery: CT, MRI, and DTI. *Journal of Neurosurgery*. 2010;7(1):5-35.
5. Geuter S, Gamer M, Onat S, Büchel C. Parametric trial-by-trial prediction of pain by easily available physiological measures. *Pain*. 2014;155(5):994-1001.